A link between smooth muscle cell death and extracellular matrix degradation during vascular atrophy

Richard D. Kenagy, PhD,[a] Seung-Kee Min, MD, PhD,[b] Eileen Mulvihill, PhD,[a] and **Alexander W. Clowes, MD,[a]** *Seattle, Wash; and Seoul, Korea*

Objective: **High blood flow induces neointimal atrophy in polytetrafluoroethylene (PTFE) aortoiliac grafts and a tight external PTFE wrap of the iliac artery induces medial atrophy. In both nonhuman primate models, atrophy with loss of smooth muscle cells and extracellular matrix (ECM) begins at ≤4 days. We hypothesized that matrix loss would be linked to cell death, but the factors and mechanisms involved are not known. The purpose of this study was to determine commonly regulated genes in these two models, which we hypothesized would be a small set of genes that might be key regulators of vascular atrophy.**

Methods: **DNA microarray analysis (Sentrix Human Ref 8; Illumina, San Diego, Calif; ~23,000 genes) was performed on arterial tissue from the wrap model (n = 9) and graft neointima from the graft model ($n = 5$) 1 day after wrapping or the switch to high flow, respectively. Quantitative reverse-transcription polymerase chain reaction (qRT-PCR) was also performed. Expression of this vascular atrophy gene set was also studied after Fas ligand-induced cell death in cultured smooth muscle cells and organ cultured arteries.**

Results: **Microarray analysis showed 15 genes were regulated in the same direction in both atrophy models: 9 upregulated and 6 downregulated. Seven of nine upregulated genes were confirmed by qRT-PCR in both models. Upregulated genes included the ECM-degrading enzymes *ADAMTS4*, tissue plasminogen activator (*PLAT*), and hyaluronidase 2; possible growth regulatory factors, including chromosome 8 open reading frame 4 and leucine-rich repeat family containing 8; a differentiation regulatory factor (musculoskeletal embryonic nuclear protein 1); a dead cell removal factor (ficolin 3); and a prostaglandin transporter (solute carrier organic anion transporter family member 2A1). Five downregulated genes were confirmed but only in one or the other model. Of the seven upregulated genes, *ADAMTS4*, *PLAT*, hyaluronidase 2, solute carrier organic anion transporter family member 2A1, leucine-rich repeat family containing 8, and chromosome 8 open reading frame 4 were also upregulated in vitro in cultured smooth muscle cells or cultured iliac artery by treatment with FasL, which causes cell death. However, blockade of caspase activity with Z-VAD inhibited FasL-mediated cell death, but not gene induction.**

Conclusion: **Seven gene products were upregulated in two distinctly different in vivo nonhuman primate vascular atrophy models. Induction of cell death by FasL in vitro induced six of these genes, including the ECM-degrading factors ADAMTS4, hyaluronidase 2, and PLAT, suggesting a mechanism by which the program of tissue atrophy coordinately removes extracellular matrix as cells die. These genes may be key regulators of vascular atrophy. (J Vasc Surg 2011;54:182-91.)**

Clinical Relevance: **This study identifies a small number of genes regulated in two distinct models of vascular atrophy in nonhuman primates. Some are involved in degradation of extracellular matrix, cell death, or cell differentiation. The function of others is less clear, but all may be fundamental regulators of vascular atrophy and may represent future therapeutic targets. A pharmacologic therapy based on the induction of vascular atrophy of established intimal lesions in restenotic stented vessels (arteries, vein grafts, and arteriovenous fistulas) would enable treatment of only those patients that develop stenosis rather than all patients as required when prevention of neointimal hyperplasia is the strategy.**

A novel approach for the treatment of restenotic stented arteries, vein grafts, and arteriovenous fistulas would be to induce atrophy of the established intimal lesion. This would enable treatment of only affected patients rather than all patients as required when prevention of neointimal hyperplasia is the strategy.[1] Intimal atrophy occurs naturally at late times in stented arteries in rats, pigs, and in most humans,[2-5] but little is known about its regulation. Therefore, we have established two different models of vascular atrophy in baboons. In the first model, neointima forms over 2 months in aortoiliac polytetrafluoroethylene (PTFE) grafts and is then induced to regress in response to a marked increase in blood flow after construction of a femoral arteriovenous fistula.[6,7] In the second model, the media of a normal iliac artery regresses in

From the Department of Surgery, University of Washington, Seattle[a]; and the Department of Surgery, Seoul National University College of Medicine, Seoul.[b]

Supported by National Institutes of Health HL30946 and RR00166.

Competition of interest: none.

Additional material for this article may be found online at www.jvascsurg.org.

Reprint requests: Alexander W. Clowes, MD, Department of Surgery, University of Washington, PO Box 356410, 1959 NE Pacific St, Seattle, WA 98195-6410 (e-mail: clowes@u.washington.edu).

The editors and reviewers of this article have no relevant financial relationships to disclose per the JVS policy that requires reviewers to decline review of any manuscript for which they may have a competition of interest.

0741-5214/$36.00

doi:10.1016/j.jvs.2010.12.070

response to a tight PTFE wrap.[8] In both models, loss of smooth muscle cells (SMCs) and matrix degradation are apparent by 4 days,[7,8] and SMC death documented by terminal deoxynucleotide transferase-mediated deoxy uridine triphosphate nick-end labeling (TUNEL) is observed in the PTFE graft model by 1 day.[9]

We hypothesized that matrix loss would be linked to cell death, but the factors and mechanisms involved are not known. For example, we previously tested the hypothesis that nitric oxide (NO) is required for graft neointimal atrophy based on the observations that endothelial NO synthase (NOS) is increased in the regressing graft endothelium[10] and that NO can inhibit SMC proliferation.[11] However, we found that pharmacologic blockade of NOS did not affect the neointima.[7] To further test the hypothesis that extracellular matrix (ECM) loss is linked to cell death, we have determined gene expression after 1 day in both baboon models of vascular atrophy to define a subset of genes common to both models and have determined the effect of FasL-induced cell death on induction of these genes in vitro.

METHODS

Animal care and procedures in this study were conducted at the University of Washington Regional Primate Research Center in accordance with state and federal laws and under protocols approved by the University of Washington Institutional Animal Care and Use Committee and the Regional Primate Research Center. Animal care and handling complied with the *Guide for the Care and Use of Laboratory Animals* issued by the Institute of Laboratory Animal Resources, Commission on Life Sciences, National Research Council, Washington, DC, National Academies Press, 1996 (http://stills.nap.edu/readingroom/books/labrats/).

Baboon model with PTFE graft. Ten male baboons received bilateral aortoiliac, 60-μm internodal distance, 4-mm unreinforced PTFE (Gore-Tex, W.L. Gore and Associates, Flagstaff, Ariz) bypass grafts, as described previously.[7] Two months after the bypass surgery, a single distal 1-cm arteriovenous fistula was created distal to a patent graft between the superficial femoral artery and the femoral vein. Femoral artery flow was measured by duplex ultrasound imaging just before and 1 day after fistula formation.

Baboon model with PTFE wrap. The common iliac arteries of 10 male baboons were tightly wrapped with a piece of 60-μm internodal distance, unreinforced PTFE graft material by wrapping the collapsed artery and a 2.5-mm diameter rod together and removing the rod after sewing the graft material closed.[8] The contralateral artery was dissected free from the surrounding tissue as a control.

RNA isolation and quantification. PTFE graft intimal tissue or wrapped and unwrapped arteries were harvested 1 day after fistula surgery or wrapping, respectively, and snap-frozen in RNAlater (Ambion, Carlsbad, Calif). Total RNA was prepared from graft neointimas and iliac arteries using the RNeasy fibrous tissue midi kit as described by the manufacturer (Qiagen, Valencia, Calif). Briefly, frozen tissue was pulverized under liquid nitrogen, homogenized in extraction buffer, and treated with proteinase K. RNA from cultured cells was obtained using the RNeasy Mini Kit (Qiagen) with the syringe and needle method of shearing. RNA preparations were treated with DNase1 before purification on the kit columns. RNA quality was assessed using the RNA 6000 Nano assay on the 2100 Bioanalyzer (Agilent, Palo Alto, Calif); $A_{260/280}$ ratios and yield were determined using the NanoDrop ND1000 spectrophotometer (Thermo Scientific, Waltham, Mass).

Microarray analysis. The Illumina Sentrix Human Ref-8 system (Illumina Inc, San Diego, Calif) was used according to the manufacturer's instructions. In brief, total RNA was used for complementary DNA (cDNA) synthesis, followed by amplification and labeling to create biotin-cRNA probes (Ambion MessageAmp kit; Ambion, Austin Tex). Hybridization, washing, blocking, development, and scanning were performed as directed by the manufacturer. Summarized bead intensities for noncontrol probes were quantile normalized. Several quality metrics were applied and indicated RNA degradation in two graft model samples and one sample of the wrap model. These three arrays plus their paired arrays were removed from the analysis. Statistical significance of gene expression differences was computed using Significance Analysis of Microarrays (SAM) software (http://www-stat.stanford.edu/~tibs/SAM/)[12] without a threshold for fold-change.

Five collections of gene sets (GO Biological Process, BP; GO Molecular Function, MF; GO Cellular Component, CC; and the C1 and C2 sets from Subramanian et al[13]) were used for gene set analysis. Information about C1 and C2 sets can be found at http://www.broad.mit.edu/gsea/msigdb/index.jsp. The software used has been described.[13,14] Analysis was restricted to gene sets with a minimum of 10 and a maximum of 500 genes. If a particular gene set is enriched in the wrapped or high-flow group, the online Results files of $\log_2$ expression contrasts (eg, wrapped to unwrapped) are presented online and have the word "positive" in the file name if a gene set is enriched in the wrapped or high-flow group and "negative" in the file name if it is enriched in the unwrapped or normal-flow group.

Quantitative reverse-transcription polymerase chain reaction. Quantitative reverse transcription polymerase chain reaction (qRT-PCR) was performed using the 7500 Fast real-time PCR system (Applied Biosystems, Foster City, Calif) according to the manufacturer's instructions using Taqman primers and probes purchased from Applied Biosystems and SensiMix master mix from Quantace Ltd (London, United Kingdom). Human probes for *Gas6* and *PLAT* did not work in baboon tissues; therefore, new primers were chosen using Primer3 (http://frodo.wi.mit.edu/cgi-bin/primer3/primer3_www.cgi) and obtained from Integrated DNA Technologies (Coralville, Iowa):

Gas6 (human): 5′-CGGAATCTGGTCATCAAGGT-3′
and 5′-TCTTCTCCGTTCAGCCAGTT-3′;

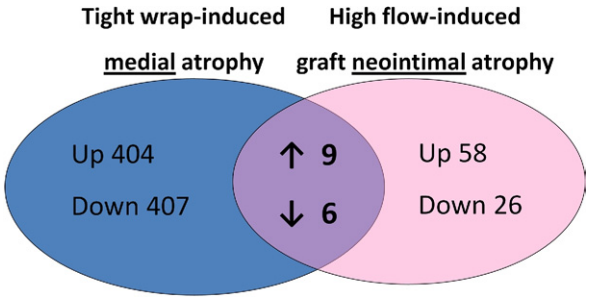

Fig 1. Venn diagram of significantly regulated genes during flow-mediated graft neointimal atrophy and wrap-mediated medial arterial atrophy. Fifteen genes were increased or decreased in both baboon models.

PLAT (human): 5′-CCCAGATCGAGACTCAAAGC-3′ and 5′-TGGGGTTCTGTGCTGTGTAA-3′;

18S (mammalian): 5′-AAACGGCTACCACATCCAAG-3′ and 5′-CCTCCAATGGATCCTCGTTA-3′.

qRT-PCR for *Gas6* and *PLAT* was performed using SYBR Green SensiMix DNA kit (Quantace) according to the manufacturer's instruction. Melting curves and size of product were tested to determine specificity. 18S was used as an endogenous control.

In vitro studies. Baboon aortic SMCs were cultured in Dulbecco's modified Eagle medium (DMEM) with 10% calf serum. SMCs were seeded at 20,000/cm^2 in six-well plates with 10% calf serum. The next day, the cell layer was washed with phosphate-buffered saline, and medium was changed to DMEM without serum plus recombinant human soluble Fas ligand (FasL)/FLAG fusion protein (50 ng/mL), anti-FLAG (2 μg/mL; both from Axxora, San Diego, Calif), and 1.5 μg/mL cycloheximide. After 6 and 24 hours RNA was extracted using RNeasy kits as described above. For experiments with Z-VAD, Z-VAD (50 μmol; BD Biosciences, San Jose, Calif) was added (or equivalent dimethyl sulfoxide to controls and FasL treated cultures) 30 minutes before the addition of FasL, anti-FLAG, and cycloheximide, as above. After 24 hours, medium was removed and spun at 1000*g* to remove floating cells for counting. Cell layers were harvested for RNA as above.

For organ culture experiments, baboon iliac arteries were obtained from the Washington National Primate Research Center tissue program. Periadventitial tissue was removed and the arteries were opened longitudinally. Arterial tissue (1.5-cm length) was incubated in a 12-well plate containing 2 mL of 10 mmol HEPES/DMEM (pH 7.4), with or without FasL/FLAG fusion protein (100 ng/mL), anti-FLAG (2 μg/mL), and 1.5 μg/mL cycloheximide. Arteries were snap-frozen 6 hours later and stored at −80°C until extraction of RNA using fibrous RNeasy kits, as described above.

Statistical analysis. Values reported are the mean ± standard error of the mean. Statistical differences (other than microarray data) were tested using a one-tailed Wilcoxon signed rank test.

RESULTS

PTFE grafts in three animals were occluded just before the fistula formation, so the fistulas were made in seven animals. RNA from one wrapped artery and two graft neointimas was degraded and was excluded from further analysis. Nine pairs of wrapped arteries and five pairs of graft intima were analyzed by microarray.

Genes regulated during vascular atrophy in vivo. Paired comparisons of gene expression by microarray were made between wrapped and unwrapped arteries and between high-flow and normal-flow PTFE graft intimas. In the wrapped arteries, we found 404 upregulated genes and 407 downregulated genes among the 24,357 genes exam-

Table I. Genes regulated in both baboon models of vascular atrophy

Gene	*RefSeq No.*	*Name*	*Wrap*	*Graft*
ADAMTS4	NM_005099	A disintegrin and metalloproteinase with thrombospondin motifs 4	2.94 (0)	1.58 (0)
FCN3	NM_173452	Ficolin 3	2.00 (0)	2.26 (0)
MUSTN1	NM_205853	Musculoskeletal embryonic nuclear protein 1 (Mustang 1)	1.98 (0)	3.00 (0)
HIST2H2AC	NM_003517	Histone 2H2ac	1.74 (0)	1.47 (0)
PLAT	NM_000931	Tissue plasminogen activator	1.66 (0)	1.47 (8.15)
LRRC8	XM_026998	Leucine-rich repeat family 8 containing	1.62 (0)	1.37 (8.15)
C8orf4	NM_020130	Thyroid cancer 1	1.49 (0)	1.81 (0)
SLCO2A1	NM_005630	Solute carrier organic anion transporter family, member 2A1 (PGT)	1.39 (0.17)	2.15 (0)
HYAL2	NM_003773	Hyaluronidase 2	1.34 (0)	1.47 (8.22)
FABP3	NM_004102	Fatty acid binding protein 3	0.74 (0.84)	0.64 (6.30)
FMOD	NM_002023	Fibromodulin	0.77 (0.71)	0.60 (6.30)
OGN	NM_014057	Osteoglycin	0.77 (0.58)	0.57 (6.30)
MATN2	NM_030583	Matrilin 2	0.77 (0.32)	0.70 (6.30)
TNNC1	NM_003280	Troponin C type 1	0.56 (0)	0.73 (8.18)
GAS6	NM_000820	Growth arrest specific protein 6	0.66 (0)	0.67 (6.30)

Values are the fold of unwrapped or normal flow, respectively. Values in parentheses are *Q* values from significance analysis of microarrays (SAM) analysis.

ined using an estimated false discovery rate of <1% (Supplementary Table I, online only). In the graft neointimas, we found 58 upregulated genes and 26 downregulated genes (Supplementary Table II, online only). In this case, we used a 10% false discovery rate for the analysis of the graft intimas because of the small number of samples.

A comparison of the genes that were significantly changed in the two models demonstrates the degree of difference between these two models (Fig 1). However, we did identify 15 genes regulated in the same direction in both models (Table I). The correlation of expression between the two models for these 15 genes was significant (Spearman $r = 0.76$, $P < .001$).

To validate the microarray data, qRT-PCR of the 15 genes was performed. All but one of the nine genes upregulated in wrapped arteries was verified (Fig 2, *A-I*). These included three genes involved in ECM regulation – *ADAMTS4*, *PLAT* (tissue plasminogen activator), and *HYAL2* (hyaluronidase 2). The other five genes were *MUSTN1* (Mustang 1), *FCN3* (ficolin 3), *SLCO2A1* (solute carrier organic anion transporter 2A1, also called the prostaglandin transporter or PGT), *C8orf4* (thyroid cancer 1 or TC1), and *LRRC8* (leucine rich repeat containing 8). In the graft intimas *PLAT*, *HYAL2, MUSTN1*, *FCN3*, *SLCO2A1*, and *C8orf4* showed the same trend ($P = .063$; only four paired samples were available for analysis), and *ADAMTS4* was previously verified at the protein and mRNA levels.[15] Among the six downregulated genes, *MATN2* (matrilin 2), *TNNC1* (troponin C), and *FABP3* (fatty acid binding protein 3) were verified in the wrap model (Fig 2, *J-O*), whereas *GAS6* and *OGN* (osteoglycin) demonstrated a trend to be decreased in the graft ($P = .063$).

Gene set analysis of atrophy in vivo. The results of gene set analysis of the microarray data were consistent with the results from analysis of individual genes. A comparison of the two atrophy models yielded a small number of gene sets regulated in common. The two models shared only four gene sets of the Biological Process collection. Three were significantly higher (GO:0045892 negative regulation of transcription, DNA-dependent; GO:0006974 response to DNA damage stimulus; and GO:0042127 regulation of cell proliferation; gene set lengths of 42, 23, and 40, respectively) and one was significantly lower (GO: 0050819 negative regulation of coagulation; gene set length of 11) comparing wrapped with unwrapped and high flow to normal flow (see Supplementary Figs I to IV, online only).

Gene regulation during apoptosis of SMCs in vitro. A small number of genes are regulated in the same manner in the two models of vascular atrophy. Because cell death is a significant aspect of both of these models, it is possible that these genes are regulated as part of a cell death pathway. To explore this possibility, we studied the effect of FasL on gene expression; we have previously shown that FasL at this dose kills ~30% of baboon SMCs by 24 hours.[15] Of the seven upregulated genes, tissue plasminogen activator (*PLAT*), the prostaglandin transporter (*SLCO2A1*), *C8orf4*, and *LRRC8* were increased by FasL in vitro (Fig 3, *A-H*), but hyaluronidase 2 (*HYAL2*), Mustang 1 (*MUSTN1*), and ficolin 3 (*FCN3*) were not changed. We have previously reported that *ADAMTS4* mRNA is increased fivefold after FasL treatment.[15] As a positive control we showed that monocyte chemoattractant protein (MCP)-1, which is induced by FasL,[16] was also increased by FasL (27 ± 18-fold and 12 ± 6-fold of control at 6 and 24 hours, respectively; mean ± SD of two experiments).

The observation that only five of seven genes that were upregulated in vivo were also upregulated in the cultured SMC death model raised the possibility that these differences may result from the lack of endothelial cells or the lack of a physiologic ECM in the in vitro model of cell death. Therefore, we also studied the effect of a 6-hour treatment with FasL on the expression of the upregulated genes in cultured baboon arteries. In contrast with the cultured SMCs, FasL induced hyaluronidase 2 in the artery (Fig 4, *B*). Tissue plasminogen activator (*PLAT*), the prostaglandin transporter (*SLCO2A1*), *C8orf4*, and *ADAMTS4* were induced in the artery to a similar degree as observed in SMCs (Fig 4. *A, D, E,* and *H*). *FCN 3* and *MUSTN1* were not induced by FasL, and the modest stimulation of *LRRC8* was not statistically significant.

To determine whether blocking apoptosis would prevent induction of the atrophy-related genes by FasL, we used the pan-caspase inhibitor, Z-VAD. This series of experiments was performed with a different baboon SMC line than the one used for data presented in Fig 3. FasL induced the prostaglandin transporter (*SLCO2A1*), *C8orf4*, and *ADAMTS4*, but not *PLAT* and *LRRC8*. This is not surprising given the variability of gene induction also observed in vivo (Fig 2). The addition of 50 μmol Z-VAD completely blocked the production of floating SMCs by FasL at 24 hours, but Z-VAD did not inhibit FasL-mediated increases in *ADAMTS4*, *C8orf4*, and *SLCO2A1* (Table II).

DISCUSSION

We have demonstrated that only a small number of genes are upregulated in both nonhuman primate models of vascular atrophy, namely medial atrophy in the tightly wrapped iliac artery and neointimal atrophy in a PTFE graft subjected to a switch from normal to high blood flow. The comparison of two distinctly different models of atrophy, one caused by changes in shear stress and the other caused by changes in wall stress, was purposely used to narrow the results obtained from microarray analysis. We chose the 1-day time, at which time there is increased cell death and decreased cell proliferation in the PTFE graft model, but before large changes occur in the wall mass.[9] Because there is essentially no proliferation in the artery model, we expected that there might be changes in both models in genes related to cell death. Our results support the conclusion that these commonly regulated genes may play a fundamental role in vascular atrophy. In addition, the fact that six of the seven atrophy-associated genes are also induced by

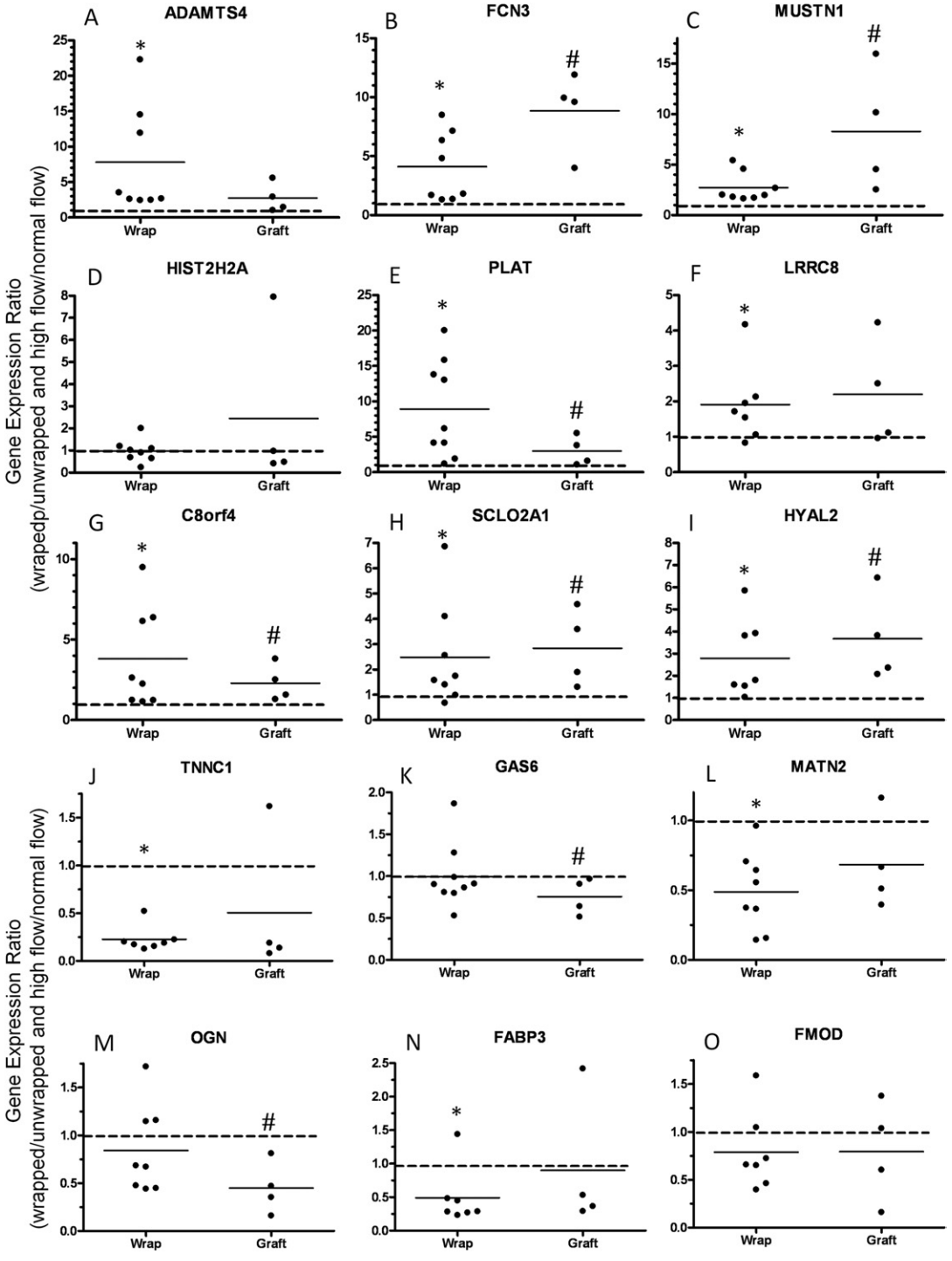

Fig 2. qRT-PCR of genes found by microarray analysis to be regulated in the PTFE wrap and PTFE graft models of vascular atrophy. **A,** *ADAMTS4* (see Kenagy et al[15] for graft data), **(B)** Ficolin 3 (*FCN3*), **(C)** Mustang 1 (*MUSTN1*), **(D)** Histone 2H2A (*HIST2H2A*), **(E)** tissue plasminogen activator (*PLAT*), **(F)** *LRRC8*, **(G)** *C8orf4* or TC1, **(H)** *SCLO2A1* or the prostaglandin transporter, PGT, **(I)** hyaluronidase 2 (*HYAL2*), **(J)** troponin C (*TNNC1*), **(K)** GAS6, **(L)** matrilin 2 (*MATN2*), **(M)** osteoglycin (*OGN*), **(N)** fatty acid binding protein 3 (*FABP3*), and **(O)** fibromodulin (*FMOD*). Each point represents a triplicate determination of paired samples of RNA from an individual animal's iliac arteries or PTFE graft intimas. Values are expressed as the ratio of wrapped/unwrapped or high blood flow/normal blood flow. The *dotted line* represents a ratio of 1, and the *solid line* shows the mean value. $^{*}P < .02$; $^{\#}P = .063$.

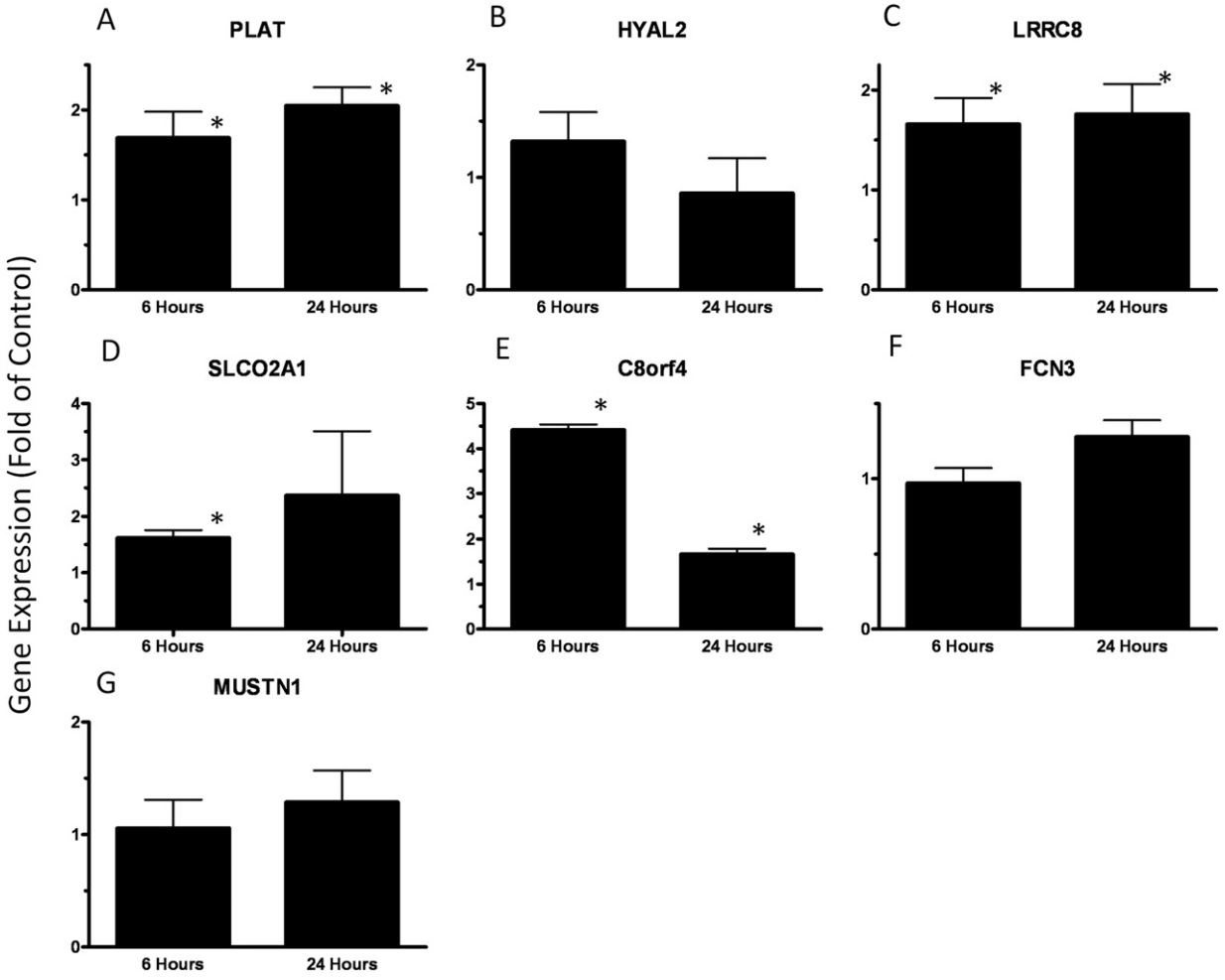

Fig 3. The effect of FasL on expression of **(A)** tissue plasminogen activator (*PLAT*), **(B)** hyaluronidase2 (*HYAL2*), **(C)** *LRRC8*, **(D)** prostaglandin transporter (*SLCO2A1*), **(E)** *C8orf4* (TC-1), **(F)** ficolin 3 (*FCN3*), and **(G)** Mustang 1 (*MUSTN1*) in cultured smooth muscle cells expressed as fold of 6- or 24-hour control. $*P < .05$ vs control; mean ± SEM of 3 experiments.

the ligand for the death receptor Fas further suggests that these genes are an important part of the vascular cell death program. These ideas are supported by the observation that ficolin 3 binds to and mediates the uptake of apoptotic cells by macrophages.[17] Although there are few macrophages in the regressing tissue in the baboon atrophy models,[7,8] SMCs also can phagocytose dead cells.[18] Also, one-third of the upregulated genes degrade components of the ECM, loss of which is a major feature of vascular atrophy. For example, the ECM constitutes ~80% of neointimal volume,[6,19] and loss of cross sectional area at 4 days in both models occurs with no change in nuclear density, consistent with a loss of ECM along with cells. Although there is a preferential loss of versican in the PTFE graft ECM, components of the ECM appear to be lost proportionately in the wrapped arteries.[8,20]

Tissue plasminogen activator activates plasminogen to plasmin, and plasmin degrades numerous ECM components and can also activate some matrix-degrading matrix metalloproteinase (MMP) family members.[21,22] Hyaluronidase 2 degrades the promigratory and proproliferative ECM that hyaluronan forms with versican,[23] and it also generates ~20-kDa fragments of hyaluronan that may induce MCP-1 and other inflammatory factors.[24,25] ADAMTS4 can degrade a number of ECM proteins, including versican, aggrecan, biglycan, matrilins, and brevican.[26-30]

Cell death and ECM degradation. Our data add to the literature linking cell death to enzymatic degradation of ECM. Several classes of proteases are increased in dying cells[31-34] and may be responsible for maintaining the cell-ECM balance by removing the ECM associated with dying cells. They can also cause cell death via reduction of matrix/cell attachment factors required for viability. For example, Leskinen et al[35] reported that chymase causes SMC death by degrading the integrin-binding matrix factor, fibronectin. Of particular relevance to our study, plasmin generated

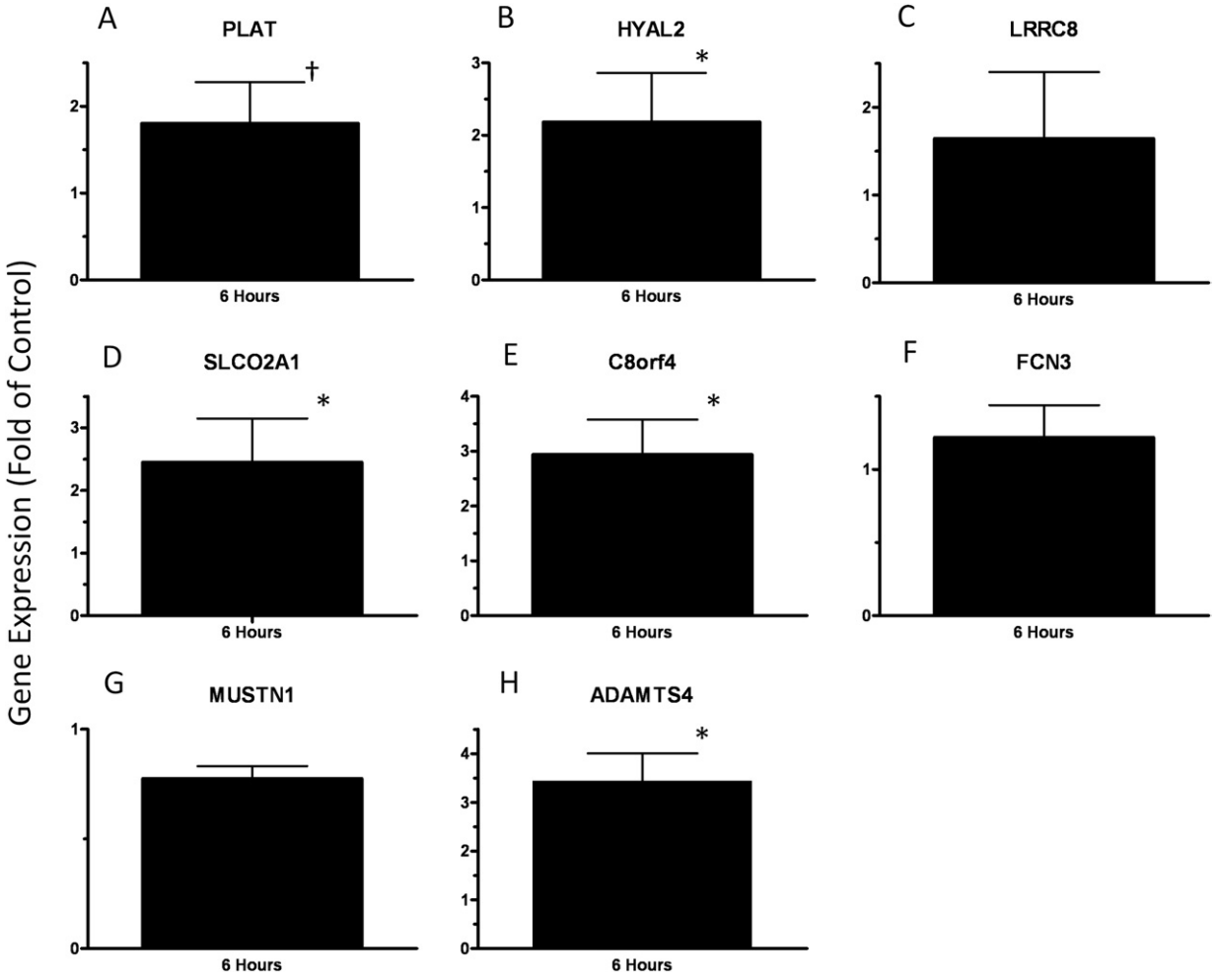

Fig 4. The effect of FasL on expression of **(A)** tissue plasminogen activator (*PLAT*), **(B)** hyaluronidase2 (*HYAL2*), **(C)** *LRRC8*, **(D)** prostaglandin transporter (*SLCO2A1*), **(E)** *C8orf4* (TC-1), **(F)** ficolin 3 (*FCN3*), **(G)** Mustang 1 (*MUSTN1*), **(H)** *ADAMTS4* in arterial organ culture expressed as fold of control. * $P < .05$ vs control; † $P = .06$; mean ± standard error of the mean of 3 to 4 experiments.

Table II. Effect of Z-VAD on FasL-induced gene expression and number of floating smooth muscle cells (*SMC*)

Gene	*FasL*	*FasL + ZVAD*
ADAMTS4	2.19 ± 0.54	2.09 ± 0.53
C8orf4	3.28 ± 0.67	3.58 ± 0.51
LRRC8	1.23 ± 0.25	1.44 ± 0.17
PLAT	0.66 ± 0.14	0.73 ± 0.15
SLCO2A1	2.50 ± 0.46	4.52 ± 1.02
Floating SMCs	12.0 ± 4.3	0.2 ± 0.1

Values are expressed as the fold of control (mean ± SEM of 3 experiments).

from plasminogen by tissue plasminogen activator can cause SMC death.[36] Because tissue plasminogen activator is induced by FasL, it may be involved in a positive feedback loop to facilitate cell death. In addition, it is intriguing that tissue plasminogen activator inhibits the accumulation of intimal SMCs and causes positive arterial remodeling after carotid artery injury.[37]

With regards to ADAMTS4, SMC death and ADAMTS4 are both increased in the PTFE graft neointima 1 day after the switch to high blood flow,[7,15] and dying intimal SMCs express ADAMTS4.[15] Furthermore, we have shown that ADAMTS4 cleaves versican, a major constituent of graft neointima.[15,26] The cleavage fragments of versican may be important during neointimal atrophy.[38] This has been shown recently for regression of cardiac outflow tract and interdigital tissue in the mouse.[39,40] ADAMTS5, -9, and -20 cooperatively clip versican at the Glu-441-Ala-442 bond (the same bond cleaved by ADAMTS4[26]) and generate an N-terminal fragment that increases apoptosis in interdigital web cells. Threshold levels of the versican N-terminal fragment may be required for tissue regression.

Potential functions of other atrophy-associated genes. The function of the other upregulated gene products associated with atrophy is less clear. SLCO2A1 (PGT) transports prostaglandins into cells where they can be degraded.[41,42] Prostaglandins of the D, E, and F series are transported at a high rate, thromboxane at an intermediate rate, and prostacyclin analogs at a low rate.[43,44] Because SMCs have been reported to synthesize PGE_2, PGI_2, and PGD_2,[45-48] increased SLCO2A1 might be expected to have the greatest impact on reducing local levels of PGE_2 and PGD_2, which use the receptors, EP_1 through EP_4 and DP_1 and DP_2, respectively. Although prostaglandin receptor expression has not been measured in these atrophy models and these receptors can mediate opposite effects (eg, PGE_2 receptors EP_1 and EP_3 induce vasoconstriction, whereas EP_2 and EP_4 induce vasodilatation[49]), it is of interest that EP_4 appears to mediate intimal hyperplasia. Activation of EP_4 increases ductus intimal cushion formation,[50] and PGE_2 may also activate the thromboxane receptor,[51,52] knockout of which leads to decreased neointima formation after arterial injury.[53] These data suggest the possibility that SLCO2A1-mediated loss of local PGE_2 might remove a pro-proliferative signal. *C8orf4*, which is overexpressed in thyroid and breast cancers,[54,55] causes anchorage-independent growth when overexpressed in immortalized epithelial cells,[56] to mediate interleukin-1β–induced proliferation of a dendritic-like cell line,[57] and to inhibit Chibby,[58] a negative regulator of β-catenin signaling, which stimulates SMC proliferation and inhibits cell death.[59,60]

Musculoskeletal embryonic nuclear protein 1 (MUSTN1) is required for differentiation of chondrocytes and myoblasts.[61,62] Whether MUSTN1 affects SMC differentiation is uncertain. Message levels of SMC differentiation genes such as SM22α (*TAGLN*), smoothelin (*SMTN*), desmin (*DES*), and calponin (*CNN1*) are decreased in the wrap model, but not in the graft neointima. Other smooth muscle differentiation genes, such as smooth muscle myosin heavy chain, smooth muscle α-actin (*ACTA2*), and caldesmon, are not altered in either model (Supplementary Tables I and II, online only). Finally, LRRC8, a putative four-pass transmembrane protein with many leucine-rich repeats in the extracellular domain, is required for B-cell development.[63] Thus, tissue plasminogen activator, SLOC2A1, and MUSTN1 may provide antiproliferative and prodifferentiation functions, and C8orf4 may be a counter-regulatory factor to moderate cell death.

Potential role of FasL in vivo. How cell death and gene expression are regulated during vascular atrophy is not evident. Nevertheless, FasL/Fas interactions mediate SMC apoptosis during spiral artery remodeling, after arterial injury, and after increased shear stress in vitro.[64-66] This pathway may be operative in the baboon models, because shear stress may be increased in the tightly wrapped artery as well as in the PTFE graft. Further, FasL induces six of the seven atrophy-associated upregulated genes in cultured SMCs and arteries (Figs 3 and 4). The observation that activation of Fas in apoptosis-resistant cells increases MMP2 and MMP9 in a caspase-independent manner[67] also links Fas activation to the baboon atrophy models, because baboon SMCs are apoptosis resistant (ie, cycloheximide is required with FasL for killing), and we have previously reported that levels of MMP2 and MMP9 are increased after 7 days of high blood flow in the PTFE graft model.[68]

The in vitro data indicate that FasL-mediated atrophy gene induction is independent of caspase-induced cell death (Table II), suggesting the possibility that a signaling cascade observed in glioblastoma cells that consists of an src kinase, PI3K, and PKB may be involved.[67] FasL also induces MCP-1 in SMCs in vitro (our results and Schaub et al[16]), and increased blood flow increases MCP-1 in the PTFE graft model after 4 days (online Table 8C in Hsieh et al[9]), but not after 1 day (Supplementary Tables I and II, online only). In addition, induction of MCP-1 is partially mediated by IL-1α (Schaub et al[16]), which also induces ADAMTS4 and hyaluronidase 2.[69,70] These data suggest that a Fas/IL-1α pathway may be operative in vivo during atrophy and account for the upregulation of some of the atrophy-associated genes.

Vascular cells expressing atrophy-associated genes. Although the cells expressing atrophy-associated genes in vivo have not been determined, we have demonstrated that cultured SMCs regulate the expression of tissue plasminogen activator, LRRC8, SLCO2A1, C8orf4, and ADAMTS4. However, endothelial cells also express tissue plasminogen activator, SLCO2A1, ADAMTS4, hyaluronidase, and ficolin 3.[71,72] The endothelium is clearly the cell exposed to the greatest shear stress, and many genes have been reported to be regulated by shear stress, including tissue plasminogen activator. Our observation that hyaluronidase 2 was not increased in cultured SMCs, but was increased in the cultured artery, is consistent with endothelial cell expression of this gene.

CONCLUSIONS

Seven genes are upregulated in two distinctly different models of nonhuman primate vascular atrophy. Most of these genes are also upregulated during induction of cell death in vitro, including the ECM-degrading factors tissue plasminogen activator, ADAMTS4, and hyaluronidase-2. Further studies are required to determine the specific roles of these and the other atrophy-associated gene products and their suitability as therapeutic targets to induce vascular atrophy in established restenotic disease.

We thank the staff of the Washington National Primate Research Center for their assistance with animal surgery and care. We thank Lynn Amon, PhD, for normalization and quality analysis of microarray data; Richard Beyer, PhD, for the gene set analysis; Steve Schwartz, MD, PhD, for helpful discussion; and Lihua Chen, PhD, for technical help with microarrays. We also thank Olivier Defawe and Suzanne Justice for assistance with the baboon operations and tissue processing.

AUTHOR CONTRIBUTIONS

Conception and design: RK, AC
Analysis and interpretation: RK, SM, AC
Data collection: RK, SM, EM
Writing the article: RK
Critical revision of the article: RK, SM, EM, AC
Final approval of the article: RK, SM, EM, AC
Statistical analysis: RK
Obtained funding: RK, AC
Overall responsibility: AC
RK and SM contributed equally to this work.

REFERENCES

1. Min SK, Kenagy RD, Clowes AW. Induction of vascular atrophy as a novel approach to treating restenosis. A review. J Vasc Surg 2008;47: 662-70.
2. Finn AV, Gold HK, Tang A, Weber DK, Wight TN, Clermont A, et al. A novel rat model of carotid artery stenting for the understanding of restenosis in metabolic diseases. J Vasc Res 2002;39:414-25.
3. Kim WH, Hong MK, Virmani R, Kornowski R, Jones R, Leon MB. Histopathologic analysis of in-stent neointimal regression in a porcine coronary model. Coron Artery Dis 2000;11:273-7.
4. Kuroda N, Kobayashi Y, Nameki M, Kuriyama N, Kinoshita T, Okuno T, et al. Intimal hyperplasia regression from 6 to 12 months after stenting. Am J Cardiol 2002;89:869-72.
5. Asakura M, Ueda Y, Nanto S, Hirayama A, Adachi T, Kitakaze M, et al. Remodeling of in-stent neointima, which became thinner and transparent over 3 years − Serial angiographic and angioscopic follow-up. Circulation 1998;97:2003-6.
6. Mattsson EJ, Kohler TR, Vergel SM, Clowes AW. Increased blood flow induces regression of intimal hyperplasia. Arterioscler Thromb Vasc Biol 1997;17:2245-9.
7. Berceli SA, Davies MG, Kenagy RD, Clowes AW. Flow-induced neointimal regression in baboon polytetrafluoroethylene grafts is associated with decreased cell proliferation and increased apoptosis. J Vasc Surg 2002;36:1248-55.
8. Min SK, Kenagy RD, Jeanette JP, Clowes AW. Effects of external wrapping and increased blood flow on atrophy of the baboon iliac artery. J Vasc Surg 2008;47:1039-47.
9. Hsieh PCH, Kenagy RD, Mulvihill ER, Jeanette JP, Wang X, Chang CMC, et al. Bone morphogenetic protein 4: Potential regulator of shear stress-induced graft neointimal atrophy. J Vasc Surg 2006;43:150-8.
10. Mattsson EJR, Kohler TR, Vergel SM, Clowes AW. Increased blood flow induces regression of intimal hyperplasia. Arterioscler Thromb Vascul Biol 1997;17:2245-9.
11. Chen L, Daum G, Forough R, Clowes M, Walter U, Clowes AW. Overexpression of human endothelial nitric oxide synthase in rat vascular smooth muscle cells and in balloon-injured carotid artery. Circ Res 1998;82:862-70.
12. Tusher VG, Tibshirani R, Chu G. Significance analysis of microarrays applied to the ionizing radiation response. Proc Natl Acad Sci U S A 2001;98:5116-21.
13. Subramanian A, Tamayo P, Mootha VK, Mukherjee S, Ebert BL, Gillette MA, et al. Gene set enrichment analysis: A knowledge-based approach for interpreting genome-wide expression profiles. Proc Natl Ac Sc U S A 2005;102:15545-50.
14. Efron B, Tibshirani R. On testing the significance of sets of genes. Ann Appl Stat 2007;1:107-29.
15. Kenagy RD, Min S-K, Clowes AW, Sandy JD. Cell death-associated ADAMTS4 and versican degradation in vascular tissue. J Histochem Cytochem 2009;57:889-97.
16. Schaub FJ, Han DK, Liles WC, Adams LD, Coats SA, Ramachandran RK, et al. Fas/FADD-mediated activation of a specific program of inflammatory gene expression in vascular smooth muscle cells. Nat Med 2000;6:790-6.
17. Honore C, Hummelshoj T, Hansen BE, Madsen HO, Eggleton P, Garred P. The innate immune component ficolin 3 (Hakata antigen) mediates the clearance of late apoptotic cells. Arthritis Rheum 2007;56:1598-607.
18. Fries DM, Lightfoot R, Koval M, Ischiropoulos H. Autologous apoptotic cell engulfment stimulates chemokine secretion by vascular smooth muscle cells. Am J Pathol 2005;167:345-53.
19. Clowes AW, Reidy MA, Clowes MM. Mechanisms of stenosis after arterial injury. Lab Invest 1983;49:208-15.
20. Kenagy RD, Fischer JW, Lara S, Sandy JD, Clowes AW, Wight TN. Accumulation and loss of extracellular matrix during shear stress-mediated intimal growth and regression in baboon vascular grafts. J Histochem Cytochem 2005;53:131-40.
21. Hu JH, Du L, Chu T, Otsuka G, Dronadula N, Jaffe M, et al. Overexpression of urokinase by plaque macrophages causes histological features of plaque rupture and increases vascular matrix metalloproteinase activity in aged apolipoprotein E-null mice. Circulation 2010;121: 1637-44.
22. Plow EF, Hoover-Plow J. The functions of plasminogen in cardiovascular disease. Trends Cardiovas Med 2004;14(5):180-6.
23. Evanko SP, Angello JC, Wight TN. Formation of hyaluronan- and versican-rich pericellular matrix is required for proliferation and migration of vascular smooth muscle cells. Arterioscler Thromb Vasc Biol 1999;19:1004-13.
24. de la Motte C, Nigro J, Vasanji A, Rho H, Kessler S, Bandyopadhyay S, et al. Platelet-derived hyaluronidase 2 Cleaves hyaluronan into Fragments that Trigger monocyte-mediated production of proinflammatory cytokines. Am J Pathol 2009;174:2254-64.
25. Jiang D, Liang J, Noble PW. Hyaluronan in tissue injury and repair. Annu Revs Cell Dev Biol 2007;23:435-61.
26. Sandy JD, Westling J, Kenagy RD, Iruela-Arispe ML, Verscharen C, Rodriguez-Mazaneque JC, et al. Versican V1 proteolysis in human aorta in vivo occurs at the Glu 441 -Ala 442 bond, a site that is cleaved by recombinant ADAMTS-1 and ADAMTS-4. J Biol Chem 2001;276: 13372-8.
27. Frank JE, Thompson VP, Brown MP, Sandy JD. Removal of O-linked and N-linked oligosaccharides is required for optimum detection of NITEGE neoepitope on ADAMTS4-digested fetal aggrecans: implications for specific N-linked glycan-dependent aggrecanolysis at Glu373–Ala374. Osteoarthritis Cartilage 2009;17:777-81.
28. Nakamura H, Fujii Y, Inoki I, Sugimoto K, Tanzawa K, Matsuki H, et al. Brevican is degraded by matrix metalloproteinases and aggrecanase-1 (ADAMTS4) at different sites. J Biol Chim 2000;275:38885-90.
29. Klatt AR, Klinger G, Paul-Klausch B, Kuhn G, Renno JH, Wagener R, et al. Matrilin-3 activates the expression of osteoarthritis-associated genes in primary human chondrocytes. FEBS Lett 2009;583:3611-7.
30. Melching LI, Fisher WD, Lee ER, Mort JS, Roughley PJ. The cleavage of biglycan by aggrecanases. Osteoarthritis Cartilage 2006;14:1147-54.
31. Piva TJ, Davern CM, Francis KG, Chojnowski GM, Hall PM, Ellem KA. Increased ecto-metallopeptidase activity in cells undergoing apoptosis. J Cell Biochem 2000;76:625-38.
32. Cowan KN, Leung WCY, Mar C, Bhattacharjee R, Zhu YH, Rabinovitch M. Caspases from apoptotic myocytes degrade extracellular matrix: a novel remodeling paradigm. FASEB J 2005:19:1848-50.
33. O'Mullane MJ, Baker MS. Loss of cell viability dramatically elevates cell surface plasminogen binding and activation. Exp Cell Res 1998;242: 153-64.
34. Levkau B, Kenagy RD, Karsan A, Weitkamp B, Clowes AW, Ross R, et al. Activation of metalloproteinases and their association with integrins: an auxiliary apoptotic pathway in human endothelial cells. Cell Death Differ 2002;9:1360-7.
35. Leskinen MJ, Lindstedt KA, Wang Y, Kovanen PT. Mast cell chymase induces smooth muscle cell apoptosis by a mechanism involving fibronectin degradation and disruption of focal adhesions. Arterioscler Thromb Vasc Biol 2003;23:238-43.
36. Meilhac O, Ho-Tin-Noe B, Houard X, Philippe M, Michel JB, Angles-Cano E. Pericellular plasmin induces smooth muscle cell anoikis. FASEB J 2003;17:1301-3.
37. Parfyonova Y, Plekhanova O, Solomatina M, Naumov V, Bobik A, Berk B, et al. Contrasting effects of urokinase and tissue-type plasminogen activators on neointima formation and vessel remodelling after arterial injury. J Vasc Res 2004;41:268-76.

38. Kenagy RD, Plaas AH, Wight TN. Versican degradation and vascular disease. Trends Cardiovasc Med 2006;16:209-15.
39. Kern CB, Norris RA, Thompson RP, Argraves WS, Fairey SE, Reyes L, et al. Versican proteolysis mediates myocardial regression during outflow tract development. Dev Dynam 2007;236:671-83.
40. McCulloch DR, Nelson CM, Dixon LJ, Silver DL, Wylie JD, Lindner V, et al. ADAMTS metalloproteases generate active versican fragments that regulate interdigital web regression. Dev Cell 2009;17:687-98.
41. Nomura T, Lu R, Pucci ML, Schuster VL. The two-step model of prostaglandin signal termination: in vitro reconstitution with the prostaglandin transporter and prostaglandin 15 dehydrogenase. Mol Pharmacol 2004;65:973-8.
42. Chang H-Y, Locker J, Lu R, Schuster VL. Failure of postnatal ductus arteriosus closure in prostaglandin transporter-deficient mice. Circulation 2010;121:529-36.
43. Kanai N, Lu R, Satriano JA, Bao Y, Wolkoff AW, Schuster VL. Identification and characterization of a prostaglandin transporter. Science 1995;268:866-9.
44. Lu R, Kanai N, Bao Y, Schuster VL. Cloning, in vitro expression, and tissue distribution of a human prostaglandin transporter cDNA(hPGT). J Clin Invest 1996;98:1142-9.
45. Okahara K, Sun B, Kambayashi J. Upregulation of prostacyclin synthesis–related gene expression by shear stress in vascular endothelial Cells. Arterioscler Thromb Vasc Biol 1998;18:1922-6.
46. Bishop-Bailey D, Pepper JR, Larkin SW, Mitchell JA. Differential induction of cyclooxygenase-2 in human arterial and venous smooth muscle--role of endogenous prostanoids. Arterioscler Thromb Vasc Biol 1998;18:1655-61.
47. Bishop-Bailey D, Warner TD. PPARgamma; ligands induce prostaglandin production in vascular smooth muscle cells: indomethacin acts as a peroxisome proliferator-activated receptor-γ antagonist. FASEB J. 2003;17:1925-7.
48. Bayston T, Ramessur S, Reise J, Jones KG, Powell JT. Prostaglandin E2 receptors in abdominal aortic aneurysm and human aortic smooth muscle cells. J Vasc Surg 2003;38:354-9.
49. Norel X. Prostanoid receptors in the human vascular wall. ScientificWorldJournal 2007;7:1359-74.
50. Yokoyama U, Minamisawa S, Quan H, Akaike T, Jin M, Otsu K, et al. Epac1 is upregulated during neointima formation and promotes vascular smooth muscle cell migration. Am J Physiol Heart Circ Physiol 2008;295:H1547-55.
51. Boersma JI, Janzen KM, Oliveira L, Crankshaw DJ. Characterization of excitatory prostanoid receptors in the human umbilical artery in vitro. Br J Pharmacol 1999;128:1505-12.
52. Davis RJ, Murdoch CE, Ali M, Purbrick S, Ravid R, Baxter GS, et al. EP4 prostanoid receptor-mediated vasodilatation of human middle cerebral arteries. Br J Pharmacol 2004;141:580-5.
53. Cheng Y, Austin SC, Rocca B, Koller BH, Coffman TM, Grosser T, et al. Role of prostacyclin in the cardiovascular response to thromboxane A2. Science 2002;296:539-41.
54. Chua EL, Young L, Wu WM, Turtle JR, Dong Q. Cloning of TC-1 (C8orf4), a novel gene found to be overexpressed in thyroid cancer. Genomic 2000;69:342-7.
55. Sunde M, McGrath KC, Young L, Matthews JM, Chua EL, Mackay JP, et al. TC-1 is a novel tumorigenic and natively disordered protein associated with thyroid cancer. Cancer Res 2004;64:2766-73.
56. Yang ZQ, Streicher KL, Ray ME, Abrams J, Ethier SP. Multiple interacting oncogenes on the 8p11-p12 amplicon in human breast cancer. Cancer Res 2006;66:11632-43.
57. Kim Y, Kim J, Park J, Bang S, Jung Y, Choe J, et al. TC1(C8orf4) is upregulated by IL-1beta/TNF-alpha and enhances proliferation of human follicular dendritic cells. FEBS Lett 2006;580:3519-24.
58. Jung Y, Bang S, Choi K, Kim E, Kim Y, Kim J, et al. TC1 (C8orf4) enhances the Wnt/beta-catenin pathway by relieving antagonistic activity of Chibby. Cancer Res 2006;66:723-8.
59. Ezan J, Leroux L, Barandon L, Dufourcq P, Jaspard B, Moreau C, et al. FrzA/sFRP-1, a secreted antagonist of the Wnt-Frizzled pathway, controls vascular cell proliferation in vitro and in vivo. Cardiovasc Res 2004;63:731-8.
60. Wang X, Xiao Y, Mou Y, Zhao Y, Blankesteijn WM, Hall JL. A role for the beta-catenin/T-cell factor signaling cascade in vascular remodeling. Circ Res 2002;90:340-7.
61. Gersch RP, Hadjiargyrou M. Mustn1 is expressed during chondrogenesis and is necessary for chondrocyte proliferation and differentiation in vitro. Bone 2009;45:330-8.
62. Liu C, Gersch RP, Hawke TJ, Hadjiargyrou M. Silencing of Mustn1 inhibits myogenic fusion and differentiation. Am J Physiol Cell Physiol 2010;298:C1100-8.
63. Sawada A, Takihara Y, Kim JY, Matsuda-Hashii Y, Tokimasa S, Fujisaki H, et al. A congenital mutation of the novel gene LRRC8 causes agammaglobulinemia in humans. J Clin Invest 2003;112:1707-13.
64. Matter CM, Chadjichristos CE, Meier P, von Lukowicz T, Lohmann C, Schuler PK, et al. Role of endogenous Fas (CD95/Apo-1) ligand in balloon-induced apoptosis, inflammation, and neointima formation. Circulation 2006;113:1879-87.
65. Harris LK. Review: trophoblast-vascular cell interactions in early pregnancy: how to remodel a vessel. Placenta 2010;31(suppl 1):S93-S8.
66. Apenberg S, Freyberg MA, Friedl P. Shear stress induces apoptosis in vascular smooth muscle cells via an autocrine Fas/FasL pathway. Biochim Biophys Res Commun 2003;310:355-9.
67. Kleber S, Sancho-Martinez I, Wiestler B, Beisel A, Gieffers C, Hill O, et al. Yes and PI3K Bind CD95 to Signal Invasion of Glioblastoma. Cancer Cell 2008;13:235-48.
68. Kenagy RD, Fischer JW, Davies MG, Berceli SA, Hawkins SM, Wight TN, et al. Increased plasmin and serine proteinase activity during flow-induced intimal atrophy in baboon PTFE grafts. Arterioscler Thromb Vasc Biol 2002;22:400-4.
69. Patwari P, Gao G, Lee JH, Grodzinsky AJ, Sandy JD. Analysis of ADAMTS4 and MT4-MMP indicates that both are involved in aggrecanolysis in interleukin-1-treated bovine cartilage. Osteoarthritis Cartilage 2005;13:269-77.
70. Tanimoto K, Yanagida T, Tanne Y, Kamiya T, Huang Y, Mitsuyoshi T, et al. Modulation of hyaluronan fragmentation by interleukin-1beta in synovial membrane cells. Ann Biomed Eng 2010;38:1618-25.
71. Ni C-W, Qiu H, Rezvan A, Kwon K, Nam D, Son DJ, et al. Discovery of novel mechanosensitive genes in vivo using mouse carotid artery endothelium exposed to disturbed flow. Blood 2010;116:e66-e73.
72. Bhasin M, Yuan L, Keskin D, Otu H, Libermann T, Oettgen P. Bioinformatic identification and characterization of human endothelial cell-restricted genes. BMC Genomics 2010;11:342.

Submitted Jul 14, 2010; accepted Dec 11, 2010.

Additional material for this article may be found online at www.jvascsurg.org.

Supplementary Table I. Genes significantly changed by a tight PTFE wrap. Data were analyzed by Significance Analysis of Microarrays (SAM) software with a false discovery rate of <1.0%.

Current settings

Input parameters

Data type?	Two class paired
Arrays centered?	FALSE
Delta	0.897748
Minimum fold change	0
Test statistic	standard
Are data are log scale?	TRUE
Number of permutations	200
Input percentile for exchangeability factor s0	Automatic choice
Number of neighbors for KNN	10
Seed for Random number generator	1234567

Computed values

Estimate of pi0 (proportion of null genes)	0.861368
Exchangibility factor s0	0.433852
s0 percentile	94.99788
False Discovery Rate (%)	0.955896

List of Significant Genes for Delta = 0.898

Positive genes (404)

Row	Gene ID	Gene Name	Score(d)	Numerator(r)	Denominator(s+s0)	Fold Change	q-value(%)
3080	IL6	NM_000600	8.05503637	3.960698155	0.491704565	11.6022788	0
7305	CHI3L1	NM_001276	6.504848601	3.628452155	0.557807318	4.382504952	0
1842	LIF	NM_002309	6.627183826	3.444769757	0.519793905	4.038447902	0
1406	SOD2	NM_000636	6.685035965	3.432563448	0.513469705	3.892974414	0
20626	SERPINA3	NM_001085	6.535787126	3.423800934	0.523854414	3.592661093	0
10924	RGS16	NM_002928	6.542959447	3.304150906	0.504993334	3.491787206	0
18942	CEBPD	NM_005195	6.160274418	3.336720022	0.541651199	3.302607993	0
1275	IER3	NM_003897	6.646385856	3.245856267	0.488364103	3.047166687	0
16839	CRISPLD2	NM_031476	3.527646966	2.849376843	0.807727324	3.026844904	0
6732	NA	XM_046677	6.770435025	3.236786462	0.478076586	2.998249951	0
22591	ADAMTS4	NM_005099	6.181779994	3.155374975	0.510431458	2.934950082	0
15553	SDC4	NM_002999	6.249794184	3.168318563	0.506947664	2.884401449	0
1525	MT1X	NM_005952	5.787120875	3.119066914	0.538966955	2.861967697	0
12867	MT1H	NM_005951	4.925269449	3.034565749	0.616121774	2.705572645	0
4745	FBXO32	NM_148177	6.07199422	3.131017002	0.515648877	2.681647287	0
6887	CHI3L2	NM_004000	5.582694346	3.027919492	0.542376011	2.620409164	0
628	TNFAIP6	NM_007115	4.71230448	2.901780041	0.615787892	2.512983372	0
479	NMB	NM_021077	6.354657469	3.093453791	0.486801028	2.437244329	0
23486	IRF1	NM_002198	2.534472688	2.253454545	0.889121653	2.424617116	0
20557	CFB	NM_001710	5.321165089	2.935271202	0.551621901	2.37109848	0
14438	KCNJ8	NM_004982	5.370301222	2.97695568	0.554336816	2.324412578	0
15441	GBP1	NM_002053	4.15185152	2.67476656	0.644234638	2.319199779	0
19498	ABCA1	NM_005502	3.185117584	2.649460473	0.831825012	2.3170094	0
21408	NA	XM_370714	4.625624639	2.796151957	0.604491755	2.261309325	0
12246	IFITM3	NM_021034	5.282863554	2.91812612	0.552375826	2.220020914	0
7148	BHLHB2	NM_003670	5.701348458	2.885410889	0.506092709	2.214963541	0
16213	NA	NM_020249	2.557632107	2.207103503	0.862947997	2.210982446	0
17467	TFPI	NM_006287	5.679821392	2.978212417	0.52434966	2.186206415	0
55	MT1M	NM_176870	4.505535902	2.78169912	0.617395839	2.179973339	0
13972	IL11	NM_000641	2.132984813	2.196222043	1.029647295	2.179888971	0.447851889
18297	CARD15	NM_022162	4.018753439	2.681531122	0.667254452	2.174138971	0
15345	PDGFRB	NM_002609	6.105913744	2.942744347	0.481949872	2.137797064	0
6417	CP	NM_000096	2.034474923	2.020836811	0.993296496	2.10147135	0.575952169
7812	RGS2	NM_002923	3.29416482	2.299538657	0.698064238	2.072762926	0
4186	FBXO32	NM_058229	4.423184944	2.731664948	0.617578732	2.070524828	0
6037	NA	XM_351747	4.017861785	2.768635752	0.68908188	2.066885323	0
23043	ADH1C	NM_000669	4.595774279	2.760173216	0.600589378	2.061790114	0
16488	MYBPH	NM_004997	4.454145242	2.708390008	0.608060551	2.032512621	0
14195	STC1	NM_003155	3.894942729	2.535618779	0.65100284	2.021201265	0
13404	TSC22D1	NM_006022	4.186840923	2.722543825	0.650262065	2.007731959	0
2839	FCN3	NM_173452	3.199316919	2.435382558	0.761219541	1.995830085	0
3209	MUSTN1	NM_205853	3.147917666	2.460322605	0.78157146	1.976907771	0
4957	THBD	NM_000361	4.00261103	2.554811152	0.638286142	1.967182554	0
883	TSHZ1	NM_005786	4.908858764	2.753347734	0.560893655	1.960785125	0
21722	EFNA1	NM_182685	5.250933171	2.740211652	0.521852319	1.954809961	0
19983	RGMA	NM_020211	5.241414009	2.8034725	0.534869502	1.944065184	0
2727	CEBPB	NM_005194	5.593524108	2.756465544	0.492795864	1.937345895	0
2378	TDO2	NM_005651	2.226916392	2.082080819	0.934961378	1.916730191	0.320211326
8814	CHRDL2	NM_015424	4.628210779	2.680812378	0.579232992	1.911958134	0
6043	TRIM8	NM_030912	4.536560276	2.66315167	0.587042056	1.883713333	0
16245	TRIB1	NM_025195	3.374917929	2.397157505	0.710286163	1.86738462	0
22024	DDIT4	NM_019058	2.611484009	2.111749772	0.808639748	1.858635663	0
18456	CDC42EP4	NM_012121	5.582565019	2.725253419	0.488172267	1.853092843	0
3212	VCAM1	NM_080682	3.164817314	2.262955784	0.715035201	1.84533239	0
10203	GPRC5C	NM_022036	4.947557655	2.689633179	0.543628466	1.84206633	0
18477	PSME2	NM_002818	2.268613356	1.971509426	0.869037212	1.82637451	0.172273693
22564	SLC25A28	NM_031212	4.508687753	2.587606441	0.573915645	1.826145878	0
1493	IL4R	NM_000418	4.208306656	2.468407326	0.586555954	1.790232908	0

Supplementary Table I. Continued

18237	FLJ20701	NM_017933	3.96348003	2.603835511	0.656956889	1.78101146	0
11523	SOX4	NM_003107	3.246248966	2.346538247	0.722846051	1.780708571	0
12170	UST	NM_005715	4.572483167	2.598718428	0.568338545	1.765231614	0
20944	GCH1	NM_000161	2.746635337	2.206826044	0.803465249	1.761576203	0
11822	HIST2H2AC	NM_003517	3.986911641	2.459129042	0.616800487	1.736723444	0
6506	CTNNB1	NM_001904	4.033469187	2.425424508	0.601324665	1.736546884	0
8325	RELB	NM_006509	3.804677959	2.489518526	0.654330945	1.735487343	0
8059	NA	XM_028067	3.012921663	2.233546754	0.741322545	1.732019285	0
1388	KIAA0999	NM_025164	4.913100322	2.577300196	0.524577156	1.730160256	0
17446	WTAP	NM_004906	4.21163376	2.48297793	0.589552195	1.729406133	0
16981	CITED4	NM_133467	3.928568404	2.499820219	0.636318364	1.725614724	0
6364	TP53BP2	NM_005426	4.375872016	2.560071106	0.5850425	1.724071783	0
16958	PTGS2	NM_000963	4.110364117	2.518191901	0.612644483	1.715876651	0
17351	TIPARP	NM_015508	3.454117475	2.264603566	0.655624362	1.707742332	0
17714	NA	XM_093799	4.483535085	2.539610243	0.566430327	1.70767984	0
19996	NA	XM_172855	4.706423922	2.588670911	0.550029269	1.699970459	0
7632	FTH1	NM_002032	2.43969713	2.193150188	0.898943628	1.690249732	0.172273693
22761	BCL3	NM_005178	4.206328604	2.442789675	0.580741522	1.689431211	0
11373	ChGn	NM_018371	4.111305436	2.454218103	0.596943755	1.680970472	0
6851	PEG3	NM_006210	3.927708375	2.436514805	0.620340049	1.677970218	0
21727	STAT3	NM_003150	4.520283658	2.465779905	0.545492295	1.672622746	0
9259	PLAT	NM_000931	4.637289702	2.526800923	0.544887442	1.664061414	0
1659	KLF4	NM_004235	3.84540975	2.373385505	0.617199638	1.655778812	0
9582	NA	XM_034000	2.847292013	2.128818554	0.747664287	1.646029212	0
6509	HIST1H1C	NM_005319	3.761896129	2.467624598	0.655952348	1.639469656	0
3202	SQRDL	NM_021199	5.161946421	2.545054827	0.493041698	1.637823346	0
2341	C1QTNF1	NM_198593	2.388717028	2.04087632	0.854381786	1.636798181	0.172273693
21017	NA	XM_054983	3.706847028	2.391733671	0.645220494	1.635946048	0
3652	BTG2	NM_006763	3.343325522	2.280836684	0.682205986	1.634085678	0
22889	NR4A2	NM_173173	1.916696433	1.842337812	0.9612048	1.633483556	0.841180142
17211	CAST	NM_001750	2.813869334	2.010271897	0.71441551	1.631441359	0
21029	KLF9	NM_001206	3.882774702	2.327386475	0.599413217	1.630486043	0
10067	IGFBP4	NM_001552	4.007261982	2.37095271	0.591664014	1.626202558	0
17531	NA	XM_026998	4.433621327	2.417336624	0.545228482	1.625052899	0
4509	GSC	NM_173849	4.024976842	2.417084387	0.600521315	1.617845842	0
1585	TCF4	NM_003199	3.785061549	2.287814966	0.604432699	1.604962497	0
460	FZD8	NM_031866	3.119352479	2.167326147	0.694800014	1.600818932	0
1706	SNF1LK	NM_173354	2.964960995	2.052118302	0.692123204	1.586553249	0
6469	HIST2H2AA	NM_003516	4.073646734	2.419294144	0.593889039	1.585351611	0
22818	PAPPA	NM_002581	4.102773253	2.38862041	0.582196544	1.584120138	0
20142	LOC387763	XM_373497	4.024531799	2.438877327	0.606002747	1.575585666	0
17480	MSC	NM_005098	3.58285438	2.218375185	0.619164205	1.568984854	0
8995	ZC3H12A	NM_025079	3.828363516	2.258357208	0.589901455	1.564400295	0
290	CCL7	NM_006273	2.338342253	1.841591396	0.78756281	1.562458281	0.172273693
16924	NFIL3	NM_005384	2.257454083	1.801855801	0.798180488	1.560791699	0.320211326
20289	RANBP9	NM_005493	2.867944088	2.117551827	0.738351852	1.558916153	0
13817	C1R	NM_001733	3.03035237	2.127083586	0.701926155	1.557731669	0
18701	FASN	NM_004104	3.768120391	2.358014851	0.625780125	1.547236552	0
3531	C1S	NM_001734	2.601220652	1.90996416	0.73425688	1.546115417	0
10184	PDZK1IP1	NM_005764	3.029641723	2.11893536	0.6994013	1.540828924	0
20121	ULK1	NM_003565	2.244574475	1.952515555	0.869882277	1.530271554	0.320211326
2217	VASN	NM_138440	3.983584828	2.319919922	0.582369906	1.529300347	0
8756	SNTB2	NM_130845	2.714209578	2.028188271	0.747248218	1.528427736	0
21748	NA	XM_375850	3.957247333	2.301531407	0.58159908	1.526956775	0
15172	ZFP36L2	NM_006887	3.038896394	2.07781915	0.683741359	1.52135508	0
9274	CARM1	NM_199141	4.069766861	2.273408864	0.558609115	1.519885037	0
17313	NA	XM_211736	3.408205659	2.180198744	0.639691076	1.51690652	0
20043	PRICKLE2	NM_198859	3.80570112	2.249495036	0.591085575	1.510324757	0
11063	NFKB1	NM_003998	3.571648422	2.239793056	0.627103452	1.505047789	0
16939	SERPING1	NM_000062	3.573918382	2.152106661	0.602170064	1.503635053	0
6250	NA	NM_016838	3.687251548	2.211957222	0.599893225	1.502987694	0
10066	H2AFZ	NM_002106	2.180933857	1.770246862	0.811692137	1.499051764	0.447851889
21105	C14orf4	NM_024496	2.820224941	2.00839033	0.712138348	1.497429844	0
11450	C8orf4	NM_020130	2.999107071	2.030628762	0.677077781	1.492869767	0
20906	SAT	NM_002970	2.572691419	1.823914799	0.708952028	1.483094824	0
15497	CD40	NM_152854	3.531305787	2.201711516	0.623483677	1.481921037	0
6207	ZFP36L1	NM_004926	2.992604463	2.073199418	0.692774285	1.481705391	0
2334	HEXIM1	NM_006460	3.711788612	2.183426739	0.588241133	1.478164976	0
20210	INTS10	NM_018142	3.402270114	2.063222755	0.606425323	1.477860054	0
21542	BCL6	NM_001706	2.594987504	1.933075605	0.744926749	1.477012142	0
476	FAM26B	NM_015916	3.28739055	2.193448167	0.667230782	1.475755374	0
7485	SIDT2	NM_015996	3.587113965	2.193472625	0.61148674	1.475197003	0
19269	OPTN	NM_021980	2.811110874	1.8856968	0.67080129	1.473217501	0
1192	USP54	NM_152586	2.805075965	1.945373944	0.693519166	1.462159955	0
6828	RAB20	NM_017817	3.719545816	2.118431551	0.569540384	1.460995775	0
20934	SIPA1L1	NM_015556	3.399063035	2.027818918	0.596581734	1.454299176	0
14120	SFRP1	NM_003012	2.890180711	1.836559168	0.635447867	1.453448567	0
12033	C10orf56	NM_153367	2.825913558	2.013142308	0.712386373	1.452218864	0
6543	NFE2L2	NM_006164	3.116766148	2.027849054	0.650625988	1.450958368	0
2175	FLOT2	NM_004475	3.837483122	2.155336865	0.561653771	1.449175167	0
580	BMPR2	NM_001204	2.063744901	1.70007287	0.823780531	1.448242636	0.575952169
19932	ACVR1B	NM_004302	2.713807269	1.919457173	0.707293106	1.442105049	0
11628	H1FX	NM_006026	3.462610907	2.118819637	0.611913869	1.440404662	0
20575	NDUFS2	NM_004550	2.708295065	1.88921778	0.697567191	1.439544293	0
120	OCIAD2	NM_152398	3.173697612	2.053140932	0.64692393	1.435859727	0
6389	LOC93349	NM_138402	2.955129678	1.919304194	0.649482224	1.434934722	0
5413	TWIST1	NM_000474	3.595983953	2.119627878	0.589443086	1.433093108	0
23440	SMOC1	NM_022137	3.750886972	2.156002052	0.574797926	1.432844008	0
21521	NA	NM_033346	2.283748887	1.734477152	0.759486808	1.431603827	0.172273693
1985	SLC25A3	NM_002635	2.087357732	1.74118047	0.834155278	1.426613742	0.553045564
14116	RARA	NM_000964	2.304035022	1.781994572	0.773423387	1.425108583	0.172273693

Supplementary Table I. Continued

17786	TMOD1	NM_003275	3.604901022	2.101536212	0.582966411	1.424901795	0
6675	UBC	NM_021009	2.717639363	1.888048979	0.694738605	1.424177631	0
13910	TNFRSF1A	NM_001065	2.869283963	1.847589557	0.643920079	1.421375026	0
4837	ITIH3	NM_002217	2.260412479	1.753482338	0.775735559	1.421197843	0.172273693
855	BZRP	NM_007311	4.243666872	2.149270167	0.506465336	1.418713715	0
835	BTG3	NM_006806	3.378651531	2.101741083	0.622065064	1.418467368	0
4587	RAB31	NM_006868	3.136105733	1.998930275	0.637392501	1.417814802	0
14865	FOXP1	NM_032682	2.980637749	1.978299275	0.663716775	1.417641473	0
6857	GALNT2	NM_004481	3.933424089	2.10749498	0.535791446	1.417200493	0
7792	SIX5	NM_175875	2.496883684	1.891089572	0.757379923	1.416219154	0.172273693
10386	MMP14	NM_004995	2.489424335	1.789686086	0.718915639	1.411668424	0.172273693
16369	ZNF659	NM_024697	2.489919241	1.789293177	0.718614945	1.410273954	0.172273693
1156	TNFAIP2	NM_006291	2.180242933	1.704844489	0.781951618	1.409715036	0.447851889
14590	EFEMP1	NM_004105	1.962149786	1.696474713	0.864600004	1.408434074	0.712856661
2632	ZFP36	NM_003407	2.417704676	1.805265885	0.746685856	1.408303467	0.172273693
22000	CLIPR-59	NM_015526	3.709829043	2.117440479	0.570764974	1.406152379	0
13731	RAB13	NM_002870	1.907935348	1.55800326	0.816591224	1.402046889	0.841180142
4248	PTPRN	NM_002846	3.075014023	1.951167153	0.63452301	1.401311745	0
9619	C9orf26	NM_033439	1.947564499	1.668074883	0.856492755	1.398733786	0.712856661
16693	NA	NM_153014	3.03346393	1.971833167	0.650026904	1.398082253	0
1503	MLL5	NM_018682	2.789268045	1.89793654	0.680442507	1.39348398	0
10998	SLCO2A1	NM_005630	2.410260584	1.727795476	0.716850073	1.393416258	0.172273693
5732	BASP1	NM_006317	2.119653044	1.663557107	0.784825192	1.392605179	0.553045564
1890	ZNF689	NM_138447	3.317869205	1.997939768	0.602175566	1.391766917	0
6462	FRMD6	NM_152330	3.399959718	2.076046915	0.610609268	1.391652013	0
15474	SELP	NM_003005	2.5323944	1.769776948	0.698855182	1.38776298	0
11423	ENPP4	NM_014936	2.332140277	1.716821368	0.736156991	1.387667513	0.172273693
15042	CIRBP	NM_001280	3.179412005	1.915022587	0.602319732	1.3865934	0
1701	ABTB2	NM_145804	3.204972683	1.982946383	0.618709293	1.385157957	0
19836	RPL18	NM_000979	2.325952549	1.68573321	0.724749613	1.384728241	0.172273693
7883	RASA3	NM_007368	2.885582511	1.914500923	0.663471211	1.384413247	0
3647	PTPN2	NM_080423	3.148559315	1.903212231	0.60447082	1.383679311	0
11560	IGFBP7	NM_001553	2.281462338	1.796733205	0.787535772	1.383655224	0.172273693
12923	USP22	XM_042698	3.241047638	1.925767201	0.594180468	1.382255156	0
14519	KIAA0247	NM_014734	2.829382795	1.868979546	0.660560865	1.381813381	0
13968	ATBF1	NM_006885	2.567846732	1.868218385	0.727542794	1.379179737	0
12568	PHLDA2	NM_003311	2.623500525	1.902256996	0.72508352	1.377873191	0
15944	CSDA	NM_003651	2.868215564	1.910276212	0.666015566	1.374663308	0
17701	ATP1A1	NM_000701	3.134047093	1.931959552	0.616442413	1.370822089	0
1467	CCL20	NM_004591	2.367483695	1.684778028	0.711632368	1.366892932	0.172273693
69	RNF122	NM_024787	3.053278532	1.861033535	0.609519739	1.366487243	0
17865	GJA4	NM_002060	2.865077098	1.898684507	0.662699272	1.362805379	0
19313	UGCG	NM_003358	2.970404759	1.963565767	0.661043166	1.362140767	0
17435	LDLR	NM_000527	2.54589944	1.785394734	0.701282504	1.360101343	0
20161	CXCL1	NM_001511	1.901105964	1.607785092	0.845710404	1.359188768	0.841180142
6634	C10orf26	NM_017787	2.691850653	1.822569408	0.677069289	1.358741779	0
11938	PSME1	NM_006263	2.348773365	1.717822767	0.731370167	1.358682269	0.172273693
1286	WIPI2	NM_016003	2.90227574	1.843932802	0.635340322	1.356620215	0
20287	LGR4	NM_018490	3.386439733	1.977780237	0.584029362	1.355057612	0
4182	PTHR1	NM_000316	2.88793374	1.812580127	0.627639098	1.354068787	0
18687	SMAD3	NM_005902	3.416271317	1.94658284	0.569797495	1.353803976	0
8827	NR2F1	NM_005654	1.983939743	1.590281287	0.801577413	1.352047986	0.712856661
19501	NINJ1	NM_004148	2.89776733	1.825170466	0.629854042	1.350902848	0
1025	XPNPEP1	NM_020383	3.13890675	1.877822208	0.598240839	1.345961325	0
15188	CXXC5	NM_016463	2.176813047	1.6550202	0.760295057	1.345922258	0.447851889
19955	C8orf72	NM_147189	2.789627421	1.812531418	0.649739605	1.343342038	0
22010	MAP4K4	NM_004834	2.738669965	1.743716371	0.6367019	1.343048234	0
5754	EP300	NM_001429	1.99644081	1.570415707	0.786607697	1.341557355	0.712856661
7846	CBR3	NM_001236	2.423465054	1.721828009	0.71048188	1.339719436	0.172273693
13645	CSNK1E	NM_001894	2.608910573	1.713761622	0.656887836	1.339687298	0
4885	B4GALT5	NM_004776	2.901267118	1.847108813	0.636655895	1.339525535	0
20752	GRAMD1A	NM_020895	2.486486226	1.696396775	0.682246601	1.335834657	0.172273693
1305	HYAL2	NM_003773	3.11069343	1.850230963	0.59479695	1.335144861	0
19340	MGC10992	NM_033212	3.576348321	1.917921037	0.53627915	1.334174664	0
8942	LRIG3	NM_153377	3.021244969	1.822337526	0.603174368	1.333355443	0
18382	FLJ10159	NM_018013	2.981616364	1.815005636	0.608732115	1.33303988	0
8159	ZNF281	NM_012482	1.995150735	1.396517816	0.699956044	1.332058837	0.712856661
581	TMEM115	NM_007024	3.120794601	1.863780597	0.597213478	1.330894434	0
12611	RPLP0	NM_001002	2.025775958	1.614126177	0.796794024	1.329186268	0.575952169
14695	BCL6B	NM_181844	2.151942354	1.552332099	0.721363236	1.328952484	0.447851889
4806	YY1	NM_003403	2.974678141	1.876780096	0.63091871	1.328846027	0
213	GNB2L1	NM_006098	2.239411635	1.745145527	0.779287515	1.328653334	0.320211326
18300	KPNA6	NM_012316	2.162432384	1.60533169	0.742373127	1.327331657	0.447851889
16196	LOC51035	NM_015853	2.242541931	1.616730531	0.720936589	1.32709027	0.320211326
7226	CDK2	NM_001798	2.135155788	1.602880693	0.750709012	1.326075818	0.447851889
5322	TEAD2	NM_003598	2.894919789	1.82116696	0.629090646	1.323815798	0
6505	3/3/2006	NM_178450	3.025348623	1.834486895	0.606372066	1.323531975	0
5170	MGP	NM_000900	2.020617077	1.499495719	0.742097915	1.322954301	0.575952169
535	LEPROT	NM_017526	2.296125192	1.584699997	0.690162715	1.322415901	0.172273693
21577	RPL12	NM_000976	2.588678448	1.703629028	0.658107626	1.322027279	0
1765	SIN3A	NM_015477	2.442595746	1.693060329	0.693139801	1.321490323	0.172273693
10653	RAB30	NM_014488	2.960349645	1.768783779	0.59749151	1.320736877	0
23304	HBP1	NM_012257	1.894387946	1.548250224	0.817282557	1.320186142	0.841180142
23102	MKL1	NM_020831	3.687506212	1.883304903	0.510725893	1.319784081	0
17650	NFKB2	NM_002502	2.494631891	1.723396099	0.690841845	1.317226578	0.172273693
21295	RBPSUH	NM_015874	2.735284566	1.730182068	0.63254189	1.316397007	0
1222	ASS	NM_000050	2.350830149	1.589238099	0.67603272	1.316300064	0.172273693
2160	CRTC3	NM_022769	2.209319889	1.662670073	0.752570998	1.316013835	0.320211326
2695	DIO2	NM_000793	2.518378988	1.692233468	0.671953457	1.315255442	0.172273693
7200	NQO1	NM_000903	2.0729643	1.604638031	0.774078951	1.313765293	0.553045564
15608	RASSF4	NM_178145	2.103745193	1.533831909	0.729095859	1.311637141	0.553045564

Supplementary Table I. Continued

11085	NA	XM_371819	2.148779944	1.572510718	0.731815616	1.308646875	0.447851889
12216	H2AFJ	NM_177925	2.306325823	1.529250706	0.663067937	1.307395946	0.172273693
20298	CHST3	NM_004273	1.93592673	1.484023232	0.766569937	1.306635612	0.841180142
2610	SQSTM1	NM_003900	2.735935853	1.721135736	0.629084828	1.30528186	0
12697	NA	NM_017574	2.796946065	1.728137893	0.617866006	1.304949859	0
14482	PBX2	NM_002586	2.276103294	1.567096153	0.688499576	1.30489999	0.172273693
14876	OSMR	NM_003999	2.178953486	1.610421131	0.739080086	1.304227386	0.447851889
18603	WDR48	NM_020839	2.739202413	1.687870576	0.616190526	1.304214839	0
15585	C12orf57	NM_138425	2.242769241	1.637407166	0.730082764	1.302716082	0.320211326
1101	UBXD1	NM_025241	2.800971236	1.724926534	0.615831577	1.299028539	0
2781	PLK2	NM_006622	1.955743966	1.410773032	0.721348529	1.297460604	0.712856661
6601	CAMK1D	NM_153498	1.925870663	1.466574104	0.761512251	1.297320014	0.841180142
10214	BMP1	NM_006129	1.957112277	1.51818968	0.775729475	1.297267368	0.712856661
6653	HTRA3	NM_053044	2.127748217	1.545212955	0.726219833	1.296726066	0.553045564
4339	DPF2	NM_006268	2.779213236	1.694809582	0.609816318	1.295540379	0
22765	WTAP	NM_152857	2.041462728	1.560356393	0.76433254	1.294047519	0.575952169
2044	WDR45	NM_007075	2.800898772	1.7192082	0.613805903	1.293351676	0
11034	CNTNAP1	NM_003632	2.722928184	1.668239108	0.612663646	1.292972848	0
21973	UBB	NM_018955	2.467176798	1.656755927	0.671518932	1.292930618	0.172273693
8895	PSMD11	NM_002815	2.676516444	1.669980078	0.623937911	1.290965455	0
15060	NA	NM_178511	1.881873702	1.369651519	0.727812668	1.289697858	0.955895955
2856	XBP1	NM_005080	2.260229111	1.489963406	0.659209015	1.289583623	0.320211326
1859	SAFB2	NM_014649	2.193635404	1.538877867	0.701519434	1.289197167	0.320211326
7075	RANBP3	NM_003624	2.745624193	1.655167988	0.602838507	1.286980832	0
18259	TSPAN12	NM_012338	2.57226346	1.583700273	0.61568354	1.285989403	0
16276	MST150	NM_032947	2.128029719	1.524319239	0.716305428	1.285507545	0.553045564
20840	HOXB4	NM_024015	2.010316932	1.573542525	0.782733558	1.282985341	0.575952169
22907	MAFG	NM_002359	2.601090776	1.611980131	0.619732362	1.282466071	0
19898	TEAD4	NM_003213	2.171198446	1.541686702	0.710062549	1.281987091	0.447851889
10762	THBS2	NM_003247	1.9310377	1.467664791	0.760039429	1.281548983	0.841180142
12675	MAN1C1	NM_020379	2.272055443	1.582043549	0.696304993	1.280664509	0.172273693
11397	RBP1	NM_002899	2.554392441	1.597915918	0.625556157	1.280048911	0
8392	RPL27A	NM_000990	2.126618553	1.580430829	0.743166106	1.279746529	0.553045564
22535	TRRAP	NM_003496	2.110780334	1.530160818	0.724926604	1.27740809	0.553045564
5942	PHLDA1	NM_007350	2.607806588	1.613083397	0.618559446	1.277342686	0
16866	HGS	NM_004712	2.420692408	1.585953965	0.655165423	1.276483098	0.172273693
18384	CSNK1D	NM_001893	2.241792776	1.509068372	0.673152483	1.27644371	0.320211326
5427	CUTL1	NM_181552	2.713619076	1.675493255	0.617438634	1.276276001	0
7919	ITGA2	NM_002203	2.393662125	1.535437655	0.641459644	1.27598766	0.172273693
8711	ELK1	NM_005229	2.475965969	1.610905751	0.650617081	1.275710967	0.172273693
17197	C1orf121	NM_016076	2.890256776	1.628708714	0.563516961	1.275092981	0
15385	GPR37	NM_005302	2.546222065	1.612087341	0.633129122	1.274680307	0
6533	MAP1LC3B	NM_022818	1.908476625	1.443431311	0.75632643	1.27362397	0.841180142
15673	ACVR2B	NM_001106	2.466949277	1.595531998	0.646763196	1.273564802	0.172273693
17484	TRH	NM_007117	1.875877446	1.366981538	0.728715802	1.272508493	0.955895955
16053	NAB1	NM_005966	2.682526495	1.635272128	0.609601482	1.270281399	0
19827	HMGB2	NM_002129	2.267657636	1.44772729	0.638424102	1.270215943	0.172273693
13636	TACC1	NM_006283	2.094790414	1.522627393	0.726863835	1.268230274	0.553045564
9121	TRAF1	NM_005658	2.042143984	1.396249386	0.683717405	1.266193735	0.575952169
14261	CAMK2N1	NM_018584	2.423201046	1.590808695	0.656490594	1.265633457	0.172273693
23081	SLC1A5	NM_005628	2.057076415	1.462831732	0.711121727	1.265202476	0.575952169
7000	PEX5	NM_000319	2.305049197	1.498221379	0.64997371	1.265083002	0.172273693
10809	SCYL1	NM_020680	2.242048721	1.549953899	0.691311426	1.264894386	0.320211326
19123	RPUSD3	NM_173659	2.41678287	1.621095231	0.670765773	1.264837265	0.172273693
19658	ZNF161	NM_007146	1.932968448	1.462718303	0.756721251	1.263714868	0.841180142
10415	KARCA1	NM_152366	2.471361991	1.621302287	0.65603594	1.263183616	0.172273693
21642	NA	XM_371390	1.862615831	1.408645619	0.756272762	1.262889428	0.955895955
7761	ZNF503	NM_032772	2.171557386	1.520183588	0.700043019	1.262120449	0.447851889
8326	S100A10	NM_002966	2.0813102	1.44835022	0.695883881	1.260246779	0.553045564
3404	ASCC3L1	NM_014014	2.498562222	1.587631541	0.635418052	1.260061843	0.172273693
21380	THRAP2	NM_015335	2.076603395	1.447297776	0.696954353	1.259962506	0.553045564
15776	CRTAC1	NM_018058	2.524683529	1.568480871	0.621258409	1.256256324	0
19385	UBC	NM_021009	2.596339554	1.604835005	0.618114454	1.254745101	0
9588	SNAI2	NM_003068	2.029332723	1.413351491	0.696461194	1.254423441	0.575952169
2538	SERPINA5	NM_000624	2.641397958	1.551556945	0.587399918	1.254081922	0
4847	ZYG11BL	NM_006336	2.156404751	1.509273644	0.699902764	1.25366824	0.447851889
12841	MXD4	NM_006454	2.001034418	1.44787992	0.723565725	1.253611396	0.712856661
13021	SHC1	NM_003029	2.660421222	1.584981314	0.595763295	1.253518296	0
2536	TRAF7	NM_032271	1.969969999	1.362278588	0.691522505	1.253386788	0.712856661
19561	KHSRP	NM_003685	2.355436114	1.541552593	0.65446589	1.252976387	0.172273693
13122	MAD2L2	NM_006341	2.268330825	1.505862542	0.663863721	1.252276988	0.172273693
7546	JAG1	NM_000214	2.317660261	1.530510167	0.660368645	1.252101249	0.172273693
22791	ACTR1A	NM_005736	1.921420126	1.458142843	0.758888087	1.251778677	0.841180142
7106	NOSIP	NM_015953	1.88075781	1.443071764	0.767282079	1.251606514	0.955895955
22268	NNMT	NM_006169	2.122583176	1.425160584	0.671427438	1.251227457	0.553045564
21953	NA	NM_172363	2.006140206	1.415263031	0.705465663	1.250703521	0.712856661
4785	PDLIM1	NM_020992	1.876477816	1.342265962	0.715311394	1.250121703	0.955895955
10854	DIP2C	NM_014974	2.412617743	1.50014171	0.621790051	1.249351905	0.172273693
16681	ACO1	NM_002197	2.99911164	1.594578444	0.53168359	1.248709875	0
3282	BCOR	NM_017745	2.396368034	1.499996605	0.625945841	1.247888356	0.172273693
2243	LOC114984	NM_138439	2.188212798	1.445248425	0.66046978	1.247723395	0.447851889
1748	MGC2408	NM_032331	2.093104818	1.436386526	0.68624682	1.247405804	0.553045564
4977	RFC5	NM_181578	2.207507943	1.446528129	0.655276523	1.247177663	0.320211326
5688	PTP4A1	NM_003463	2.057694305	1.428273479	0.694113541	1.24705089	0.575952169
9100	UBE2D3	NM_181893	1.945137237	1.451314579	0.746124516	1.246799019	0.841180142
12743	NA	XM_370738	2.392487877	1.473072118	0.615707245	1.246677838	0.172273693
2568	DHX37	NM_032656	2.665196829	1.53093525	0.574417331	1.246497776	0
10752	NYREN18	NM_016118	2.214283342	1.469935441	0.663842523	1.246435411	0.320211326
12555	TLE1	NM_005077	2.017899918	1.405709695	0.696620126	1.244807364	0.575952169
17205	MSGN1	XM_292850	2.057165339	1.444080123	0.701975721	1.244655993	0.575952169
823	PI15	NM_015886	1.986208018	1.4376519	0.723817388	1.241472949	0.712856661

Supplementary Table I. Continued

22429	ABL1	NM_007313	2.694516954	1.538828457	0.571096223	1.241400603	0
6824	UBC	NM_021009	2.719317111	1.537779243	0.565501992	1.241012116	0
16552	AKAP1	NM_003488	2.16942305	1.437177268	0.662469806	1.240762621	0.447851889
11559	C17orf61	NM_152766	2.200507513	1.438395242	0.653665226	1.238942931	0.320211326
14818	NOTCH1	NM_017617	1.908472215	1.356967733	0.711023049	1.237024866	0.841180142
14532	RAG1AP1	NM_018845	2.156785035	1.369142536	0.634807138	1.236849252	0.447851889
12306	MED25	NM_030973	2.043570503	1.370296558	0.670540388	1.236414048	0.575952169
13098	DNTTIP1	NM_052951	2.671476027	1.517919958	0.568195238	1.235791989	0
20949	KIAA1285	NM_015694	2.028914265	1.411180138	0.695534632	1.235764219	0.575952169
9899	HIF1A	NM_001530	2.097996099	1.431980697	0.682546883	1.235583729	0.553045564
17970	C21orf63	NM_058187	2.006740959	1.44642161	0.720781426	1.235355933	0.712856661
22668	ZA20D3	NM_019006	2.332985482	1.477352771	0.633245591	1.235156183	0.172273693
13216	RRS1	NM_015169	1.915752922	1.368440164	0.714309319	1.233127015	0.841180142
12506	FLJ22709	NM_024578	2.341595656	1.445309966	0.617232938	1.232029923	0.172273693
8109	UNC119	NM_005148	2.135004289	1.34540663	0.630165774	1.231778449	0.447851889
5751	KLHL21	NM_014851	2.018912516	1.37345941	0.680296645	1.230634859	0.575952169
16771	SNTB2	NM_006750	1.880106124	1.333391939	0.709210997	1.230504889	0.955895955
2273	CAMLG	NM_001745	2.941565016	1.524389983	0.518224134	1.227178274	0
8830	POLA2	NM_002689	2.089619496	1.421692791	0.680359651	1.227173645	0.553045564
21760	PNKD	NM_022572	1.873644728	1.3948261	0.744445347	1.227142704	0.955895955
18280	UBAP1	NM_016525	2.803849085	1.490609276	0.531629639	1.226962181	0
15076	TNFSF5IP1	NM_020232	2.805207387	1.479577992	0.527439789	1.226908784	0
7618	USP10	NM_005153	2.120897961	1.412401408	0.665945007	1.226150318	0.553045564
17289	BBX	NM_020235	2.315192753	1.403125406	0.606051226	1.225898612	0.172273693
21599	JAK1	NM_002227	1.968605163	1.344427231	0.682933915	1.225388319	0.712856661
19856	TCEAL1	NM_004780	2.059074954	1.374976614	0.667764236	1.225146529	0.575952169
15828	NA	XM_050793	1.861370095	1.325314559	0.712010235	1.224819417	0.955895955
2895	CTPS2	NM_019857	1.881769449	1.39682412	0.74229291	1.224286841	0.955895955
14804	SDK1	NM_152744	1.936245872	1.366589572	0.705793408	1.222795278	0.841180142
8206	PSMB2	NM_002794	1.876274222	1.310957208	0.69870235	1.222000175	0.955895955
2288	HARS	NM_002109	1.979335184	1.367360981	0.690818307	1.221520071	0.712856661
9240	SERINC3	NM_006811	2.045708138	1.367324856	0.668387064	1.220139202	0.575952169
15457	DNAJC1	NM_022365	2.477041904	1.428638963	0.576752037	1.217736313	0.172273693
5027	FAM38A	NM_014745	2.224350978	1.361677812	0.612168594	1.217498879	0.320211326
7253	SPG7	NM_003119	2.005257862	1.298932902	0.647763526	1.215588264	0.712856661
21318	PIR	NM_003662	2.229710179	1.406717001	0.630896793	1.215268622	0.320211326
16382	SLU7	NM_006425	2.016286779	1.337369472	0.663283362	1.214322167	0.575952169
9410	C7orf27	NM_152743	1.941721962	1.303158684	0.671135574	1.213966042	0.841180142
14808	NA	XM_045271	2.193505768	1.352949928	0.61679798	1.21393	0.320211326
21789	SLC39A8	NM_022154	2.194195316	1.389042096	0.633053077	1.213265433	0.320211326
20032	RBM14	NM_006328	1.968044476	1.320788819	0.671117363	1.212711229	0.712856661
12548	NCOA1	NM_147233	2.196837545	1.333861411	0.607173441	1.212368705	0.320211326
9168	NKX3-1	NM_006167	2.092050752	1.320163278	0.631037883	1.211153242	0.553045564
15178	ABCF1	NM_001090	2.235789589	1.31499994	0.588159077	1.210305445	0.320211326
14206	CCNI	NM_006835	1.905916273	1.304282173	0.684333405	1.209594647	0.841180142
17665	NA	XM_351827	1.862050303	1.238451635	0.665101063	1.209434957	0.955895955
3453	ZNF574	NM_022752	1.944378693	1.313794405	0.675688543	1.209373642	0.841180142
20939	SLC25A6	NM_001636	1.96969408	1.31843693	0.669361269	1.20848508	0.712856661
16886	PIK4CA	NM_002650	1.895202711	1.298372755	0.685083842	1.205391223	0.841180142
21476	WDR40A	NM_015397	1.871070938	1.237328976	0.66129453	1.204463952	0.955895955
15575	ZBTB20	NM_015642	2.021547425	1.297095392	0.641634906	1.20404298	0.575952169
21535	ADH1A	NM_000667	2.268643779	1.371999997	0.604766605	1.202694274	0.172273693
22514	HADH2	NM_004493	1.932025171	1.296448856	0.671031038	1.199392303	0.841180142
623	MANEAL	NM_152496	2.012918536	1.255676348	0.623808826	1.199226534	0.575952169
1341	C9orf23	NM_148178	1.890462495	1.310723036	0.693334589	1.199139974	0.841180142
2683	HNRPA1	NM_002136	2.020790459	1.277850459	0.632351788	1.198713164	0.575952169
1380	DYRK3	NM_003582	1.926405963	1.259529026	0.653823259	1.197752861	0.841180142
3581	FUS	NM_004960	1.9846003	1.2793542	0.644640737	1.197470321	0.712856661
8480	MYST1	NM_032188	1.923478392	1.263977255	0.657130988	1.19581003	0.841180142
14839	HOXA6	NM_024014	1.906918592	1.224582856	0.642178885	1.193668812	0.841180142
9846	MGC3123	NM_024107	2.193076292	1.26745933	0.577936725	1.193348615	0.447851889
21369	LOC391769	XM_373079	2.131867461	1.283757499	0.602175099	1.193175585	0.447851889
8750	NA	XM_290667	1.92468651	1.237722742	0.64307758	1.192983578	0.841180142
23084	TRAF3IP2	NM_147200	2.129271917	1.274393537	0.59851141	1.191414511	0.447851889
20982	SVIL	NM_003174	2.099704634	1.278529853	0.608909383	1.190428267	0.553045564
10782	BTF3	NM_001207	2.185547781	1.289012189	0.589789068	1.189326343	0.447851889
9347	NDUFA11	NM_175614	1.98800414	1.24898724	0.628261891	1.189130898	0.712856661
18889	MRPL10	NM_145255	1.925619208	1.22958416	0.638539621	1.185699495	0.841180142
953	SLC16A9	NM_194298	1.919687389	1.235050479	0.643360208	1.180901248	0.841180142
19306	OACT5	NM_005768	2.025318261	1.182134197	0.58367824	1.175464435	0.575952169
7985	C16orf48	NM_032140	1.989378426	1.142334661	0.574216874	1.163561059	0.712856661
16479	QARS	NM_005051	1.926482574	1.127860144	0.585450478	1.160557575	0.841180142
7294	CCDC25	NM_018246	1.881422916	1.084537315	0.576445256	1.153425353	0.955895955

Negative genes (407)

Row	Gene ID	Gene Name	Score(d)	Numerator(r)	Denominator(s+s0)	Fold Change	q-value(%)
923	ANKRD1	NM_014391	-5.841479977	-3.480368324	0.595802492	0.283573284	0
23485	NRXN3	NM_138970	-5.261097148	-3.275899035	0.622664616	0.36071643	0
23261	PRG4	NM_005807	-5.586012558	-3.097098869	0.554438222	0.386366161	0
13902	COLQ	NM_080544	-5.233500179	-3.001407796	0.573499129	0.412640418	0
9326	RGC32	NM_014059	-4.00918833	-2.970867632	0.741014736	0.424219198	0
13739	UACA	NM_018003	-5.066891561	-2.995345178	0.591160308	0.431045164	0
14309	ARHGDIB	NM_001175	-3.379807508	-2.809818405	0.831354566	0.435911623	0
22361	SERPINE1	NM_000602	-5.098399462	-2.92118529	0.572961242	0.451810065	0
10256	NA	XM_090844	-3.745415674	-2.765817646	0.738454123	0.480935632	0
13982	NA	XM_167711	-3.820927139	-2.694656176	0.70523621	0.488019334	0
6261	DES	NM_001927	-4.951647329	-2.805085333	0.56649538	0.491545161	0

Supplementary Table I. Continued

22013	SYTL2	NM_032379	-5.418584438	-2.773556113	0.511859905	0.496993537	0
14988	THBS1	NM_003246	-4.030995516	-2.71387007	0.67325058	0.498227561	0
18682	ECGF1	NM_001953	-3.937503329	-2.700908535	0.685944445	0.500190367	0
21609	HSPB7	NM_014424	-4.053956119	-2.677969154	0.660581683	0.506389805	0
12320	SYNC1	NM_030786	-5.163240549	-2.744870385	0.531617762	0.507778524	0
9816	CRYAB	NM_001885	-3.945976336	-2.690421781	0.681813967	0.515496721	0
11208	DNAJB4	NM_007034	-4.268335314	-2.685554194	0.629180699	0.518825382	0
7780	INPP5A	NM_005539	-4.853658113	-2.71601617	0.55958127	0.522957659	0
1260	MAP2	NM_031845	-4.821843171	-2.677501402	0.555285875	0.530877334	0
8664	PNCK	NM_198452	-4.498833682	-2.660138393	0.591295118	0.534222432	0
19776	DOC1	NM_014890	-4.240782369	-2.646142081	0.623974977	0.538110803	0
19691	TNNC1	NM_003280	-2.766022578	-2.370242408	0.856913615	0.555195104	0
19041	NCF1	NM_000265	-2.04709307	-2.210933862	1.08003583	0.558586376	0.575952169
17219	KCNA5	NM_002234	-4.266573489	-2.55365895	0.598526887	0.562621891	0
19771	DCN	NM_133507	-4.209936256	-2.530329951	0.601037592	0.562844666	0
8386	AIF1	NM_032955	-2.632704067	-2.353120978	0.89380383	0.567036055	0
6181	HLA-DPB1	NM_002121	-2.63428213	-2.372145504	0.900490299	0.56731701	0
17053	RYR2	NM_001035	-4.666196618	-2.48435554	0.532415529	0.581230798	0
13022	ZNF364	NM_014455	-4.674231552	-2.497322494	0.534274451	0.583368235	0
13803	EFHD1	NM_025202	-4.275917952	-2.481397026	0.580319139	0.584628602	0
3688	ATP1B1	NM_001677	-4.823683649	-2.514383678	0.521257997	0.586911345	0
480	C5orf13	NM_004772	-4.591753081	-2.483099781	0.540773804	0.597379335	0
23180	TNFRSF12A	NM_016639	-3.895470349	-2.47331789	0.634921503	0.598004944	0
4688	MNDA	NM_002432	-2.126921208	-2.408286577	1.132287632	0.598068702	0.553045564
3687	PPP1R14A	NM_033256	-2.966932664	-2.320403795	0.782088459	0.601641271	0
253	FCAR	NM_133279	-3.619621267	-2.322288855	0.641583382	0.604172302	0
20323	HSPA1A	NM_005345	-3.725221485	-2.387739632	0.640965817	0.604385906	0
16665	CFL2	NM_021914	-4.348792482	-2.450034967	0.563382819	0.605678454	0
1495	SHRM	NM_020859	-3.923704962	-2.411985966	0.614721542	0.606126948	0
6111	NET1	NM_005863	-3.252004471	-2.305727807	0.709017416	0.606464637	0
12415	ALPL	NM_000478	-2.162413346	-2.172178584	1.004515898	0.607012801	0.447851889
7889	CXCR4	NM_003467	-2.404035422	-2.182379869	0.907798549	0.609331852	0.20411575
7633	IGFBP2	NM_000597	-3.158101187	-2.304448969	0.729694469	0.610227208	0
1119	DOC1	NM_014890	-2.778547373	-2.212484677	0.796273873	0.616282523	0
5211	LRRFIP1	NM_004735	-3.176122462	-2.222812856	0.699851118	0.617113475	0
20385	CSF1R	NM_005211	-2.107669928	-2.218674913	1.052667158	0.617318037	0.553045564
19531	ACTG2	NM_001615	-2.687801886	-2.222345881	0.82682652	0.619017771	0
4128	HSPA1B	NM_005346	-3.330541444	-2.270188702	0.681627519	0.619337791	0
5854	HCFC1R1	NM_017885	-2.63653738	-2.212433786	0.83914372	0.620008169	0
20373	IGFBP6	NM_002178	-4.084775986	-2.363094143	0.578512543	0.620020507	0
8276	STK38L	NM_015000	-3.426425829	-2.266789247	0.661560868	0.621361633	0
908	TEP1	NM_007110	-3.102422926	-2.227269449	0.717912903	0.623387243	0
21658	ITM2A	NM_004867	-3.64332481	-2.345374959	0.643745777	0.626358468	0
7906	TMEM47	NM_031442	-4.493116931	-2.355280062	0.524197366	0.63019673	0
21020	FOS	NM_005252	-2.70009747	-2.123186422	0.786336955	0.631486931	0
18441	PIK3CD	NM_005026	-2.783306721	-2.166256202	0.778303083	0.634722667	0
8588	SPOP	NM_003563	-2.81145641	-2.192066364	0.779690681	0.636285965	0
19744	NA	NM_182588	-3.62387062	-2.211512751	0.610262612	0.637509783	0
3291	P2RX1	NM_002558	-2.954636603	-2.196394405	0.743372096	0.639558333	0
1831	NA	NM_198278	-4.188991268	-2.273483533	0.542728162	0.640398496	0
21419	SLC2A5	NM_003039	-2.432409139	-2.061983982	0.847712644	0.641305288	0.20411575
5492	TPD52L1	NM_003287	-3.609370146	-2.278220168	0.631196047	0.641399079	0
4800	GIMAP4	NM_018326	-3.508213806	-2.264174633	0.64539243	0.642744529	0
16346	NA	XM_379377	-3.014213834	-2.110093207	0.700047616	0.642954024	0
9753	ZNF665	NM_024733	-3.323967939	-2.179442665	0.655674996	0.644242593	0
4370	ACTN4	NM_004924	-2.572201064	-2.139535779	0.83179181	0.644553275	0
15507	AMIGO2	NM_181847	-3.798741293	-2.254540845	0.593496812	0.645081689	0
8045	RNASET2	NM_003730	-3.902811891	-2.230350888	0.571472813	0.645107341	0
3660	NA	XM_351837	-2.200686182	-1.992980332	0.905617688	0.646039202	0.447851889
21878	LMO3	NM_018640	-3.213076618	-2.168654235	0.674946319	0.646084009	0
18409	TTF2	NM_003594	-2.873102686	-2.144893723	0.74654266	0.648705994	0
20758	NA	XM_378933	-2.70893396	-2.123568182	0.783912865	0.649579793	0
23066	FUT6	NM_000150	-2.836765455	-2.101043789	0.740647693	0.6499543	0
22752	COL1A2	NM_000089	-3.975473677	-2.267440199	0.570357241	0.652930909	0
21103	IFI30	NM_006332	-2.08293671	-2.018032091	0.968839851	0.65365617	0.553045564
3524	APOE	NM_000041	-3.029857835	-2.089672051	0.689693103	0.653882998	0
3114	TMEM113	NM_025222	-3.353420579	-2.148371964	0.640650916	0.654967383	0
13435	NRCAM	NM_005010	-4.189412904	-2.228319707	0.531893074	0.657106506	0
15651	ZNF549	NM_153263	-3.080929267	-2.081993382	0.675767991	0.658288723	0
7333	DKK3	NM_013253	-3.350530564	-2.191559509	0.654093275	0.658405141	0
18998	GAS6	NM_000820	-2.767326098	-2.107714807	0.761643092	0.658615759	0
18581	CASQ2	NM_001232	-2.990111401	-2.099390261	0.702111052	0.659115897	0
14401	SYAP1	NM_032796	-2.898474031	-2.037339916	0.702900869	0.659175148	0
1638	DNAJA4	NM_018602	-2.79654959	-2.082765146	0.744762458	0.65945981	0

Supplementary Table I. Continued

7177	BIRC4	NM_001167	-3.187695167	-2.099680254	0.658682886	0.660455547	0
16038	MMP25	NM_022468	-1.932954546	-1.955493918	1.011660581	0.661067414	0.841180142
7625	LOC151194	NM_145280	-3.052845102	-2.05101553	0.671837405	0.661707611	0
8371	ANKRD41	NM_152363	-3.327963	-2.116571808	0.635996196	0.662016416	0
6779	MMP23B	NM_006983	-3.646597977	-2.175353295	0.596543219	0.662114063	0
21381	CSTA	NM_005213	-2.838636378	-2.060337141	0.725819326	0.663217526	0
8635	ARHGAP4	NM_001666	-2.647981162	-1.99081963	0.75182545	0.663552654	0
15405	WEE1	NM_003390	-3.92015516	-2.184889744	0.557347772	0.664548558	0
13799	LILRB3	NM_006864	-1.908245284	-1.880854069	0.985645863	0.665321123	0.841180142
19917	MGC16703	NM_145042	-2.844815688	-2.035518885	0.715518722	0.66638358	0
16864	LRRC1	NM_018214	-3.561613359	-2.155268547	0.60513827	0.667371253	0
15395	KLF6	NM_001300	-3.732640284	-2.156140637	0.577644904	0.667627862	0
5367	CATSPER2	NM_172097	-2.852102385	-2.027666758	0.710937577	0.667740574	0
3278	CD37	NM_001774	-2.059395381	-2.114259138	1.026640711	0.668150486	0.575952169
363	NA	XM_371054	-2.879530796	-2.037841239	0.707699061	0.669261778	0
12918	EFHD2	NM_024329	-2.760947401	-2.055409233	0.744457947	0.669812285	0
20404	NA	XM_038576	-2.617411578	-2.012086607	0.768731454	0.672095306	0
353	HLA-DPA1	NM_033554	-2.087333106	-1.950317921	0.934358735	0.673492095	0.553045564
7813	ENO3	NM_053013	-3.530334444	-2.158629171	0.611451749	0.675182117	0
23195	VWA1	NM_022834	-2.643919239	-2.023961548	0.765515647	0.675541762	0
20495	BAMBI	NM_012342	-3.179500042	-2.105967465	0.662358056	0.675805163	0
12942	MRP63	NM_024026	-2.636051272	-1.946001038	0.738225792	0.67598601	0
12183	MARCO	NM_006770	-2.045607105	-1.844096632	0.901491116	0.676354489	0.575952169
21056	HSD17B7	NM_016371	-2.911030937	-2.007115743	0.689486229	0.676835502	0
15645	SPINT2	NM_021102	-2.459887746	-2.017477813	0.820150357	0.676896615	0.20411575
3061	MSH3	NM_002439	-2.749456739	-1.97910535	0.719816872	0.678478696	0
20478	DUSP19	NM_080876	-2.845380151	-1.979751639	0.695777553	0.678562996	0
16019	STXBP2	NM_006949	-2.196339319	-1.930770614	0.879085757	0.678673286	0.447851889
6045	PRKCB1	NM_002738	-3.274402597	-2.085319069	0.636854818	0.679147861	0
7861	WAS	NM_000377	-2.013599951	-1.961262571	0.974008054	0.679904567	0.575952169
21430	C5orf24	NM_152409	-2.521104701	-1.948541224	0.772891829	0.680131835	0.20411575
22040	NT5C2	NM_012229	-2.817834978	-1.988104496	0.705543267	0.681372865	0
189	C14orf125	XM_113763	-2.323426964	-1.910170394	0.8221349	0.681406477	0.20411575
1600	CTSH	NM_148979	-2.742690239	-2.043384803	0.745029378	0.681452017	0
14051	ASPN	NM_017680	-2.928506271	-2.052166563	0.700755393	0.681760984	0
8704	CORO1A	NM_007074	-2.561652652	-1.985057032	0.774912645	0.681765654	0
15029	C21orf7	NM_020152	-2.698901793	-1.959272659	0.725951816	0.68208543	0
22422	GPR155	NM_152529	-2.93922604	-1.985906091	0.67565613	0.68258254	0
3855	PHYHIPL	NM_032439	-2.646150405	-1.952162444	0.737736767	0.68455451	0
7672	CD4	NM_000616	-2.032571269	-1.868384413	0.919222092	0.685927934	0.575952169
2306	RARRES1	NM_002888	-2.61316716	-1.915863325	0.733157585	0.687254031	0
20522	DSCR1L1	NM_005822	-2.134287834	-1.842183094	0.863137139	0.687868514	0.553045564
12775	SEMA3E	NM_012431	-2.233269031	-1.791308824	0.802101672	0.688924648	0.320211326
19685	NFAT5	NM_173215	-2.60543483	-1.904759037	0.731071457	0.689045867	0
454	ACTB	NM_001101	-2.756099805	-1.993425015	0.723277514	0.690135825	0
12403	CNN1	NM_001299	-2.620558231	-1.977152365	0.754477554	0.690165469	0
79	CREB1	NM_004379	-2.385711347	-1.890347753	0.79236231	0.69018067	0.20411575
2032	RP4-692D3.1	NM_025030	-2.696621595	-1.913116726	0.709449457	0.690229602	0
12875	NA	NM_032710	-2.868733713	-1.91561388	0.667755906	0.690345527	0
15879	FCER1G	NM_004106	-2.054420204	-1.862184031	0.906428017	0.690481107	0.575952169
19940	CENTB1	NM_014716	-2.9942278	-2.003751275	0.669204686	0.691331081	0
14573	C2orf15	NM_144706	-2.602062187	-1.912933112	0.735160413	0.692263379	0
3442	C1orf33	NM_016183	-2.556205043	-1.881234377	0.735948152	0.693881874	0
22563	C9orf85	NM_198394	-2.69399747	-1.90728542	0.707975951	0.694390484	0
15975	PBOV1	NM_021635	-2.669532373	-1.897951012	0.710967595	0.694524261	0
6622	DOCK2	NM_004946	-1.970367326	-1.883039472	0.955679404	0.696733336	0.712856661
1992	C9orf5	NM_032012	-2.781734613	-1.926841059	0.692676091	0.696968257	0
7272	CTSK	NM_000396	-3.881725209	-2.082747082	0.536551912	0.69750874	0
11514	ZNF430	NM_025189	-2.756697098	-1.894776029	0.687335591	0.698858351	0
16243	C19orf39	NM_175871	-1.905277631	-1.724562468	0.905150221	0.698859307	0.841180142
20308	ZNF136	NM_003437	-2.568388018	-1.860256475	0.724289501	0.698992675	0
7249	LOX	NM_002317	-2.367074399	-1.878671251	0.79366802	0.69924277	0.20411575
9759	NA	XM_351658	-2.50997984	-1.868996678	0.744626171	0.699406883	0.20411575
21920	FKBP14	NM_017946	-2.631972417	-1.862310817	0.707572315	0.699797643	0
11353	NA	NM_014006	-2.441362148	-1.841422051	0.754260097	0.700869435	0.20411575
11469	SCN11A	NM_014139	-3.218882488	-1.96401509	0.610154331	0.701338037	0
8617	DIP2B	NM_173602	-1.852373966	-1.70367142	0.919723259	0.701392213	0.955895955
12282	GNPNAT1	NM_198066	-2.475311822	-1.83189866	0.740067835	0.701772748	0.20411575
21063	SRPX	NM_006307	-3.757960081	-2.057518107	0.547509304	0.70231879	0
4091	LRAP	NM_022350	-2.706025598	-1.877370276	0.693774027	0.702535797	0
9005	TADA3L	NM_133480	-2.726557217	-1.881097191	0.689916639	0.703216321	0
626	CALM1	NM_006888	-3.53051113	-2.06325555	0.584407038	0.703277566	0
746	ZNF454	NM_182594	-3.088145659	-1.938095414	0.627591969	0.703342248	0
1145	FAM46B	NM_052943	-2.799096595	-1.956170409	0.698857772	0.703469466	0
13787	ARHGAP9	NM_032496	-2.347293815	-1.856587807	0.790948196	0.704827803	0.20411575

Supplementary Table I. Continued

9196	TRIM74	NM_198853	-2.024589492	-1.756520263	0.867593293	0.704956883	0.575952169
9615	COL16A1	NM_001856	-3.420604543	-1.989905959	0.581741015	0.706230494	0
13510	TRIM58	NM_015431	-2.15120788	-1.777110471	0.826098903	0.706472612	0.447851889
11902	FAM73A	NM_198549	-2.187752652	-1.767570195	0.807938774	0.707106501	0.447851889
9296	NA	NM_017932	-2.374684758	-1.800788222	0.758327275	0.707615122	0.20411575
15708	CUGBP2	NM_006561	-3.037471033	-1.945825708	0.640607165	0.708264097	0
10490	LENG12	NM_033206	-2.707865386	-1.851857862	0.683881064	0.708349601	0
1120	CCDC85A	XM_055636	-3.416959462	-1.999792171	0.585254872	0.708462448	0
16408	TPM2	NM_003289	-2.360023894	-1.908708568	0.808766629	0.709490014	0.20411575
17133	SSH2	NM_033389	-2.439710934	-1.900983881	0.779184064	0.70980017	0.20411575
22310	C6orf32	NM_015864	-1.904194651	-1.878731074	0.98662764	0.709920467	0.841180142
15275	GNL3L	NM_019067	-2.322945782	-1.81816432	0.782697699	0.710247414	0.20411575
13584	SYK	NM_003177	-2.468096132	-1.914623238	0.775749053	0.71047786	0.20411575
14691	NA	NM_024977	-3.042350714	-1.921282254	0.631512417	0.710683801	0
16484	LAPTM5	NM_006762	-2.474972673	-1.900991739	0.768085951	0.71087173	0.20411575
3261	TMEM19	NM_018279	-2.508304744	-1.814169769	0.723265294	0.711969589	0.20411575
20813	TMEM17	NM_198276	-2.584032833	-1.801915235	0.697326757	0.712009741	0
5941	SGK3	NM_170709	-2.33114217	-1.76548762	0.757348755	0.713244525	0.20411575
12189	NA	XM_351675	-3.08196553	-1.939891325	0.629433167	0.71407335	0
4602	DCN	NM_001920	-1.870600064	-1.731440245	0.925606856	0.714406692	0.955895955
2841	SMTN	NM_006932	-1.903153398	-1.856197261	0.975327193	0.715001811	0.841180142
11773	CAMK4	NM_001744	-2.540032971	-1.865672243	0.734507097	0.716049065	0.20411575
96	SMTN	NM_134269	-2.110569014	-1.813110661	0.859062485	0.71620662	0.553045564
10950	HSPB1	NM_001540	-2.222802413	-1.811136142	0.814798531	0.716641589	0.320211326
13384	C3orf34	NM_032898	-2.294511125	-1.737597608	0.757284456	0.71737707	0.20411575
10296	PCDH18	NM_019035	-2.751832782	-1.865042971	0.677745749	0.717646452	0
12046	ITCH	NM_031483	-2.320616575	-1.759760343	0.758315856	0.717744432	0.20411575
723	PKN1	NM_002741	-3.574528078	-1.98827773	0.556235029	0.718206036	0
4900	MMP3	NM_002422	-2.374542143	-1.823273991	0.767842338	0.718448866	0.20411575
8265	C1orf176	NM_022774	-2.684651173	-1.798653793	0.669976722	0.720202883	0
9824	BTBD5	NM_017658	-2.121097535	-1.70867523	0.805561839	0.721670869	0.553045564
1623	PDLIM5	NM_006457	-2.104968895	-1.736595304	0.824998083	0.721748481	0.553045564
21667	DKFZp762I137	NM_152411	-1.885314586	-1.647810368	0.874024091	0.7217536	0.841180142
17614	LMCD1	NM_014583	-2.192766399	-1.713829697	0.781583345	0.721851237	0.447851889
22165	FLJ21657	NM_022483	-2.125423277	-1.698076669	0.798935764	0.721875465	0.553045564
10088	USP14	NM_005151	-2.101532625	-1.69994549	0.808907495	0.723153879	0.553045564
19829	ITGB1	NM_033668	-2.659441691	-1.874806131	0.7049623	0.723707849	0
21681	TUBB6	NM_032525	-2.776471996	-1.898487108	0.68377679	0.723744394	0
23243	EFNB2	NM_004093	-2.978753288	-1.897641228	0.637058878	0.723878743	0
10919	C9orf58	NM_031426	-1.998987309	-1.730663226	0.865769992	0.724079577	0.575952169
15650	MYLK	NM_053031	-2.090166091	-1.739159429	0.832067574	0.72444276	0.553045564
17617	CXorf41	NM_173494	-2.409644367	-1.763130559	0.731697417	0.724680049	0.20411575
1634	ECOP	NM_030796	-3.156132853	-1.930467106	0.611655845	0.726255398	0
1377	PLAC8	NM_016619	-1.919252035	-1.828031524	0.952470801	0.726427903	0.841180142
243	C21orf77	NM_018277	-2.354339579	-1.751438048	0.743919044	0.726448982	0.20411575
15198	PTPLA	NM_014241	-2.680018678	-1.857566075	0.693116839	0.726784037	0
1883	IL17B	NM_014443	-2.09816598	-1.785294334	0.850883272	0.72721801	0.553045564
14760	YWHAH	NM_003405	-3.137810736	-1.896874594	0.604521672	0.728388852	0
6031	NA	XM_351316	-2.06817871	-1.689685307	0.816991926	0.728751787	0.553045564
1597	COL12A1	NM_080645	-3.135870983	-1.889366899	0.602501477	0.729785986	0
17471	FSTL3	NM_005860	-2.593885594	-1.843997381	0.710901585	0.729795149	0
20392	UNQ1940	NM_205855	-2.779003851	-1.878105537	0.675819696	0.729810723	0
16092	SCRN1	NM_014766	-3.152068773	-1.876379471	0.595285067	0.730523726	0
6401	HLA-DMB	NM_002118	-2.432345224	-1.80663724	0.742755273	0.731033006	0.20411575
18793	AK5	NM_174858	-2.589568649	-1.809358651	0.698710441	0.731845328	0
17538	MS4A6A	NM_022349	-1.970469503	-1.704658305	0.865102607	0.732164966	0.712856661
20412	PTPN6	NM_080548	-2.52052124	-1.831292979	0.726553282	0.732249794	0.20411575
12152	GP1BB	NM_000407	-2.295026124	-1.775037202	0.773427886	0.732994236	0.20411575
1780	NPY	NM_000905	-1.954266297	-1.666842594	0.852925006	0.733042749	0.712856661
9054	MYH10	NM_005964	-2.467443996	-1.774816164	0.719293393	0.733265789	0.20411575
18540	VAMP8	NM_003761	-2.709184494	-1.858246785	0.685906327	0.733893627	0
7752	RNASE2	NM_002934	-2.609434204	-1.809599201	0.693483361	0.734118044	0
12722	NA	XM_048747	-2.762235856	-1.80659366	0.654033093	0.734279207	0
10965	PRPSAP1	NM_002766	-2.702128015	-1.803005184	0.667253799	0.734425936	0
9137	NTF3	NM_002527	-2.127573505	-1.671534951	0.785653209	0.734620453	0.553045564
20584	C7orf38	NM_145111	-1.979894974	-1.623924626	0.820207459	0.735169544	0.712856661
2633	DUSP8	NM_004420	-2.28185892	-1.693350218	0.742092424	0.735595551	0.20411575
17201	PDLIM7	NM_005451	-3.042654239	-1.857962469	0.610638713	0.735991465	0
18245	CSPG2	NM_004385	-1.90929705	-1.642214055	0.860114488	0.736262272	0.841180142
9395	DMC1	NM_007068	-2.062634177	-1.653512006	0.801650639	0.736370205	0.575952169
6856	LAMC1	NM_002293	-2.799511935	-1.82546528	0.652065546	0.736704962	0
21582	STON1	NM_006873	-2.710289574	-1.772215755	0.653884283	0.737999321	0
22982	SCHIP1	NM_014575	-3.246857672	-1.902772061	0.586034946	0.73819855	0
2929	PAFAH2	NM_000437	-3.128292129	-1.815878479	0.580469599	0.739200456	0
9949	SIGLEC8	NM_014442	-2.371864878	-1.728071486	0.728570798	0.739466433	0.20411575

Supplementary Table I. Continued

3204	FBLN1	NM_001996	-2.602161946	-1.774602666	0.681972415	0.739875126	0
5030	TUBB2A	NM_001069	-2.37874536	-1.750666167	0.735961989	0.740281785	0.20411575
21130	DAPP1	NM_014395	-2.202255472	-1.699309119	0.771622158	0.740347971	0.447851889
3820	GPSM3	NM_022107	-2.085001222	-1.708831706	0.819583072	0.741626726	0.553045564
8164	FABP3	NM_004102	-1.90367999	-1.603788673	0.842467579	0.741777519	0.841180142
5098	NA	XM_211460	-2.106846784	-1.650725902	0.783505433	0.743193855	0.553045564
7828	HLA-DRB3	NM_022555	-2.413752	-1.770771426	0.733617797	0.743240016	0.20411575
19616	SDF2L1	NM_022044	-2.572866606	-1.823320451	0.708672749	0.744114659	0
16094	NA	NM_016158	-1.992489273	-1.641596608	0.823892319	0.744231612	0.712856661
10259	C11orf1	NM_022761	-2.034493879	-1.625150873	0.798798605	0.746495193	0.575952169
7271	MAGEB10	NM_182506	-2.549378225	-1.699807363	0.6667537	0.74811455	0
19381	ATP6AP2	NM_005765	-2.77212253	-1.778362727	0.641516638	0.74866171	0
15034	ALOX5AP	NM_001629	-1.893863459	-2.145950081	1.133107073	0.750392557	0.841180142
22110	FBLN1	NM_001996	-2.488413047	-1.704265457	0.684880454	0.750801299	0.20411575
11631	CDK2AP2	NM_005851	-2.097079965	-1.663739746	0.793360183	0.751545376	0.553045564
714	MBNL1	NM_021038	-2.272221744	-1.671496872	0.73562225	0.7517658	0.20411575
3105	ARSG	NM_014960	-2.291798661	-1.644818142	0.717697488	0.752289298	0.20411575
15037	NA	XM_352661	-1.974710235	-1.641493964	0.831258144	0.752803962	0.712856661
19255	STAB1	NM_015136	-2.63688646	-1.74265977	0.660877818	0.753020381	0
5702	XRCC2	NM_005431	-2.712487474	-1.707068294	0.629336839	0.753092251	0
14585	FNBP1	NM_015033	-2.795115879	-1.782813313	0.637831628	0.753809377	0
6924	METTL2A	NM_181725	-2.570453677	-1.680490934	0.653772114	0.754298316	0
1797	ADD3	NM_019903	-2.63679224	-1.729378487	0.655864524	0.754867728	0
8520	USP16	NM_006447	-3.227953226	-1.804026097	0.558876158	0.755119915	0
7136	DNAJB1	NM_006145	-2.243858821	-1.677230251	0.747475837	0.755786371	0.320211326
18360	C14orf132	NM_020215	-2.102561463	-1.590769666	0.756586523	0.755977662	0.553045564
4041	SULT1A1	NM_001055	-1.866915724	-1.551933065	0.831281801	0.756370778	0.955895955
11124	YIF1B	NM_033557	-2.281420081	-1.671564998	0.732686195	0.75753959	0.20411575
8930	WDR17	NM_170710	-2.655118553	-1.738011927	0.654589199	0.757641236	0
2365	LGI2	NM_018176	-2.131975454	-1.596244601	0.748716219	0.757877662	0.553045564
22516	ZNF554	NM_152303	-2.470861576	-1.674406245	0.677660886	0.758441073	0.20411575
16758	VEPH1	NM_024621	-2.598965913	-1.706849738	0.656741872	0.75902685	0
11795	CNR1	NM_016083	-1.996800313	-1.567122759	0.784816964	0.759188694	0.712856661
3541	FLJ21106	NM_025097	-2.568160536	-1.664587453	0.648163318	0.759245287	0
6270	PCDH9	NM_020403	-1.952028042	-1.580234857	0.809534916	0.759322826	0.712856661
16769	FLJ10803	NM_018224	-2.245396474	-1.647376845	0.733668581	0.759470797	0.320211326
10623	ADRA2C	NM_000683	-1.859503262	-1.618271711	0.870270972	0.759480854	0.955895955
15312	TM6SF1	NM_023003	-3.049207074	-1.757219218	0.576287269	0.759978082	0
2831	WIG1	NM_152240	-2.00382951	-1.546959388	0.7720015	0.761375162	0.575952169
17888	NA	XM_379632	-2.181125861	-1.690998655	0.77528706	0.76159122	0.447851889
10178	UNC13B	NM_006377	-2.56840941	-1.690592679	0.658225543	0.761775427	0
22461	UGP2	NM_006759	-2.950258223	-1.750689757	0.593402213	0.76223643	0
21036	NA	XM_114317	-2.302280189	-1.607769996	0.69833811	0.763051056	0.20411575
2122	FES	NM_002005	-2.213224368	-1.584870173	0.716091055	0.763716104	0.320211326
15538	NRXN3	NM_138970	-3.421641442	-1.795428908	0.524727368	0.763812425	0
22100	JUND	NM_005354	-2.368219705	-1.65847399	0.700304109	0.764630765	0.20411575
6033	RPESP	NM_153225	-2.005993042	-1.612330433	0.803756742	0.7647691	0.575952169
16972	NA	NM_018589	-2.032312611	-1.549993747	0.762674865	0.764998237	0.575952169
14357	ZNF440	NM_152357	-2.645199605	-1.645059911	0.621903885	0.765234873	0
8672	FREQ	NM_014286	-2.191585946	-1.633443656	0.745324937	0.765277495	0.447851889
14800	EDG6	NM_003775	-2.033663028	-1.634674561	0.803807976	0.765485987	0.575952169
21371	NA	XM_351558	-2.591892553	-1.699110066	0.655548033	0.765621744	0
5662	FZD1	NM_003505	-1.898097861	-1.511201829	0.796166446	0.765675707	0.841180142
11596	AHSA1	NM_012111	-2.140827463	-1.671088342	0.780580579	0.7657485	0.447851889
12477	VGLL3	NM_016206	-3.369767634	-1.775764992	0.526969567	0.766463541	0
3481	C12orf43	NM_022895	-2.263596123	-1.622910246	0.716961047	0.766896681	0.320211326
10516	FMOD	NM_002023	-1.97343729	-1.541190737	0.780967678	0.767172249	0.712856661
13726	UHRF1	NM_013282	-2.637576092	-1.701307834	0.645027015	0.767217201	0
22904	ITGB2	NM_000211	-1.873299547	-1.600354964	0.854297417	0.76727023	0.955895955
983	OGN	NM_014057	-2.018871204	-1.52630344	0.756018233	0.767853181	0.575952169
11917	CD34	NM_001773	-2.146111681	-1.554920088	0.724528971	0.768338371	0.447851889
13027	CTHRC1	NM_138455	-2.229165503	-1.593276589	0.714741273	0.768764139	0.320211326
4071	TNFSF15	NM_005118	-2.437235893	-1.595062826	0.654455661	0.769195564	0.20411575
4682	RIMS3	NM_014747	-2.727377674	-1.677474194	0.615050204	0.769922262	0
16064	ABLIM3	NM_014945	-2.785060188	-1.660354238	0.59616458	0.771129417	0
17332	SELPLG	NM_003006	-2.082445058	-1.571359668	0.75457437	0.772462419	0.553045564
13350	GARNL3	NM_032293	-2.521078958	-1.681822571	0.667104283	0.772480956	0.20411575
16878	TMEM71	NM_144649	-1.857300809	-1.52932434	0.823412305	0.772489908	0.955895955
3361	MYOCD	NM_153604	-2.429659982	-1.645480097	0.677247067	0.772765998	0.20411575
10631	MATN2	NM_030583	-2.236997687	-1.593829675	0.712486063	0.773169097	0.320211326
2541	TUBA6	NM_032704	-2.034368564	-1.574704952	0.774050966	0.773248153	0.575952169
8821	EXOC6	NM_019053	-2.940878219	-1.6991193	0.57775915	0.775233451	0
16045	RASSF2	NM_170773	-2.16094447	-1.583333403	0.732704345	0.775434945	0.447851889
18273	SGCD	NM_172244	-2.210927357	-1.621394455	0.73335492	0.77545628	0.320211326
14145	TRIB2	NM_021643	-1.91925177	-1.54518016	0.805095081	0.775553821	0.841180142

Supplementary Table I. Continued

22941	IGF1	NM_000618	-2.46037414	-1.606720357	0.653039036	0.77558972	0.20411575
10093	WDR1	NM_005112	-2.529430694	-1.674368836	0.661954819	0.775758385	0.20411575
16338	PALLD	NM_016081	-2.506217871	-1.594867732	0.63636436	0.775796058	0.20411575
22618	GPRC5B	NM_016235	-2.541807392	-1.665138392	0.655100145	0.776498692	0.20411575
19376	GAP43	NM_002045	-2.657223456	-1.654393783	0.622602431	0.777939841	0
3179	FPRL2	NM_002030	-2.037125527	-1.542576591	0.757231977	0.779310123	0.575952169
20871	FBXL22	NM_203373	-2.319676033	-1.539095666	0.663495955	0.77953702	0.20411575
13388	PHLDA3	NM_012396	-1.912212681	-1.463043094	0.765104796	0.780910492	0.841180142
17600	RGL1	NM_015149	-2.245568328	-1.552493512	0.691358839	0.783444015	0.320211326
16596	PFN2	NM_002628	-2.213605097	-1.511291052	0.682728394	0.784964617	0.320211326
12557	KIR3DL3	NM_153443	-2.051565161	-1.46781818	0.715462618	0.785351335	0.575952169
20105	KCNB2	NM_004770	-2.161433263	-1.520036562	0.703253988	0.78619115	0.447851889
3913	ACTR5	NM_024855	-2.578072845	-1.646228276	0.638549946	0.786222503	0
4804	TKT	NM_001064	-2.484993052	-1.604598644	0.645715545	0.786430054	0.20411575
103	LY86	NM_004271	-2.490454323	-1.615308195	0.648599807	0.787666321	0.20411575
1211	SGK	NM_005627	-2.020301544	-1.541438336	0.762974389	0.78767177	0.575952169
13760	HRASLS3	NM_007069	-2.220867928	-1.536038289	0.691638737	0.789093301	0.320211326
17156	MFAP5	NM_003480	-2.207977201	-1.558940394	0.706049135	0.789496717	0.320211326
8110	VIL2	NM_003379	-1.969430171	-1.507504371	0.765452055	0.789526004	0.712856661
10156	RASA1	NM_022650	-2.309699274	-1.52272526	0.659274252	0.790704112	0.20411575
20612	ZNFN1A1	NM_006060	-1.97692589	-1.461105294	0.739079447	0.790839905	0.712856661
5481	LMOD1	NM_012134	-2.082493191	-1.510315342	0.725243832	0.791051567	0.553045564
3491	TMEM61	NM_182532	-2.211936713	-1.513522287	0.684252076	0.791736112	0.320211326
11363	AGTPBP1	NM_015239	-2.394743001	-1.548877231	0.646782235	0.794285623	0.20411575
11179	PRO1853	NM_018607	-1.908628384	-1.40733612	0.737354705	0.794510187	0.841180142
22844	TMEM51	NM_018022	-2.001328926	-1.435708073	0.717377366	0.795583141	0.575952169
22499	HEXB	NM_000521	-2.709249299	-1.587304921	0.58588367	0.796095562	0
19434	LIMA1	NM_016357	-2.360081217	-1.537574395	0.651492154	0.796830604	0.20411575
2046	B3GALTL	NM_194318	-1.870336848	-1.420737569	0.759615879	0.79688174	0.955895955
21955	IL11RA	NM_004512	-2.376344157	-1.480349972	0.622952685	0.796981748	0.20411575
10683	ANXA11	NM_001157	-2.195285413	-1.509927972	0.687804858	0.797473409	0.447851889
19416	COL15A1	NM_001855	-2.642487519	-1.548239686	0.585902365	0.799334068	0
7419	GPBAR1	NM_170699	-2.089507671	-1.466069415	0.7016339	0.799838375	0.553045564
8747	INSIG2	NM_016133	-2.568393577	-1.547327064	0.602449359	0.800379014	0
1711	LOC399888	XM_374880	-2.121395589	-1.482996204	0.699066318	0.800574148	0.553045564
22497	AP3S1	NM_001284	-2.107316074	-1.480340889	0.702476912	0.800804333	0.553045564
3124	LASP1	NM_006148	-2.087189234	-1.514928646	0.725822374	0.801034967	0.553045564
2418	DPT	NM_001937	-2.474548282	-1.536705623	0.621004502	0.801515167	0.20411575
10778	VCL	NM_003373	-1.909959867	-1.353136479	0.708463305	0.802356967	0.841180142
8351	HSPD1	NM_002156	-2.210060483	-1.454738731	0.658234805	0.802897267	0.320211326
2181	LYZ	NM_000239	-1.917069898	-1.418352348	0.739854269	0.803163761	0.841180142
6614	GDF10	NM_004962	-2.015754553	-1.410494533	0.699735259	0.803369906	0.575952169
14996	NA	NM_032031	-2.049086018	-1.437852952	0.701704535	0.803421881	0.575952169
2788	ISOC1	NM_016048	-1.995922508	-1.45981079	0.731396527	0.804447582	0.712856661
22133	ITGB1BP2	NM_012278	-2.257780743	-1.504289498	0.66626908	0.804507953	0.320211326
17051	DDAH1	NM_012137	-2.152027304	-1.440749693	0.669484857	0.804745412	0.447851889
7463	KIAA0408	NM_014702	-1.980718493	-1.41899442	0.716403884	0.805269469	0.712856661
5168	FHL2	NM_001450	-2.618236928	-1.513000636	0.577870024	0.805513713	0
15233	RNASE1	NM_002933	-2.451129686	-1.490066203	0.607909982	0.806886051	0.20411575
22846	PPT1	NM_000310	-1.9390168	-1.416083896	0.730310277	0.807633761	0.712856661
22066	NA	XM_353207	-2.360292758	-1.475033957	0.624936865	0.809636152	0.20411575
18605	CCND3	NM_001760	-2.588248517	-1.504751102	0.581378138	0.809702671	0
21839	SDHC	NM_003001	-2.007747551	-1.424878933	0.709690286	0.81068122	0.575952169
18366	FAM49B	NM_016623	-1.962558264	-1.394236217	0.710417745	0.810735711	0.712856661
4967	GUSB	NM_000181	-2.811903055	-1.523783821	0.541904821	0.810977475	0
8022	CRELD2	NM_024324	-2.14393088	-1.424207014	0.664297076	0.812795375	0.447851889
4327	SPRYD3	NM_032840	-1.870911738	-1.319753168	0.705406429	0.812990391	0.955895955
19159	SUSD5	XM_171054	-2.077172082	-1.373303575	0.661140975	0.813201017	0.553045564
22381	CKAP1	NM_001281	-1.989142113	-1.392100607	0.699849748	0.814240599	0.712856661
5055	C4orf18	NM_016613	-2.288985154	-1.441005094	0.629538855	0.816027577	0.20411575
9923	INPP4B	NM_003866	-1.945771617	-1.373751113	0.706018682	0.818776853	0.712856661
13414	MTMR11	NM_181873	-2.366199281	-1.438040011	0.607742561	0.818900767	0.20411575
17359	GALNT12	NM_024642	-2.035185796	-1.391121411	0.683535338	0.821819778	0.575952169
16741	ACADM	NM_000016	-2.49951042	-1.415239705	0.566206763	0.821877246	0.20411575
6916	RAP2C	NM_021183	-1.955082027	-1.320288812	0.675311211	0.822433316	0.712856661
3125	DAAM1	NM_014992	-2.070580794	-1.355323412	0.654561955	0.823067514	0.553045564
16687	FAM101B	NM_182705	-2.073847122	-1.364694608	0.658049763	0.823509077	0.553045564
12011	CCT8	NM_006585	-1.894159819	-1.319331053	0.696525731	0.82355264	0.841180142
1586	PPP1R15A	NM_014330	-2.06985335	-1.382273423	0.66781225	0.823648902	0.553045564
13288	PCYOX1	NM_016297	-2.061241974	-1.341836842	0.650984629	0.823666066	0.575952169
21517	FKBP1A	NM_000801	-2.032023847	-1.370831301	0.674613786	0.823757143	0.575952169
10457	NA	NM_017808	-1.856793609	-1.278255659	0.688420971	0.823883309	0.955895955
2486	WBSCR17	NM_022479	-2.247754003	-1.377102037	0.612656917	0.825187031	0.320211326
986	SEC11L3	NM_033280	-1.972860704	-1.334937454	0.676650638	0.826113873	0.712856661
5461	CENTA2	NM_018404	-1.866243123	-1.304629406	0.699067228	0.826747168	0.955895955

Supplementary Table I. Continued

14560	CRIM1	NM_016441	-2.137747935	-1.367159246	0.639532483	0.826866906	0.447851889
11787	PLCL2	NM_015184	-2.220159593	-1.3599434	0.612543082	0.827297464	0.320211326
11441	DULLARD	NM_015343	-1.917145231	-1.35154559	0.704978198	0.828673926	0.841180142
18308	MAPRE1	NM_012325	-2.245615495	-1.35419804	0.603040923	0.829184071	0.320211326
5759	MORC4	NM_024657	-1.931117012	-1.29907002	0.672703939	0.829479179	0.841180142
5880	BDNF	NM_170734	-2.17333496	-1.340396678	0.616746476	0.829725643	0.447851889
10764	HEBP2	NM_014320	-1.997930181	-1.321046881	0.66120773	0.830934157	0.575952169
18147	AKAP6	NM_004274	-2.270643307	-1.347659025	0.593514191	0.831537241	0.20411575
12391	MTMR4	NM_004687	-2.405625345	-1.362066811	0.566200724	0.832095434	0.20411575
12181	BIN1	NM_139351	-2.036933516	-1.324166059	0.650078193	0.832142715	0.575952169
6485	GCLC	NM_001498	-2.017288231	-1.334165413	0.661365784	0.832253951	0.575952169
15361	GMPR	NM_006877	-1.892888233	-1.281820728	0.677177186	0.832459064	0.841180142
461	OLFML3	NM_020190	-2.224362676	-1.362093487	0.612352249	0.834327482	0.320211326
6313	PDXK	NM_003681	-2.115741943	-1.315646747	0.621837059	0.838401773	0.553045564
16751	CYP4F3	NM_000896	-1.933309859	-1.260285857	0.65187991	0.844056001	0.841180142
14870	RABGGTB	NM_004582	-2.060542483	-1.255357278	0.6092363	0.844226714	0.575952169
10753	C20orf20	NM_018270	-1.864761804	-1.237130322	0.663425388	0.846082302	0.955895955
15908	DENND4C	NM_017925	-2.067370769	-1.262437513	0.610648816	0.846452972	0.553045564
21255	CABLES1	NM_138375	-2.057279851	-1.217658071	0.591877702	0.850795223	0.575952169
98	NA	XM_031104	-1.998477228	-1.226594238	0.613764431	0.851886259	0.575952169
7669	ARL6IP	NM_015161	-1.977266515	-1.179714148	0.596638915	0.854032276	0.712856661
21685	FLJ35779	NM_152408	-1.881193657	-1.161303183	0.617322506	0.854264553	0.841180142

Estimated Miss rates for Delta=0.897747607952323

Quantiles	Cutpoints	Miss Rate(%)
0 -> 0.05	-1.849 -> -0.9	62.91
0.05 -> 0.1	-0.908 -> -0.6	21.18
0.1 -> 0.15	-0.654 -> -0.51	10.31
0.15 -> 0. 2	-0.511 -> -0.4	5.58
0.2 -> 0.25	-0.406 -> -0.3	4.04
0.25 -> 0.75	-0.321 -> 0.326	0.3
0.75 -> 0.8	0.326 -> 0.411	3.89
0.8 -> 0.85	0.411 -> 0.515	7.84
0.85 -> 0.9	0.515 -> 0.653	14.59
0.9 -> 0.95	0.653 -> 0.896	23.15
0.95 -> 1	0.896 -> 1.849	60.58

Significant: 811
Median number of false positives: 7.75
False Discovery Rate (%): 0.96

SAM Plotsheet

Tail strength (%): 27
se (%): 8.8

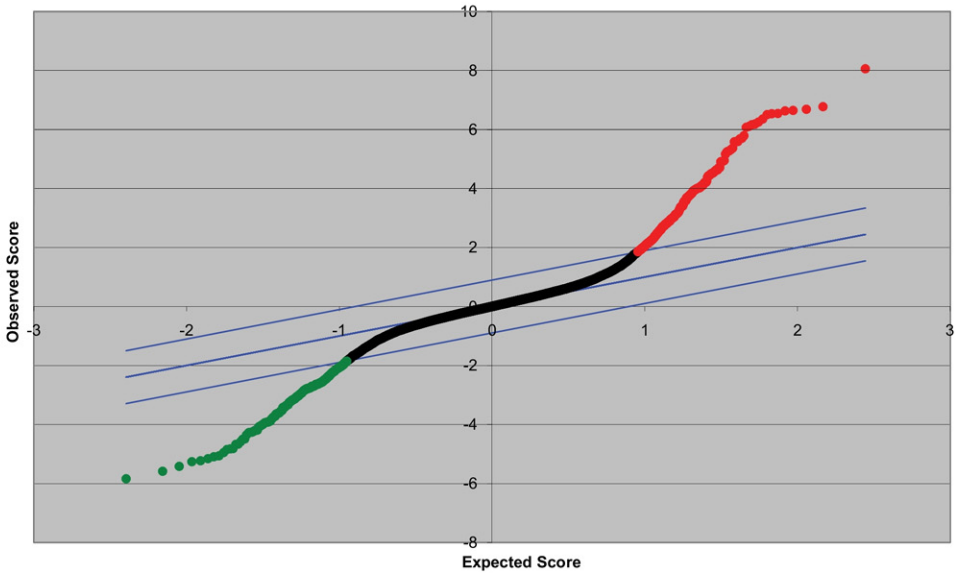

Supplementary Table II. Genes significantly changed by high flow in a PTFE graft. Data were analyzed by Significance Analysis of Microarrays (SAM) software with a false discovery rate of 10%.

Current settings

Input parameters

Data type?	Two class paired
Arrays centered?	FALSE
Delta	0.267427
Minimum fold change	0
Test statistic	standard
Are data are log scale?	TRUE
Number of permutations	200
Input percentile for exchangeability factor s0	Automatic choice
Number of neighbors for KNN	10
Seed for Random number generator	1234567

Computed values

Estimate of pi0 (proportion of null genes)	0.944944
Exchangibility factor s0	1.346388
s0 percentile	99.99589
False Discovery Rate (%)	10.1244

List of Significant Genes for Delta = 0.267

Positive genes (58)

Row	Gene ID	Gene Name	Score(d)	Numerator(r)	Denominator(s+s0)	Fold Change	q-value(%)
16513	COL5A3	NM_015719	2.259874	3.267324406	1.445799468	2.230378841	0
3228	MUSTN1	NM_205853	2.236295	3.494620175	1.562683282	2.998131637	0
11056	SLCO2A1	NM_005630	1.993018	3.104891317	1.557884337	2.151683371	0
13266	IGFBP5	NM_000599	1.948903	2.990345643	1.534373934	2.159877065	0
18545	PLA2G2A	NM_000300	1.928421	2.838375118	1.471864719	1.725450075	0
4628	DCN	NM_001920	1.885166	2.738884755	1.452861308	1.677453418	0
11508	C8orf4	NM_020130	1.872169	2.844381037	1.519296873	1.812281217	0
11977	CD34	NM_001773	1.799393	2.816210332	1.565089429	1.832272678	0
11643	NA	XM_351265	1.735766	2.752114719	1.585532841	1.93434844	0
6926	CLEC3B	NM_003278	1.674844	2.490778769	1.487170941	1.525405585	0
24085	ADAMTS6	NM_197941	1.655247	2.629314812	1.588473112	1.599896563	0
2856	FCN3	NM_173452	1.603059	2.920951919	1.822111126	2.262747384	0
11650	JAG2	NM_145159	1.594815	2.610578039	1.63691593	1.723542096	0
3043	RAMP2	NM_005854	1.568354	2.599116113	1.657224946	1.759685309	0
13771	CLEC14A	NM_175060	1.502388	2.482775345	1.652552782	1.816571626	0
11723	MDK	NM_002391	1.497042	2.863626871	1.912856135	2.315960936	0
11880	HIST2H2AC	NM_003517	1.485151	2.265835967	1.525659983	1.468017692	0
21728	ADAM15	NM_003815	1.478605	2.624925285	1.775271632	1.851431911	0
23403	ADAMTS4	NM_005099	1.441664	2.374421648	1.64700104	1.585081098	0
2321	RARRES1	NM_002888	1.43377	2.939526747	2.050207439	2.711026709	0
17363	CLDN5	NM_003277	1.428885	2.24981617	1.574525173	1.491827804	0
5913	BDNF	NM_170734	1.322441	2.346977695	1.774731638	1.834078992	4.108451994
11537	RASIP1	NM_017805	1.317729	2.271855113	1.724068468	1.528843678	4.108451994
3421	ENPP2	NM_006209	1.298207	2.391945945	1.842500211	1.668309462	5.062199778
16091	TUBB3	NM_006086	1.297833	2.005144791	1.544994297	1.344984865	5.062199778
20419	DOC1	NM_014890	1.293539	2.297460121	1.776104172	1.759128793	5.062199778
11609	FLJ10986	NM_018291	1.290071	2.025462515	1.570039643	1.398671239	5.062199778
8952	SATB2	NM_015265	1.287445	1.825418078	1.417860483	1.297248596	5.062199778
19513	CXCL9	NM_002416	1.269117	2.304331897	1.815696312	1.643973986	6.299626391
10309	NA	XM_090844	1.252213	2.418820598	1.931637415	2.034803991	8.146068609
13555	AUTS2	NM_015570	1.238762	1.964133446	1.585561925	1.371873499	8.146068609
14099	PBXIP1	NM_020524	1.236886	1.839964407	1.487578096	1.309832637	8.146068609
17285	THBS4	NM_003248	1.218883	2.252291666	1.847832315	1.563523344	8.146068609
18034	NA	XM_026998	1.217166	1.917981505	1.575776229	1.369437393	8.146068609
10103	SLPI	NM_003064	1.214802	2.758758513	2.270953773	2.681802851	8.146068609
17228	ENC1	NM_003633	1.213223	1.852317524	1.526773988	1.307075151	8.146068609
9306	PLAT	NM_000931	1.208204	2.031260717	1.681223546	1.466801556	8.146068609
13997	ABI3BP	NM_015429	1.202544	2.190437099	1.821502175	1.525251423	8.146068609
1219	SGK	NM_005627	1.173636	1.943896245	1.656301945	1.399281789	8.216903988
6726	CNN3	NM_001839	1.169674	2.076265488	1.775081077	1.501904328	8.216903988
20414	DCN	NM_133507	1.165614	2.208592296	1.894788289	1.533622173	8.216903988
23541	MYBL2	NM_002466	1.165111	1.836193434	1.575981001	1.325718892	8.216903988
23303	EVI1	NM_005241	1.158818	2.039986136	1.760403193	1.419739553	8.216903988
13966	CMTM8	NM_178868	1.158332	2.078456053	1.794353135	1.444559955	8.216903988
19653	PTPRB	NM_002837	1.15738	1.869005266	1.614859323	1.370518273	8.216903988
12337	HSD11B1	NM_005525	1.156732	2.004553313	1.732945367	1.429151268	8.216903988
7711	C9orf65	NM_138818	1.153946	2.045268271	1.772412875	1.58963112	8.216903988

Supplementary Table II. Continued

1313	HYAL2	NM_003773	1.147602	2.010763771	1.752143409	1.469560258	8.216903988
19602	NA	XM_351624	1.137195	1.727099357	1.518736423	1.278224951	8.703431198
9103	DONSON	NM_145795	1.135602	1.821336842	1.603851998	1.330021111	8.703431198
19947	HNRPU	NM_004501	1.12167	1.849194299	1.648608406	1.331121516	8.703431198
14689	IQGAP3	NM_178229	1.117983	1.801588377	1.611463817	1.301041452	8.703431198
20999	MCM7	NM_005916	1.116799	1.946937377	1.74332011	1.369993427	8.703431198
4151	HSPA1B	NM_005346	1.107158	1.975049336	1.783891448	1.600332371	9.332779838
182	NA	XM_351477	1.098412	1.750440307	1.593610677	1.30713518	9.332779838
19364	GPR3	NM_005281	1.094596	1.713227793	1.565169233	1.277011813	9.332779838
4852	NA	NM_004702	1.092365	1.771283675	1.621513122	1.299306846	9.332779838
2853	PIP5K1A	NM_003557	1.083108	1.744530923	1.610670932	1.301245489	10.12439956

Negative genes (26)

Row	Gene ID	Gene Name	Score(d)	Numerator(r)	Denominator(s+s0)	Fold Change	q-value(%)
10571	FMOD	NM_002023	-1.61225	-2.624305513	1.62773195	0.602321802	6.299626391
21416	NOV	NM_002514	-1.58471	-2.758478335	1.740684341	0.576641447	6.299626391
19584	GAS6	NM_000820	-1.46957	-2.435441154	1.657245644	0.672337564	6.299626391
21267	ATOH8	NM_032827	-1.46685	-2.747872433	1.873309318	0.598376682	6.299626391
8204	FABP3	NM_004102	-1.44347	-2.482189554	1.719601792	0.645991567	6.299626391
2207	ODC1	NM_002539	-1.43607	-2.06671665	1.439145033	0.731015492	6.299626391
21093	PTGIS	NM_000961	-1.42707	-2.463144785	1.726012122	0.646307981	6.299626391
10687	MATN2	NM_030583	-1.40678	-2.201695595	1.565059273	0.704936281	6.299626391
22627	SMAD6	NM_005585	-1.39544	-2.83973892	2.035010667	0.559458726	6.299626391
383	AGC1	NM_001135	-1.39448	-2.203797696	1.580367736	0.70885958	6.299626391
313	CCDC3	NM_031455	-1.3915	-2.581561758	1.855235616	0.58550121	6.299626391
9455	AGC1	NM_013227	-1.37865	-2.278786366	1.652908818	0.699608983	6.299626391
16763	COPZ2	NM_016429	-1.36215	-2.190132761	1.607852054	0.692174203	6.299626391
4248	ANKMY2	NM_020319	-1.35527	-2.056040982	1.517065946	0.733943298	6.299626391
7555	C1QTNF5	NM_015645	-1.35325	-2.301108505	1.700425371	0.700104544	6.299626391
15497	CXXC5	NM_016463	-1.34375	-2.238938386	1.66618672	0.699936577	6.299626391
989	OGN	NM_014057	-1.33164	-2.751117605	2.065956752	0.570317231	6.299626391
20329	TNNC1	NM_003280	-1.32142	-2.080143428	1.574178117	0.72823014	8.177399642
738	GADD45B	NM_015675	-1.3124	-2.022025964	1.540713669	0.742180704	8.177399642
402	RRAS	NM_006270	-1.30148	-2.287555909	1.757660821	0.687262864	8.177399642
20411	COL8A2	NM_005202	-1.25921	-2.225897818	1.767699555	0.701453413	8.216903988
2279	MCHR1	NM_005297	-1.25467	-2.138503153	1.704440894	0.715185165	8.216903988
22805	CCDC51	NM_024661	-1.24538	-1.915449884	1.538046133	0.74762743	9.061106452
16407	UROS	NM_000375	-1.21131	-1.962134247	1.619839243	0.746951548	9.332779838
12515	NA	XM_370710	-1.20827	-1.954448446	1.617564827	0.732447806	9.332779838
10502	FGFR3	NM_022965	-1.20655	-2.029386275	1.681967664	0.728148609	9.332779838

Estimated Miss rates for Delta=0.267427157138977

Quantiles	Cutpoints	Miss Rate(%)
0 -> 0.05	-1.186 -> -0.443	25.59
0.05 -> 0.1	-0.443 -> -0.336	11.19
0.1 -> 0.15	-0.336 -> -0.269	7.78
0.15 -> 0.2	-0.269 -> -0.219	8.85
0.2 -> 0.25	-0.219 -> -0.176	7.2
0.25 -> 0.75	-0.176 -> 0.169	0.08
0.75 -> 0.8	0.169 -> 0.213	0.95
0.8 -> 0.85	0.213 -> 0.268	0
0.85 -> 0.9	0.268 -> 0.34	1.23
0.9 -> 0.95	0.34 -> 0.455	9.25
0.95 -> 1	0.455 -> 1.072	32.5

Supplementary Table II. Continued

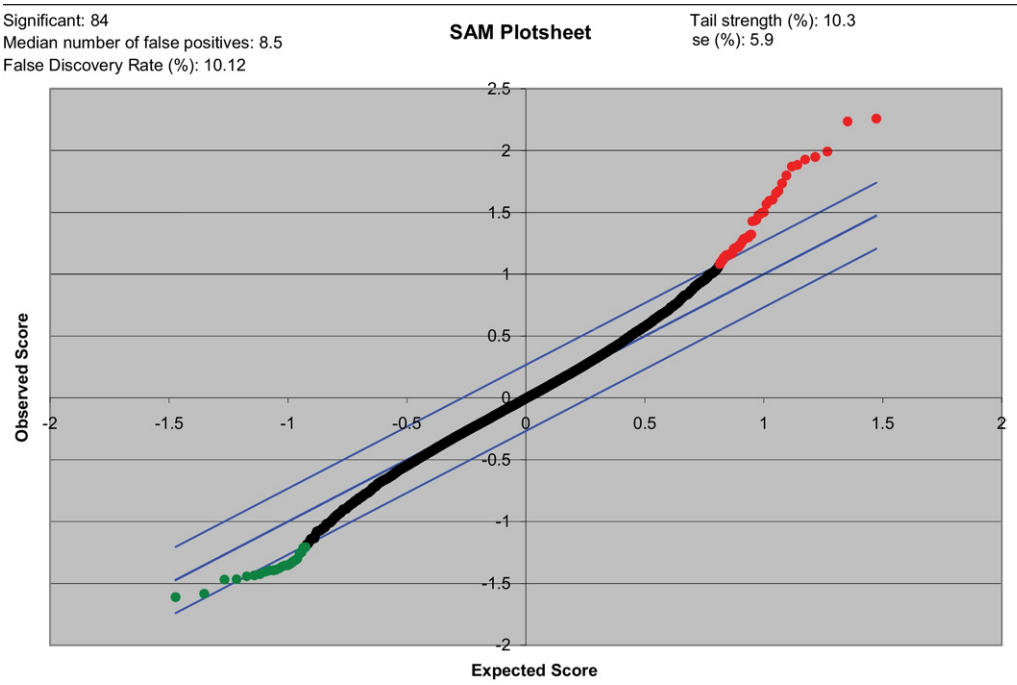

GO:0045892

negative regulation of transcription, DNA-dependent

Gene_set	2711
Gene_set_name	GO:0045892
Score	0.4094692
p-value	0.035
FDR	0.5834118
Gene_set_length	42
Gene_set_description	negative regulation of transcription, DNA-dependent

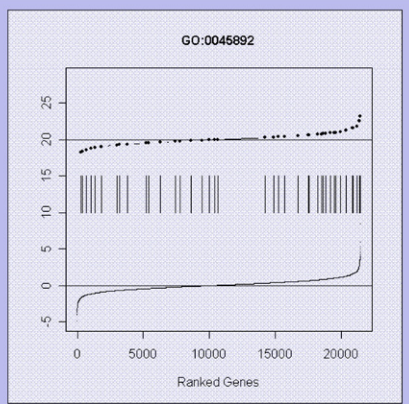

Supplementary Fig I (online only). Gene set GO:0045892 "negative regulation of transcription, DNA-dependent" was significantly enriched in **(A)** high-flow graft neointimas and **(B)** wrapped arteries compared with unwrapped arteries and normal flow grafts, respectively.

	Gene	Score	links
1	ILF3	3.15230539446884	EntrezGene|Source|GeneCard
2	PA2G4	2.50995838033778	EntrezGene|Source|GeneCard
3	TCF7L1	1.81314852110493	EntrezGene|Source|GeneCard
4	TBX3	1.55010504679832	EntrezGene|Source|GeneCard
5	SMARCC2	1.52231828717278	EntrezGene|Source|GeneCard
6	NCOR2	1.23302045887417	EntrezGene|Source|GeneCard
7	CUTL2	1.07787001846078	EntrezGene|Source|GeneCard
8	SIN3A	0.972620151616902	EntrezGene|Source|GeneCard
9	REST	0.943292233822652	EntrezGene|Source|GeneCard
10	DNMT1	0.882046811117962	EntrezGene|Source|GeneCard
11	HNRPAB	0.79899790867625	EntrezGene|Source|GeneCard
12	ZHX2	0.773766317612851	EntrezGene|Source|GeneCard
13	FOXF2	0.752429604026593	EntrezGene|Source|GeneCard
14	KLF4	0.706800190678441	EntrezGene|Source|GeneCard
15	TBX20	0.611899811012897	EntrezGene|Source|GeneCard
16	SMARCE1	0.604061279602447	EntrezGene|Source|GeneCard
17	SIN3B	0.511929483748753	EntrezGene|Source|GeneCard
18	HIVEP1	0.510243324285222	EntrezGene|Source|GeneCard
19	DNAJB6	0.402435032344929	EntrezGene|Source|GeneCard
20	BHLHB2	0.360851782178301	EntrezGene|Source|GeneCard
21	TSG101	0.322847287438982	EntrezGene|Source|GeneCard
22	DAXX	0.265660178465005	EntrezGene|Source|GeneCard
23	MECP2	-0.0209140324233863	EntrezGene|Source|GeneCard
24	NCOR1	-0.0382648718662586	EntrezGene|Source|GeneCard
25	SOX9	-0.0742316406787132	EntrezGene|Source|GeneCard
26	PURB	-0.11973313983431	EntrezGene|Source|GeneCard
27	NFKB1	-0.183625500939374	EntrezGene|Source|GeneCard
28	RPS14	-0.250596824278106	EntrezGene|Source|GeneCard
29	HIC2	-0.278088084135577	EntrezGene|Source|GeneCard
30	DMAP1	-0.382037262857903	EntrezGene|Source|GeneCard
31	CTBP2	-0.38470215931321	EntrezGene|Source|GeneCard
32	NR0B1	-0.46599578649445	EntrezGene|Source|GeneCard
33	TRPS1	-0.485578767291999	EntrezGene|Source|GeneCard
34	PURA	-0.644831741602892	EntrezGene|Source|GeneCard
35	LDB1	-0.721124596070924	EntrezGene|Source|GeneCard
36	ING4	-0.747791010513826	EntrezGene|Source|GeneCard
37	PHF12	-0.971160374580516	EntrezGene|Source|GeneCard
38	FOXP3	-1.10696400142227	EntrezGene|Source|GeneCard
39	NOSTRIN	-1.21228585293278	EntrezGene|Source|GeneCard
40	ZHX1	-1.38798859979598	EntrezGene|Source|GeneCard
41	BCOR	-1.63212637440909	EntrezGene|Source|GeneCard
42	ZNF396	-1.80180017154897	EntrezGene|Source|GeneCard

Supplementary Fig I, A (online only). Continued.

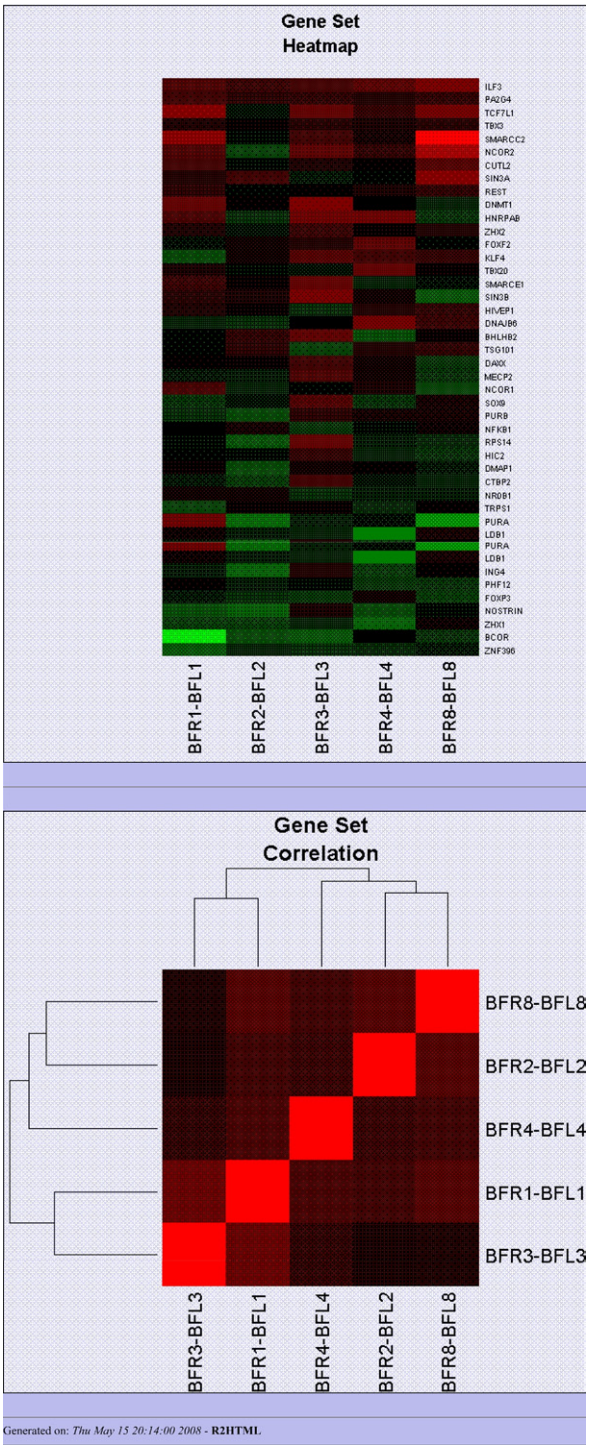

Supplementary Fig I, A (online only). Continued.

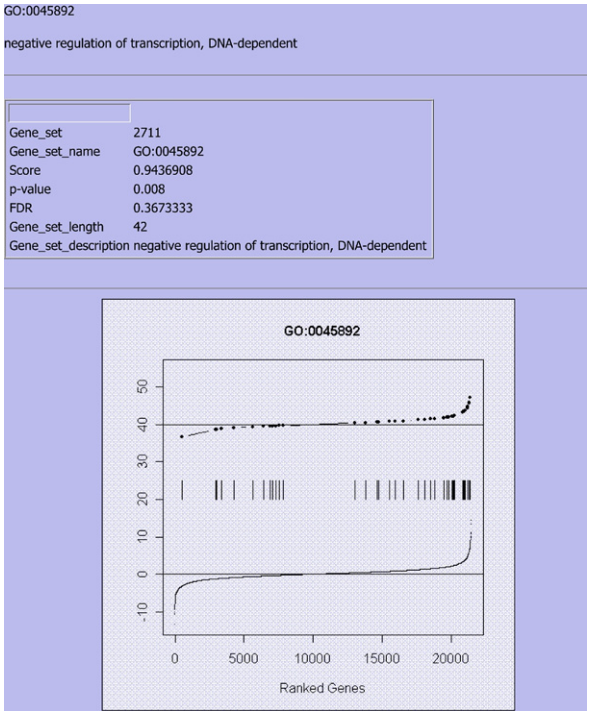

Supplementary Fig I, B (online only). Continued.

	Gene	Score	links
1	NFKB1	7.17095861292666	EntrezGene|Source|GeneCard
2	BHLHB2	7.11042750309384	EntrezGene|Source|GeneCard
3	KLF4	5.7442601868846	EntrezGene|Source|GeneCard
4	BCOR	5.61619695480129	EntrezGene|Source|GeneCard
5	SIN3A	4.77227995406333	EntrezGene|Source|GeneCard
6	DAXX	4.35340613453568	EntrezGene|Source|GeneCard
7	CTBP2	3.66613675570752	EntrezGene|Source|GeneCard
8	ING4	3.5239337504694	EntrezGene|Source|GeneCard
9	TBX3	3.35832405636225	EntrezGene|Source|GeneCard
10	ZHX2	3.21123827372764	EntrezGene|Source|GeneCard
11	PA2G4	2.28337416346075	EntrezGene|Source|GeneCard
12	SIN3B	2.20190127902266	EntrezGene|Source|GeneCard
13	RPS14	2.15461879797641	EntrezGene|Source|GeneCard
14	HNRPAB	2.15018919158734	EntrezGene|Source|GeneCard
15	LDB1	2.10287612563771	EntrezGene|Source|GeneCard
16	DMAP1	1.92408956448457	EntrezGene|Source|GeneCard
17	SOX9	1.85385348848701	EntrezGene|Source|GeneCard
18	SMARCC2	1.72831310381143	EntrezGene|Source|GeneCard
19	ILF3	1.45991565102074	EntrezGene|Source|GeneCard
20	ZNF396	1.37240127966915	EntrezGene|Source|GeneCard
21	SMARCE1	1.24407418915654	EntrezGene|Source|GeneCard
22	TBX20	1.12308853777409	EntrezGene|Source|GeneCard
23	NCOR1	0.88164675133455	EntrezGene|Source|GeneCard
24	NCOR2	0.781910926865337	EntrezGene|Source|GeneCard
25	NR0B1	0.71392396570911	EntrezGene|Source|GeneCard
26	PURB	0.591772029864592	EntrezGene|Source|GeneCard
27	HIVEP1	0.573676429820187	EntrezGene|Source|GeneCard
28	DNAJB6	0.448375801325090	EntrezGene|Source|GeneCard
29	CUTL2	0.332059254449260	EntrezGene|Source|GeneCard
30	PHF12	-0.348596332798477	EntrezGene|Source|GeneCard
31	HIC2	-0.395295199705449	EntrezGene|Source|GeneCard
32	FOXF2	-0.396432150893273	EntrezGene|Source|GeneCard
33	FOXP3	-0.423364468544569	EntrezGene|Source|GeneCard
34	DNMT1	-0.463303362102042	EntrezGene|Source|GeneCard
35	TSG101	-0.489925857329576	EntrezGene|Source|GeneCard
36	MECP2	-0.562876033048477	EntrezGene|Source|GeneCard
37	PURA	-0.693551451197524	EntrezGene|Source|GeneCard
38	REST	-0.948516206742221	EntrezGene|Source|GeneCard
39	TRPS1	-1.18646385582757	EntrezGene|Source|GeneCard
40	TCF7L1	-1.29673513226598	EntrezGene|Source|GeneCard
41	NOSTRIN	-1.30964694711830	EntrezGene|Source|GeneCard
42	ZHX1	-3.35626191987719	EntrezGene|Source|GeneCard

Supplementary Fig I, B (online only). Continued.

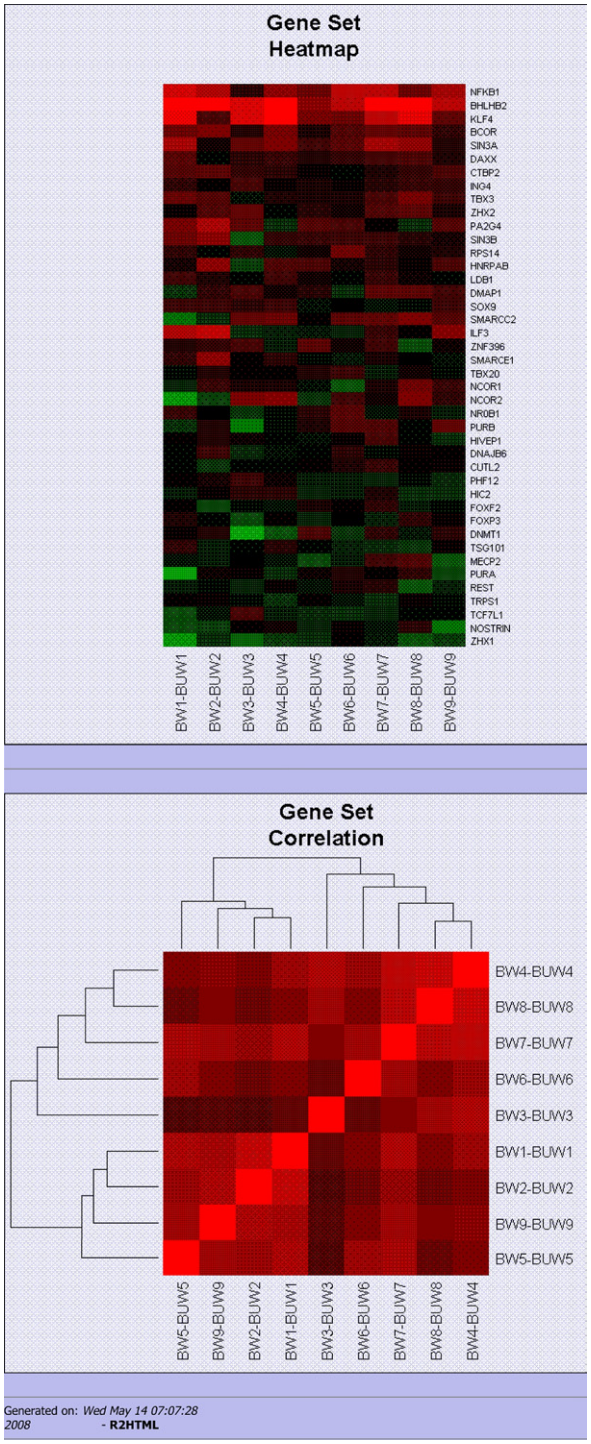

Supplementary Fig I, B (online only). Continued.

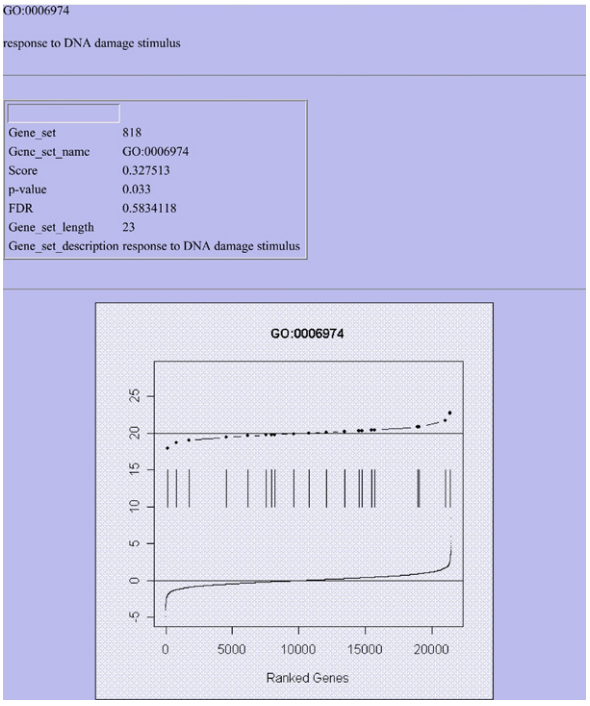

Supplementary Fig II (online only). Gene set GO:0006974 "response to DNA damage stimulus" was significantly enriched in **(A)** high-flow graft neointimas and **(B)** wrapped arteries compared with unwrapped arteries and normal flow grafts, respectively.

	Gene	Score	links
1	SGK	2.80261025061431	EntrezGene|Source|GeneCard
2	MCM7	2.59477145230217	EntrezGene|Source|GeneCard
3	PPP1R15A	1.62948736943821	EntrezGene|Source|GeneCard
4	BCL6	0.855263540412638	EntrezGene|Source|GeneCard
5	TLK2	0.847045886175068	EntrezGene|Source|GeneCard
6	MLH3	0.823377451354393	EntrezGene|Source|GeneCard
7	MAPK1	0.403456560351392	EntrezGene|Source|GeneCard
8	SESN1	0.38047938688319	EntrezGene|Source|GeneCard
9	APC	0.311700081036876	EntrezGene|Source|GeneCard
10	BARD1	0.290935204537427	EntrezGene|Source|GeneCard
11	TP53	0.197355442193255	EntrezGene|Source|GeneCard
12	TOPORS	0.0881003877297543	EntrezGene|Source|GeneCard
13	TLK1	-0.00851240068155202	EntrezGene|Source|GeneCard
14	PARG	-0.102996463231899	EntrezGene|Source|GeneCard
15	BRE	-0.221386892256092	EntrezGene|Source|GeneCard
16	NEK1	-0.234803823398909	EntrezGene|Source|GeneCard
17	TP53AP1	-0.268303368721230	EntrezGene|Source|GeneCard
18	RAD23A	-0.391144002484534	EntrezGene|Source|GeneCard
19	BCL3	-0.39567799953148	EntrezGene|Source|GeneCard
20	DDIT3	-0.555445538163646	EntrezGene|Source|GeneCard
21	CIB1	-0.993121020074338	EntrezGene|Source|GeneCard
22	CDKN1A	-1.30633059076816	EntrezGene|Source|GeneCard
23	BAX	-2.13038392660532	EntrezGene|Source|GeneCard

Supplementary Fig II, A (online only). Continued.

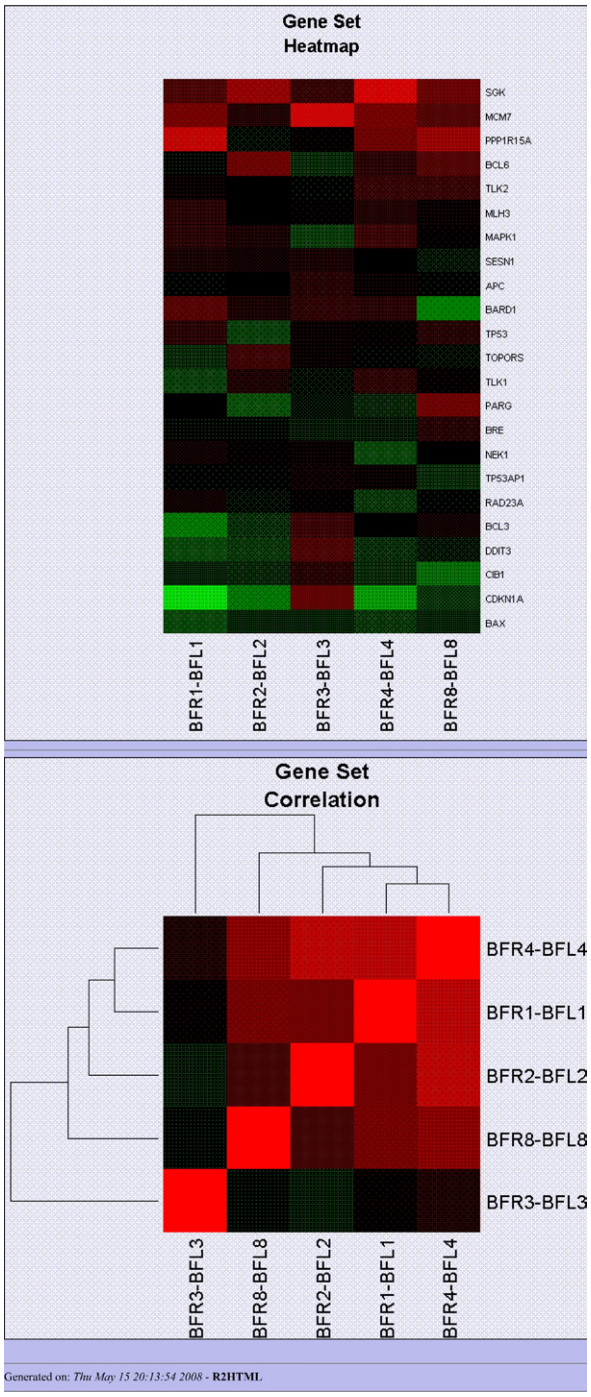

Supplementary Fig II, A (online only). Continued.

GO:0006974

response to DNA damage stimulus

Gene_set	818
Gene_set_name	GO:0006974
Score	0.5945776
p-value	0.039
FDR	0.6482353
Gene_set_length	23
Gene_set_description	response to DNA damage stimulus

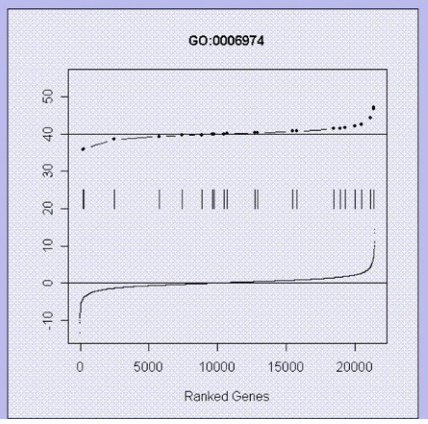

Supplementary Fig II, B (online only). Continued.

	Gene	Score	links
1	BCL3	7.04966647364937	EntrezGene|Source|GeneCard
2	CDKN1A	6.67934342656543	EntrezGene|Source|GeneCard
3	BCL6	4.25047264063508	EntrezGene|Source|GeneCard
4	CIB1	2.56334009307653	EntrezGene|Source|GeneCard
5	MCM7	2.06106997856247	EntrezGene|Source|GeneCard
6	BAX	2.05777039368670	EntrezGene|Source|GeneCard
7	TLK2	1.63376731750371	EntrezGene|Source|GeneCard
8	TOPORS	1.50606844388264	EntrezGene|Source|GeneCard
9	SESN1	1.34341024494405	EntrezGene|Source|GeneCard
10	APC	0.748171844308398	EntrezGene|Source|GeneCard
11	BRE	0.70296184806854	EntrezGene|Source|GeneCard
12	TLK1	0.31329325603105	EntrezGene|Source|GeneCard
13	RAD23A	0.293168147847414	EntrezGene|Source|GeneCard
14	TP53	0.0257606475505974	EntrezGene|Source|GeneCard
15	MLH3	-0.00621270232596164	EntrezGene|Source|GeneCard
16	NEK1	-0.0873282021540831	EntrezGene|Source|GeneCard
17	DDIT3	-0.103772307821797	EntrezGene|Source|GeneCard
18	TP53AP1	-0.209857085185033	EntrezGene|Source|GeneCard
19	PARG	-0.404311363718452	EntrezGene|Source|GeneCard
20	BARD1	-0.672255525243434	EntrezGene|Source|GeneCard
21	MAPK1	-1.47490289443499	EntrezGene|Source|GeneCard
22	SGK	-4.02956830436901	EntrezGene|Source|GeneCard
23	PPP1R15A	-4.29737064750016	EntrezGene|Source|GeneCard

Supplementary Fig II, B (online only). Continued.

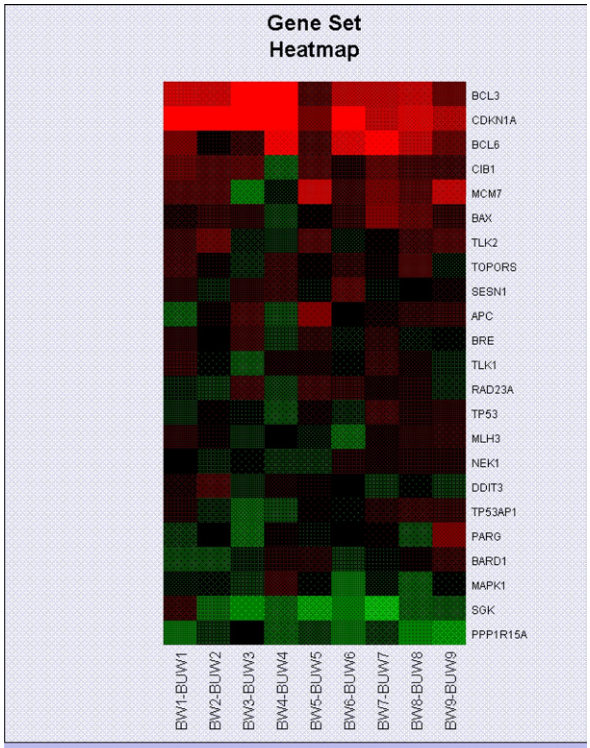

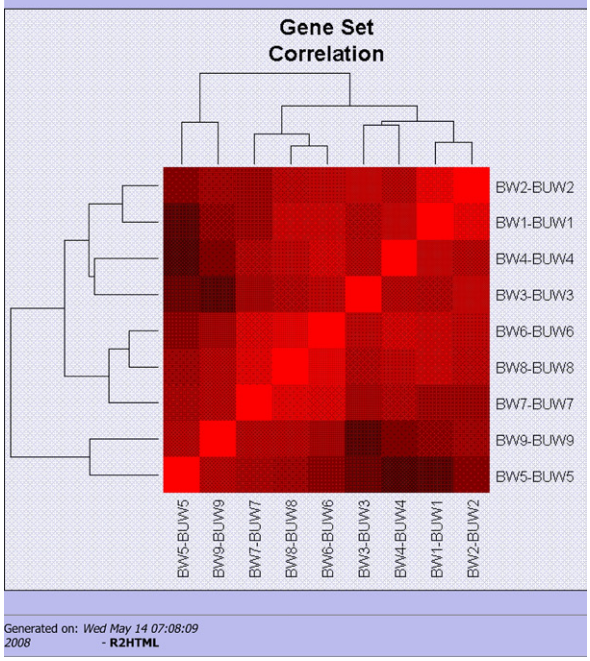

Generated on: *Wed May 14 07:08:09 2008* - **R2HTML**

Supplementary Fig II, B (online only). Continued.

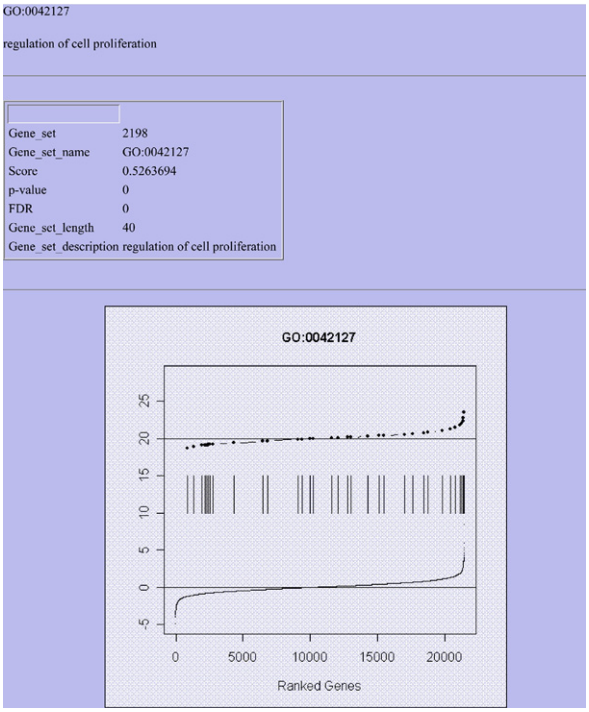

Supplementary Fig III (online only). Gene set GO:0042127 "regulation of cell proliferation" was significantly enriched in **(A)** high-flow graft neointimas and **(B)** wrapped arteries compared with unwrapped arteries and normal flow grafts, respectively.

	Gene	Score	links
1	JAG2	3.49255410628517	EntrezGene|Source|GeneCard
2	EVI1	2.75209821283839	EntrezGene|Source|GeneCard
3	MYC	2.34816856712383	EntrezGene|Source|GeneCard
4	HHEX	2.04577510347270	EntrezGene|Source|GeneCard
5	CHRNA10	1.97098766634045	EntrezGene|Source|GeneCard
6	MAFG	1.76530246400387	EntrezGene|Source|GeneCard
7	ARHGEF2	1.47208578402387	EntrezGene|Source|GeneCard
8	CTNNB1	1.25543460503349	EntrezGene|Source|GeneCard
9	RBM9	1.24170204135636	EntrezGene|Source|GeneCard
10	SCGB3A1	1.04381208038298	EntrezGene|Source|GeneCard
11	INHA	0.793149378995158	EntrezGene|Source|GeneCard
12	DUSP22	0.740078276933897	EntrezGene|Source|GeneCard
13	CFDP1	0.62155646305119	EntrezGene|Source|GeneCard
14	FANCL	0.548900184678322	EntrezGene|Source|GeneCard
15	NFKBIA	0.383498467257032	EntrezGene|Source|GeneCard
16	CDK4	0.346361649940464	EntrezGene|Source|GeneCard
17	PDGFB	0.274331479232568	EntrezGene|Source|GeneCard
18	STAT6	0.165953652725386	EntrezGene|Source|GeneCard
19	TNF	0.148875049855458	EntrezGene|Source|GeneCard
20	HOXD13	0.0886371948772558	EntrezGene|Source|GeneCard
21	TOPORS	0.0881003877297543	EntrezGene|Source|GeneCard
22	DHCR7	0.0505012720463564	EntrezGene|Source|GeneCard
23	TCFL5	-0.0499886381328429	EntrezGene|Source|GeneCard
24	LAMA5	-0.0732649379409301	EntrezGene|Source|GeneCard
25	SOX9	-0.0742316406787132	EntrezGene|Source|GeneCard
26	ARX	-0.124897204987137	EntrezGene|Source|GeneCard
27	FGFR1	-0.146064906606277	EntrezGene|Source|GeneCard
28	DBH	-0.149702136931881	EntrezGene|Source|GeneCard
29	PPP1R9B	-0.329976168992863	EntrezGene|Source|GeneCard
30	BRCA1	-0.368188342885146	EntrezGene|Source|GeneCard
31	TBX19	-0.584199461448677	EntrezGene|Source|GeneCard
32	E2F4	-0.7813006279963	EntrezGene|Source|GeneCard
33	ANXA1	-0.825748185937246	EntrezGene|Source|GeneCard
34	CDCA7	-0.84655295072533	EntrezGene|Source|GeneCard
35	GRPR	-0.848215143859	EntrezGene|Source|GeneCard
36	FANCA	-0.864034649266264	EntrezGene|Source|GeneCard
37	PIN1	-0.898009244203468	EntrezGene|Source|GeneCard
38	JAG1	-0.935369545302141	EntrezGene|Source|GeneCard
39	DBP	-1.09811820794645	EntrezGene|Source|GeneCard
40	BMPR2	-1.29069683352785	EntrezGene|Source|GeneCard

Supplementary Fig III, A (online only). Continued.

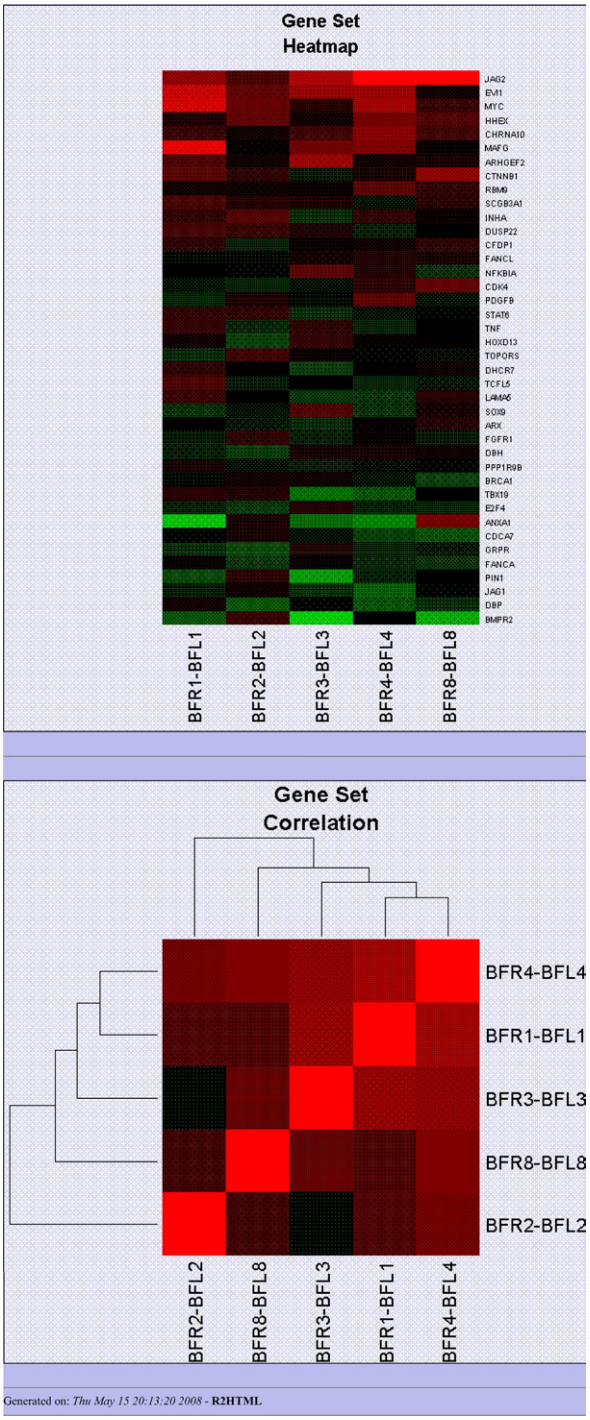

Supplementary Fig III, A (online only). Continued.

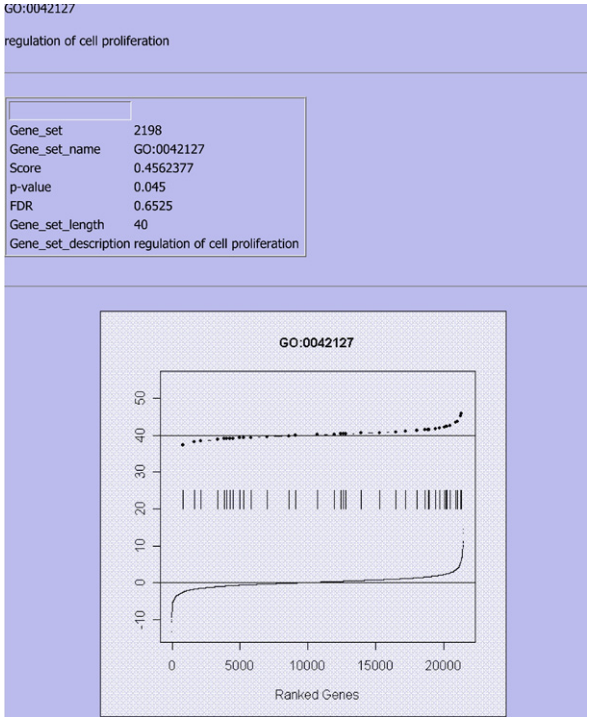

Supplementary Fig III, B (online only). Continued.

	Gene	Score	links
1	MAFG	5.74049596808015	EntrezGene|Source|GeneCard
2	JAG1	5.14656524826306	EntrezGene|Source|GeneCard
3	CTNNB1	5.1265923240615	EntrezGene|Source|GeneCard
4	BMPR2	3.67941783540555	EntrezGene|Source|GeneCard
5	JAG2	3.37863150018995	EntrezGene|Source|GeneCard
6	MYC	2.56732289800295	EntrezGene|Source|GeneCard
7	FANCL	2.28832427175525	EntrezGene|Source|GeneCard
8	STAT6	2.21831089936373	EntrezGene|Source|GeneCard
9	EVI1	2.21543825498486	EntrezGene|Source|GeneCard
10	RBM9	2.12026731897931	EntrezGene|Source|GeneCard
11	SOX9	1.85385348848701	EntrezGene|Source|GeneCard
12	ARHGEF2	1.70088496633126	EntrezGene|Source|GeneCard
13	TOPORS	1.50606844388264	EntrezGene|Source|GeneCard
14	FANCA	1.48387656583953	EntrezGene|Source|GeneCard
15	CDK4	1.40000993914564	EntrezGene|Source|GeneCard
16	DHCR7	1.21859221112766	EntrezGene|Source|GeneCard
17	ARX	1.02978818258172	EntrezGene|Source|GeneCard
18	LAMA5	0.878859857554796	EntrezGene|Source|GeneCard
19	TCFL5	0.666779626115225	EntrezGene|Source|GeneCard
20	PPP1R9B	0.46386506737742	EntrezGene|Source|GeneCard
21	DUSP22	0.302950282492755	EntrezGene|Source|GeneCard
22	HOXD13	0.276671559109385	EntrezGene|Source|GeneCard
23	NFKBIA	0.255482356398652	EntrezGene|Source|GeneCard
24	GRPR	0.189018486163113	EntrezGene|Source|GeneCard
25	CHRNA10	0.0264014932860080	EntrezGene|Source|GeneCard
26	FGFR1	-0.178031210664718	EntrezGene|Source|GeneCard
27	DBP	-0.181554204543748	EntrezGene|Source|GeneCard
28	SCGB3A1	-0.244430589535177	EntrezGene|Source|GeneCard
29	TBX19	-0.472072275337557	EntrezGene|Source|GeneCard
30	BRCA1	-0.659161662918341	EntrezGene|Source|GeneCard
31	TNF	-0.76063016762063	EntrezGene|Source|GeneCard
32	E2F4	-0.808183344334742	EntrezGene|Source|GeneCard
33	INHA	-0.906144289610844	EntrezGene|Source|GeneCard
34	CDCA7	-0.952382960150164	EntrezGene|Source|GeneCard
35	PIN1	-1.0025012356394	EntrezGene|Source|GeneCard
36	CFDP1	-1.05868292154210	EntrezGene|Source|GeneCard
37	ANXA1	-1.18033908831312	EntrezGene|Source|GeneCard
38	HHEX	-1.63525135946524	EntrezGene|Source|GeneCard
39	DBH	-1.90912592475633	EntrezGene|Source|GeneCard
40	PDGFB	-2.74101229506604	EntrezGene|Source|GeneCard

Supplementary Fig III, B (online only). Continued.

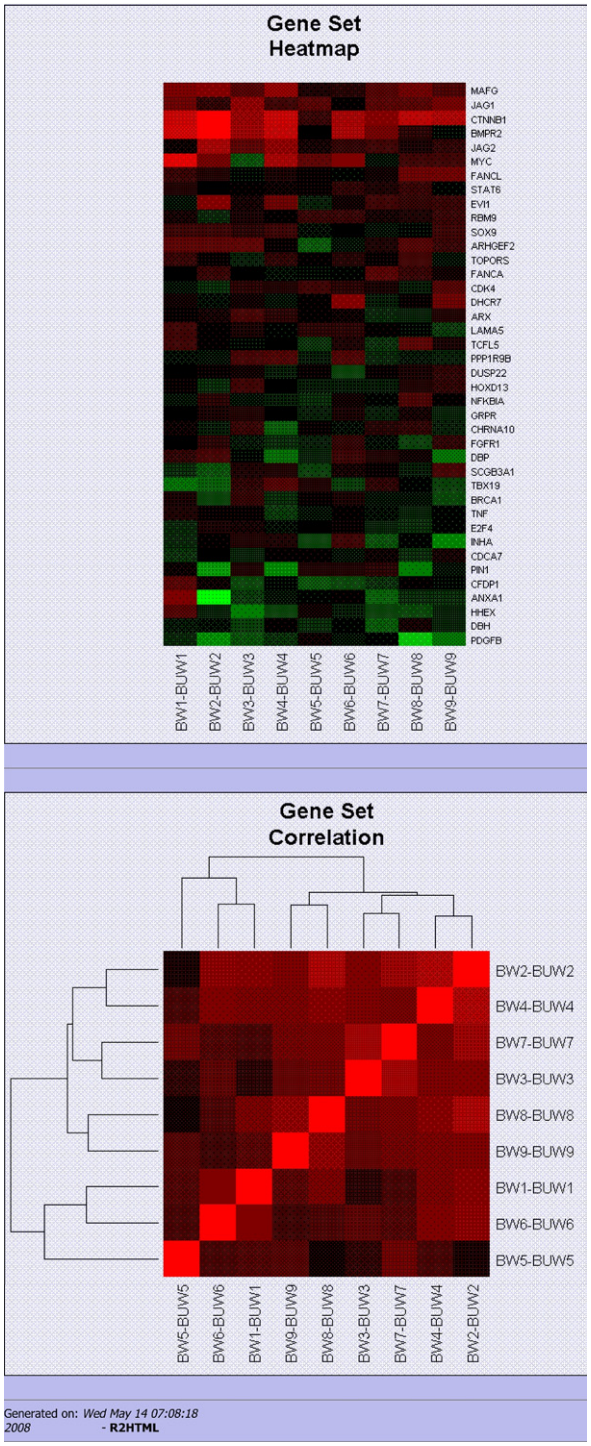

Supplementary Fig III, B (online only). Continued.

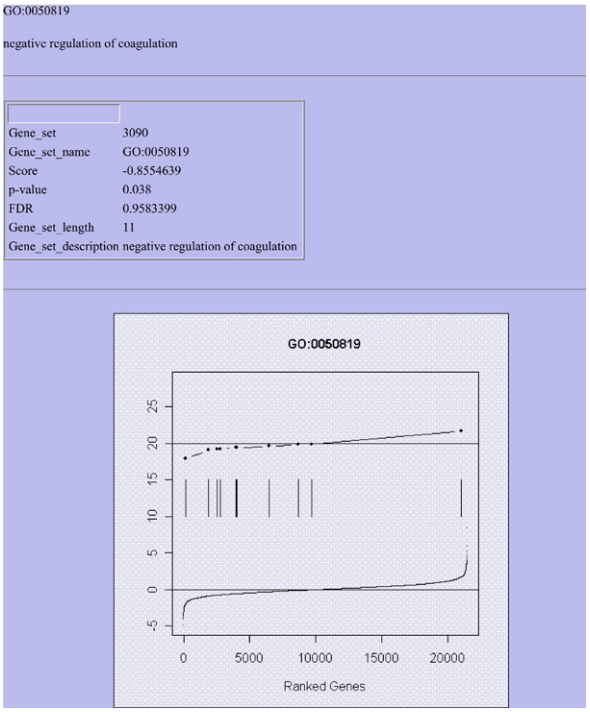

Supplementary Fig IV (online only). Gene set GO:0050819 "negative regulation of coagulation" was significantly enriched in **(A)** normal flow graft neointimas and **(B)** unwrapped arteries compared with high-flow grafts and wrapped arteries, respectively.

	Gene	Score	links
1	ANXA3	1.65329357277804	EntrezGene|Source|GeneCard
2	ANXA9	-0.0975225536344933	EntrezGene|Source|GeneCard
3	HS3ST5	-0.183098990790436	EntrezGene|Source|GeneCard
4	ANXA10	-0.364713334394912	EntrezGene|Source|GeneCard
5	ANXA6	-0.616198008367344	EntrezGene|Source|GeneCard
6	ANXA4	-0.619451491443513	EntrezGene|Source|GeneCard
7	ANXA8	-0.782332272325127	EntrezGene|Source|GeneCard
8	ANXA1	-0.825748185937246	EntrezGene|Source|GeneCard
9	ANXA5	-0.950889876263313	EntrezGene|Source|GeneCard
10	ANXA2	-0.954137250114775	EntrezGene|Source|GeneCard
11	ANXA11	-2.12824969870469	EntrezGene|Source|GeneCard

Supplementary Fig IV, A (online only). Continued.

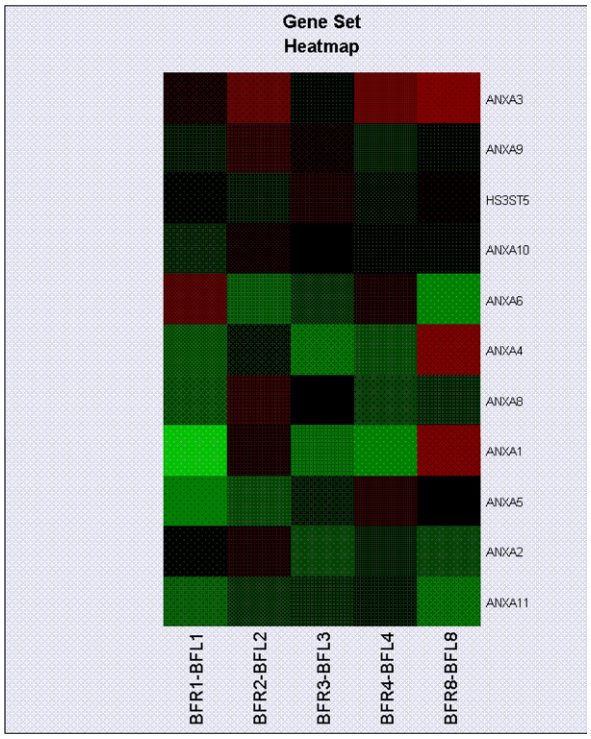

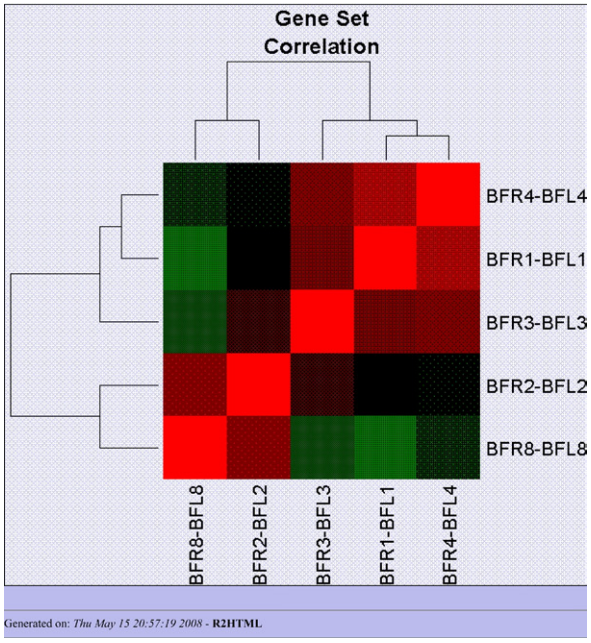

Supplementary Fig IV, A (online only). Continued.

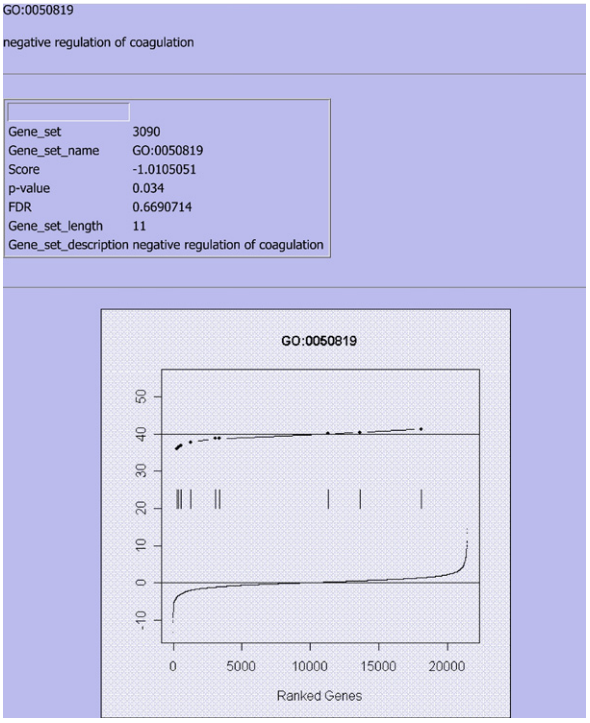

Supplementary Fig IV, B (online only). Continued.

	Gene	Score	links
1	HS3ST5	1.23443946870770	EntrezGene|Source|GeneCard
2	ANXA8	0.419928715910400	EntrezGene|Source|GeneCard
3	ANXA9	0.104902654942738	EntrezGene|Source|GeneCard
4	ANXA1	-1.18033908831312	EntrezGene|Source|GeneCard
5	ANXA2	-1.18624117477357	EntrezGene|Source|GeneCard
6	ANXA10	-1.27960462292079	EntrezGene|Source|GeneCard
7	ANXA5	-2.16916598131854	EntrezGene|Source|GeneCard
8	ANXA4	-2.18260221898958	EntrezGene|Source|GeneCard
9	ANXA6	-3.13516370354977	EntrezGene|Source|GeneCard
10	ANXA3	-3.68924236672235	EntrezGene|Source|GeneCard
11	ANXA11	-4.01655875738525	EntrezGene|Source|GeneCard

Supplementary Fig IV, B (online only). Continued.

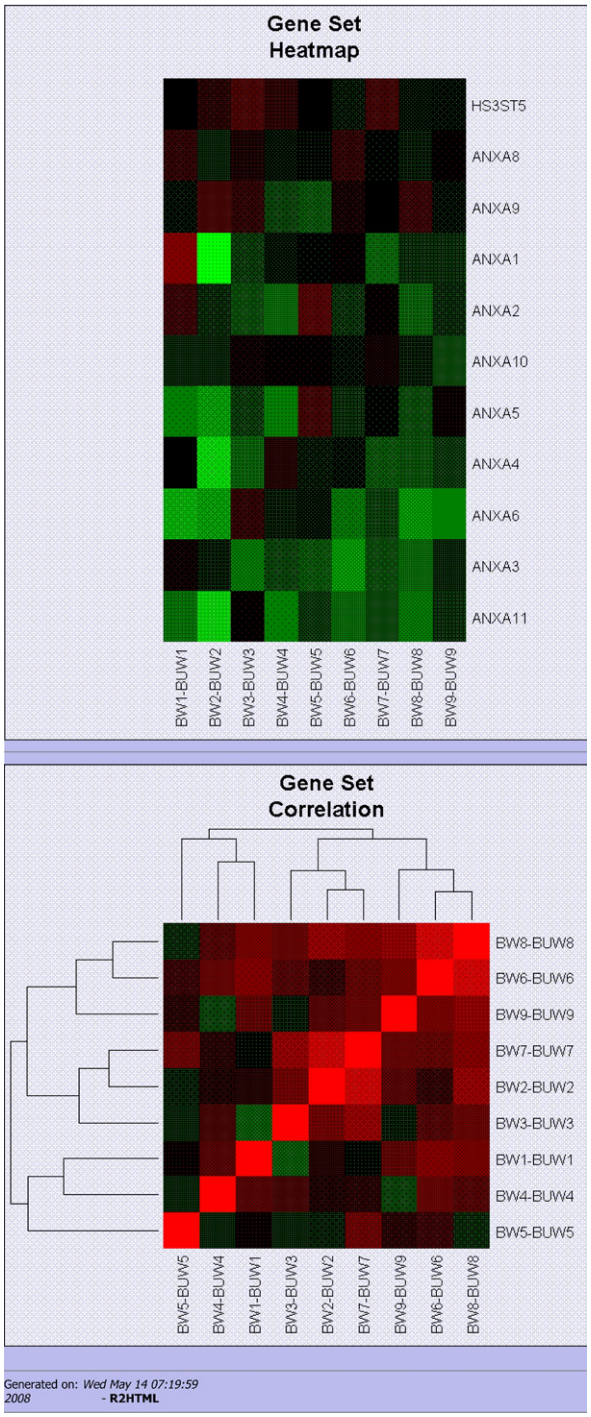

Supplementary Fig IV, B (online only). Continued.